Cloning, Expression of Δ^5-Elongase Gene from *Pavlova* sp. CCMP459 and Determination of Polyunsaturated Fatty Acid Production in *Physcomitrella patens*

Pichit Chodok

A Thesis Submitted in Partial Fulfillment of the Requirements for the Degree of Doctor of Philosophy in Pharmaceutical Sciences

Prince of Songkla University

2012

Thesis Title	Cloning, Expression of Δ^5-Elongase Gene from *Pavlova* sp. CCMP459 and Determination of Polyunsaturated Fatty Acid Production in *Physcomitrella patens*
Author	Mr. Pichit Chodok
Major Program	Pharmaceutical Sciences

Major Advisor :

……..
(Dr. Sireewan Kaewsuwan)

Examining Committee :

…….....Chairperson
(Assoc. Prof. Dr. Wanna Choorit)

Co-advisor :

…….....
(Assist. Prof. Dr. Akkharawit Kanjana-Opas)

……..….....
(Dr. Sireewan Kaewsuwan)

…….….....
(Assist. Prof. Dr. Akkharawit Kanjana-Opas)

…….....
(Assist. Prof. Dr. Juraithip Wungsintaweekul)

The Graduate School, Prince of Songkla University, has approved this thesis as partial fulfillment of the requirements for the Doctor of Philosophy Degree in Pharmaceutical Sciences

..……...……
(Prof. Dr. Amornrat Phongdara)
Dean of Graduate School

ชื่อวิทยานิพนธ์ การโคลน การแสดงออกของยีน Δ^5-elongase จาก *Pavlova* sp. CCMP459 และการผลิตกรดไขมันไม่อิ่มตัวสูงใน *Physcomitrella patens*
ผู้เขียน นายพิชิต โชดก
สาขาวิชา เภสัชศาสตร์
ปีการศึกษา 2554

บทคัดย่อ

กรดอะดรีนิก และกรดโอเมก้า 3 โดโคซาเพนทาอีโนอิกเป็นกรดไขมันไม่อิ่มตัวสูงในกลุ่มโอเมก้า 6 และโอเมก้า 3 ตามลำดับ ที่มีศักยภาพนำไปใช้เป็นยารักษาโรค ปัจจุบันมีการศึกษากระบวนการชีวสังเคราะห์ของน้ำมันจากพืช ตลอดจนการศึกษาทางด้านพันธุวิศวกรรมของพืชกันอย่างแพร่หลาย ดังนั้นการปรับเปลี่ยนวิถีชีวสังเคราะห์ของกรดไขมันเพื่อให้พืชผลิตกรดไขมันไม่อิ่มตัวสูงชนิดใหม่จึงเป็นทางเลือกหนึ่งที่น่าสนใจ การศึกษาครั้งนี้ได้นำยีน Δ^5-elongase จากสาหร่าย *Pavlova* sp. CCMP459 ที่เกี่ยวข้องกับการสังเคราะห์กรดไขมันไม่อิ่มตัวสูงที่มีความยาว 22 คาร์บอน มาศึกษาในมอส *Physcomitrella patens* เพื่อให้มอสผลิตกรดอะดรีนิกและกรดโอเมก้า 3 โดโคซาเพนทาอีโนอิก พบว่ายีน Δ^5-elongase สามารถแสดงออกได้ใน *P. patens* ภายใต้การควบคุมของ 35S promoter จำนวน 2 ชุดซ้ำกัน โดยทำให้ *P. patens* สามารถผลิตกรดอะดรีนิกได้เท่ากับ 0.15±0.04 ถึง 6.97±0.74 มิลลิกรัมต่อลิตร จากสารตั้งต้นกรดอะราชิโดนิคที่มีอยู่ใน *P. patens* และจากการปรับปรุงสภาวะของการเพาะเลี้ยง transgenic *P. patens* C6 โดยวิธี response surface methodology (RSM) พบว่า *P. patens* สามารถผลิตกรดอะดรีนิกได้เพิ่มขึ้นอย่างมีนัยสำคัญทางสถิติได้เท่ากับ 4.48 มิลลิกรัมต่อลิตร มากกว่าสภาวะที่ไม่ได้มีการปรับปรุงการเพาะเลี้ยงถึง 10.6 เท่า (0.42 มิลลิกรัมต่อลิตร) นอกจากนี้ยังพบว่าการปรับปรุงวิถีชีวสังเคราะห์ด้วยยีน Δ^5-elongase จากสาหร่าย *Pavlova* sp. ร่วมกับการเติมน้ำมันพืช พบว่าประสบความสำเร็จในการกระตุ้นให้ *P. patens* สร้างทั้งกรดอะดรีนิกและกรดโอเมก้า 3 โดโคซาเพนทาอีโนอิก โดยสะสมกรดอะดรีนิกและกรดโอเมก้า 3 โดโคซะเพนทาโนอิกเพิ่มขึ้นถึง 24.3 และ 11.7 มิลลิกรัมต่อลิตร ตามลำดับ หรือ 2.3 และ 1.1 เปอร์เซ็นต์ของกรดไขมันรวม ตามลำดับ การศึกษานี้จึงเป็นรายงานแรกในการผลิตกรดโอเมก้า 3 โดโคซะเพนทาโนอิกซึ่งเป็นสารตั้งต้นในการสังเคราะห์โดโคซาเฮกซาอีโนอิก (ดีเอชเอ) ใน *P. patens*

Thesis Title	Cloning, Expression of Δ^5-Elongase Gene from *Pavlova* sp. CCMP459 and Determination of Polyunsaturated Fatty Acid Production in *Physcomitrella patens*
Author	Mr. Pichit Chodok
Major Program	Pharmaceutical Sciences
Academic Year	2011

ABSTRACT

Adrenic acid (ADA) and ω-3 docosapentaenoic acid (ω-3 DPA), an ω-6 and ω-3 polyunsaturated fatty acids (PUFAs), respectively, has attracted much interest due to their pharmaceutical potential. Exploiting the wealth of information currently available in *planta* oil biosynthesis, and coupling this information with the tool of genetic engineering, it is now feasible to deliberately alter fatty acid biosynthetic pathways to generate unique oils in commodity crops. In this study, a Δ^5-elongase gene from the algae *Pavlova* sp. CCMP459 related to the biosynthesis of C_{22}-PUFAs was targeted to enable production of ADA and ω-3 DPA in the moss *Physcomitrella patens*. Heterologous expression of this gene under the control of a tandemly duplicate 35S promoter in *P. patens* resulted in the production of C_{22}-PUFA, ADA (0.15±0.04 to 6.97±0.74 mg/l) from endogenous arachidonic acid (ARA). In an attempt to maximize ADA production in transgenic *P. patens* C6, medium optimization by the response surface methodology (RSM), resulted in a significant elevation of ADA (4.48 mg/l) production under optimum conditions, which was 10.6-fold higher, respectively, than production rates in the non-optimization study (0.42 mg/l ADA). Therefore, metabolic engineering with a gene from a marine algae *Pavlova* sp. encoding Δ^5-elongase together with vegetable oil supplementation successfully activated both ADA and ω-3 DPA in *P. patens*. The accumulation of ADA and ω-3 DPA were dramatically increased to 24.3 and 11.7 mg/l, respectively, and accounted for 2.3 and 1.1% of total fatty acids, respectively. To the best of our knowledge, this is the first report on producing ω-3 DPA, docosahexaenoic acid (DHA) precursor, in *P. patens*.

ACKNOWLEDGEMENTS

I would like to express my greatest and sincere gratitude to advisory committee, Dr. Sireewan Kaewsuwan and Assist. Prof. Dr. Akkharawit Kanjana-Opas for their kindness, valuable advises and suggestions, supporting, encouragement, guidance, and criticism throughout of my study program.

I also would like to express my greatest and sincere gratitude to examining committee, Assoc. Prof. Dr. Wanna Choorit and Assist. Prof. Dr. Juraithip Wungsintaweekul for their valuable suggestions.

This work was supported by the Marine Natural Products Research Unit (MNP) from the Faculty of Pharmaceutical Sciences, Prince of Songkla University.

I would like to extend my sincere thank to Department of Pharmacognocy and Pharmaceutical Botany, Faculty of Pharmaceutical Sciences, Prince of Songkla University for providing laboratory facilities.

I would like to thank all staff of Faculty of Pharmaceutical Sciences, Prince of Songkla University for their kindness and help.

Finally, I would like to express my sincere gratitude and appreciation to my dear parent and also the members of my family for their love, pushing up, cheerfulness, devoting and encouragement throughout my life.

Pichit Chodok

CONTENTS

CONTENTS (CONTINUED)

CONTENTS (CONTINUED)

CONTENTS (CONTINUED)

LIST OF TABLES

LIST OF TABLES (CONTINUED)

LIST OF FIGURES

LIST OF FIGURES (CONTINUED)

LIST OF FIGURES (CONTINUED)

LIST OF FIGURES (CONTINUED)

LIST OF ABBREVIATIONS AND SYMBOLS

ABRC	=	Arabidopsis biological resource center
ACC	=	Acetyl-CoA carboxylase
ACP	=	Acyl carrier protein
Act1	=	Rice actin
ATP	=	Adenosine-5'-triphosphate
AD	=	Alzheimer's disease
ADA	=	Adrenic acid
ALA	=	α-Linolenic acid
Am^r	=	Ampicillin resistance
ANOVA	=	Analysis of variance
ARA	=	Arachidonic acid
α	=	Alpha
bp	=	Base pair
by wt	=	By weight
β	=	Beta
CaMV35S	=	Cauliflower mosaic virus 35S
CaPW	=	Calcium protoplast wash
CCD	=	Central composite design
CCMP	=	Center for culture of marine phytoplankton
cDNA	=	Complementary DNA
C.E.	=	Coefficient estimate
CO_2	=	Carbon dioxide
cm	=	Centimeter
Cm^r	=	Chloramphenicol resistance
COP1	=	Constitutively photomorphogenic 1
C_{18}-PUFAs	=	C_{18}-polyunsaturated fatty acids
C_{20}-PUFAs	=	C_{20}-polyunsaturated fatty acids
C_{22}-PUFAs	=	C_{22}-polyunsaturated fatty acids
CSPD	=	Chemi-luminescent substrate
Da	=	Dalton

LIST OF ABBREVIATIONS AND SYMBOLS (CONTINUED)

DCW	=	Dry cell weight
Df	=	Degree of freedom
^{o}C	=	Degree Celsius
^{o}C/min	=	Degree Celsius per minutes
Δ	=	Delta
DHA	=	Docosahexaenoic acid
DHGLA	=	Di-homo-γ-linolenic acid
DNA	=	Deoxyribonucleic acid
dNTPs	=	Deoxynucleotide triphosphates
DO	=	Dissolved oxygen
DTT	=	Dichlorodiphenyltrichloroethane
EDA	=	Eicosadienoic acid
ELO	=	Elongase
EM	=	Early-methionine
EPA	=	Eicosapentaenoic acid
Eqs	=	Equations
ER	=	Endoplasmic reticulum
ETA	=	Eicosatetraenoic acid
ETrA	=	Eicosatrienoic acid
eV	=	Electron volt
FACES	=	Fatty acid chain elongation system
FAD	=	Fatty acid desaturase
FAE	=	Fatty acid elongase
FAMEs	=	Fatty acid methyl esters
FAS	=	Fatty acid synthase
FtsZ	=	Filamentous temperature-sensitive Z
g	=	Gram
GC	=	Gas chromatography
GC-MS	=	Gas chromatography-mass spectrometry

LIST OF ABBREVIATIONS AND SYMBOLS (CONTINUED)

GFP	=	Green fluorescence protein
GLA	=	γ-Linolenic acid
G6PDH	=	Glucose-6-phosphate dehydrogenase
g/g	=	Gram per gram
g/l	=	Gram per liter
HAD	=	Hexadecadienoic acid
h	=	Hours
Hyg^r	=	Hygromycin resistance
IHF	=	Integration host factor
Int	=	Integrase
IPTG	=	Isopropyl thiogalactoside
JA	=	Jasmonic acid
kbp	=	Kilo base pair
Km^r	=	kanamycin resistance
KNO_3	=	Potassium nitrate
l	=	Liter
LA	=	Linoleic acid
LB	=	Luria-bertani
LC-FA	=	Long chain fatty acid
LC-PUFAs	=	Long-chain polyunsaturated fatty acids
LDL	=	Low density lipoproteins
l/min/l	=	liter per minute per liter
liq.N_2	=	Liquid nitrogen
LT	=	Leukotrienes
λ	=	Lamda
Mbp	=	Mega base pair
µg	=	Microgram
µl	=	Microliter
µm	=	Micrometer
µM	=	Micromolar

LIST OF ABBREVIATIONS AND SYMBOLS (CONTINUED)

µg/ml	=	Microgram per milliliter
µmol/m^2/s^1	=	Micromol per metre squared per second
M	=	Molar
m	=	Meter
mg	=	Milligram
mg/dl	=	Micrograms per decilitre
mg/l	=	Milligram per liter
min	=	Minutes
ml	=	Milliliter
ml/l	=	Milliliter per liter
m/z	=	Mass-to-charge ratio
mm	=	Millimeter
mM	=	Millimolar
MMM	=	D-mannitol/$MgCl_2$/MES
mRNA	=	Messenger ribonucleic acid
MS	=	Mean square
MUFA	=	Monounsaturated fatty acid
NADPH	=	Nicotinamide adenine dinucleotide phosphate
ng	=	Nanogram
Nos ter	=	Nos terminator
O_2	=	Oxygen
OA	=	Oleic acid
OPDA	=	(9S, 13S)-12-Oxo-phytodienoic acid
ORF	=	Open reading frame
ω-3 DPA	=	Omega-3 docosapenaenoic acid
ω-6 DPA	=	Omega-6 docosapentaenoic acid
ω-3 LC-PUFAs	=	Omega-3 long-chain polyunsaturated fatty acids
ω	=	Omega

LIST OF ABBREVIATIONS AND SYMBOLS (CONTINUED)

ω-6 LC-PUFAs	=	Omega-6 long-chain polyunsaturated fatty acids
ω-3 PUFA	=	Omega-3 polyunsaturated fatty acid
PA	=	Palmitic acid
pBR322 ori	=	pBR322 origin of replication
PC	=	Phosphatidylcholine
PCR	=	Polymerase chain reaction
PEG	=	Polyethylene-glycol
%	=	Percentage
%TFA	=	Percentage total fatty acid
%w/w	=	Percentage weight by weight
%w/v	=	Percentage weight by volume
PG	=	Prostaglandins
pH	=	The negative logarithm of the concentration of hydrogen ions
PRMB	=	Protoplast regeneration medium-bottom
PRMT	=	Protoplast regeneration medium-top
Pro	=	Promoter
PUFAs	=	Polyunsaturated fatty acids
R^2	=	Coefficient of regression
RNA	=	Ribonucleic acid
RNAi	=	Ribonucleic acid
rpm	=	Round per minutes
RSM	=	Response surface methodology
RT	=	Retention time
RT-PCR	=	Reverse transcriptase-polymerase chain reaction
SDA	=	Stearidonic acid
SDS	=	Sodium dodecyl sulfate

LIST OF ABBREVIATIONS AND SYMBOLS (CONTINUED)

S.E.	=	Standard error
SFA	=	Saturated fatty acid
Spn^r	=	Spectinomycin resistance
Spn pro	=	Spectinomycin promoter
SS	=	Sum of square
SSC	=	Saline sodium citrate
TAG	=	Triacylglycerol
Ter	=	Terminator
TF	=	Tissue factor
TX	=	Thromboxanes
U/µl	=	Unit per microliter
UV	=	Ultraviolet
v/v	=	Volume by volume
WT	=	Wild type
w/v	=	Weight by volume
w/w	=	Weight by weight
X-Gal	=	5-Bromo-4-chloro-3-indolyl-beta-D-galactopyranoside
Xis	=	Excisionase

CHAPTER 1

INTRODUCTION

1.1 General introduction

Long-chain (C≥20) polyunsaturated fatty acids (LC-PUFAs) including the omega-3 (ω-3) eicosapentaenoic acid (EPA, 20:5 $\Delta^{5,8,11,14,17}$) and docosahexaenoic acid (DHA, 22:6 $\Delta^{4,7,10,13,16,19}$) are essential to human health and development. Several studies have indicated that deficiencies in these fatty acids increase the risk of cardiovascular disease (vonSchacky, 2006), hypertension (Ueshima *et al*., 2007), inflammatory diseases, rheumatoid arthritis (Simopoulos, 2002) and neuropsychiatric disorders including dementia and depression (Freeman *et al*., 2006; Schaefer *et al*., 2006). DHA is an ω-3 PUFA found in fish and certain algae, makes up 60% of the fatty acid in human neuronal cell membranes, and is particularly concentrated in synaptic membranes (Bazan and Scott, 1990) and in myelin sheaths (Ansari and Shoeman, 1990). DHA is essential for prenatal brain development as well as normal healthy brain functioning. Supplemental DHA has also been shown to have a protective effect against cognitive decline or Alzheimer's disease (AD) which may involve triacylglycerols (TAGs) lowering (Kelley *et al*., 2007; Cunnane *et al*., 2009). Furthermore, DHA has strong medical benefit implications since it has been positively linked to the prevention of numerous human afflictions including cancer and heart disease (Stilwell and Wassall, 2003).

Humans, particularly infants, are unable to synthesize DHA and other LC-PUFAs to any great extent and must therefore obtain them through their diet. The human consumption of LC-PUFAs is steadily increasing, but the production of fish oil, the main source of LC-PUFAs for human consumption, is declining (Takeuchi, 2001). Generally, the cost of the commercial processing, refining, and stabilizing the fish oils is very high, and the decline in production due to over-fishing continues to drive up the cost of fish oils (Sargent and Tacon, 1999). The recent finding of toxic compounds in fish oil has further raised safety concerns on the consumption of fish oils (Guallar *et al*., 2002).

Increasing demand has consequently raised an interest in obtaining these PUFAs from alternative sources that are more economical and sustainable. Plant oils could be a sustainable alternative source of fatty acids. However, plants do not synthesize LC-PUFAs owing to the lack of Δ^6- and Δ^5-position-specific desaturase and the absence of an elongase. Plant oils are therefore rich in C_{18}-PUFAs, linoleic acid (LA, 18:2 $\Delta^{9,12}$), α-linolenic acid (ALA, 18:3 $\Delta^{9,12,15}$) and γ-linolenic acid (GLA, 18:3 $\Delta^{6,9,12}$), but not in LC-PUFAs, EPA and DHA (Wallis *et al*., 2002). An attractive possibility is to genetically engineer plants to produce LC-PUFAs.

In algae, DHA can be synthesized from EPA in a two-step process that involves: (a) the elongation of EPA by Δ^5-elongase to generate ω-3 docosapenaenoic acid (ω-3 DPA, $\Delta^{7,10,13,16,19}$): and (b) the desaturation of ω-3 DPA by a Δ^4-desaturase to generate DHA (Pereira *et al*., 2004b). A number of elongases have been identified from mammals, zebra fish, marine and fresh water teleost fish that can recognize and elongate multiple chain-length PUFAs, such as C_{18}-, C_{20}- and C_{22}-PUFAs (Leonard *et al*., 2000; Agaba *et al*., 2004; Agaba *et al*., 2006). Recently, elongases specific for C_{20}-PUFAs have been identified from algae and demonstrated to function in the production of DHA (Meyer *et al*., 2004; Pereira *et al*., 2004b).

In addition, the moss *Physcomitrella patens* produces several PUFAs, especially arachidonic acid (ARA, 20:4 $\Delta^{5,8,11,14}$) and EPA (Kaewsuwan *et al*., 2006) which are C_{20}-PUFAs required for the synthesis of the LC-PUFAs, adrenic acid (ADA, $\Delta^{7,10,13,16}$) and ω-3 DPA, respectively by Δ^5-elongase (Pereira *et al*., 2004b). Although ADA is a minor fatty acid in the brain, it is suggested to be an important component for myelination of neural tissue (O'Brien and Sampson, 1965) and also serves as an eicosanoid precursor in tissue (VanRollins *et al*., 1985). Moreover, ω-3 DPA is a precursor of DHA which has attracted much interest due to its pharmaceutical potential mentioned above.

Development of transgenic oil plants capable of producing C_{22}-PUFAs, ADA and ω-3 DPA is therefore an attractive route to improve commercial-scale DHA production. In this study the primary step for activation of C_{22}-PUFAs, ADA and ω-3 DPA, from C_{20}-PUFAs, ARA and EPA, respectively in *P. patens* is carried out by heterologous expression of the marine algae *Pavlova* sp. Δ^5-elongase and vegetable oil supplementation.

1.2 Objectives

1.2.1 To clone the algae *Pavlova* sp. Δ^5-elongase gene

1.2.2 To construct the plant expression vector and obtain the stable transgenic *P. patens* producing C_{22}-PUFAs, ω-6 ADA and ω-3 DPA

1.2.3 To determine the polyunsaturated fatty acid products of *Pavlova* sp. Δ^5-elongase gene in *P. patens*

1.2.4 To optimize the medium composition for high production of ω-6 ADA and ω-3 DPA in transgenic *P. patens*

CHAPTER 2

LITERATURE REVIEW

2.1 *Physcomitrella patens* (Hedw.) B.S.G.

The moss *Physcomitrella patens*, non-vascular and multicellular organism, is a monoecious land plant belonging to the Funariaceae (Bryophyte). Both sexual organs, male (antheridia) and female (archegonia) are produced on the same gametophore (Cove, 2005; Frank *et al*, 2005). *P. patens* is widely distributed in temporal zones. Its isolate is available from Japan, Australia, Africa, North America and Europe (Cove, 2005; McDaniel *et al*., 2010). It's an ephemeral moss that develops in late summer from overwintered spores and grows on banks of ponds, lakes and rivers that have been exposed by lowering water levels (Cove, 2005). However, it develops sexual organs in the fall, triggered by lowered temperatures and shortened days (Hohe *et al*., 2002a). Recently, *P. patens* the first bryophyte and the fourth land plant genome of which has been completely sequenced (Rensing *et al*., 2008) after *Arabidopsis*, rice and poplar (Reski, 2005). The haploid genome size of *P. patens* is estimated to be around 511 Mbp (Schween *et al*., 2003) distributed among 27 chromosomes (Reski *et al*., 1994), which is about three fold bigger than the *Arabidopsis* genome (Cho *et al*., 2007).

Interestingly, *P. patens* was originally chosen as a model system to study a variety of plant gene functions (Table 2.1). Among them *P. patens* emerged as a powerful model species for molecular genetics due to (Prigge and Bezanilla, 2010): First, this moss has a dominant haploid gametophyte in its life cycle and a very high frequency of integrate transformed DNA molecules by homologous recombination, enabling gene targeting studies to be performed to analyze gene function (Schaefer and Zryd, 1997; Schaefer, 2001; Cove, 2005; Kamisugi *et al*., 2006). Second, *P. patens* is easily propagated vegetatively. At any developmental stage, if *P. patens* tissues, such as protonemata, gametophores or sporophytes, are mechanically disrupted, then the cells in the disrupted area change into chloronemal apical cells producing a new filamentous network. As a consequence, mutant strains with a wide range of developmental defects can be maintained indefinitely. Additionally, tissues

Table 2.1 Various gene functional studies in *P. patens*.

Functional characterization	**Gene**	**Reference**
Auxin homeostasis	GH3-like proteins	Bierfreund *et al*., (2004); Ludwig-Muller *et al*., (2009)
Cellulose biosynthesis	Cellulose synthase	Roberts and Bushoven, (2007); Wise *et al*., (2011)
Chloroplast division, chloroplast shaping, cell patterning, plant development and gravity sensing	Filamentous temperature-sensitive Z (ftsZ)	Gremillon *et al*., (2007); Suppanz *et al*., (2007); Martin *et al*., (2009a); Martin *et al*., (2009b)
Fatty acid biosynthesis	Δ^6-desaturase	Girke *et al*., (1998)
	Δ^6-elongase	Zank *et al*., (2002)
	Δ^5-desaturase	Kaewsuwan *et al*., (2006)
Favonoid biosynthesis	Chalcone synthase	Jiang *et al*., (2006); Koduri *et al*., (2010)
	C9-aldehydes	Stumpe *et al*., (2006)
Hexose metabolism	Hexokinases	Nilsson *et al*., (2011)
Jasmonic acid (JA) and (9S, 13S)-12-oxo-phytodienoic acid (*cis*-(+)-OPDA) biosynthesis	Allene oxide cyclases	Stumpe *et al*., (2010)
N-glycosylation	*N*-acetylglucosaminyl-transferase I, α1,3-fucosyl-transferase and β1,2-xylosyltransferase	Koprivova *et al*., (2003)
Sulfate assimilation	Adenosine 5’-phosphosulfate reductase	Koprivova *et al*., (2002)
	Sulfate reductase	Wiedemann *et al*., (2010)

can be disrupted by cell wall-digesting enzymes, producing a suspension of single cells known as protoplasts. Given osmotically controlled medium, protoplasts rebuild their cell walls and then regenerate into protonemal tissue. Third, transformation of DNA is routine in *P. patens*. It is generally performed by polyethylene-glycol (PEG)-mediated transformation of protoplasts (Schaefer *et al*., 1991). Stable transformants, with the transformed DNA integrated into the genome, can be selected within 4-6 weeks, which is remarkably fast compared with any other plant system. DNA can integrate by homologous recombination or randomly if the transformed DNA lacks any sequences homologous to the genome. However, the efficiency of generating non-targeted stable transformants is one-tenth of that achieved when mediated by homologous recombination (Schaefer, 2001).

2.1.1 The life cycle of *P. patens* (Cove, 2000; Frank *et al*., 2005; Prigge and Bezanilla, 2010)

The life cycle of *P. patens* is characterized by an alternation of two generations, the haploid gametophyte and the diploid sporophyte (Figure 2.1). However, this moss has a dominant haploid gametophyte in its life cycle. In the sporophyte stage, a large number of haploid spores of *P. patens* are produced by meiosis from the diploid generation. *P. patens* germinates from a haploid spore, producing a linear array of cells that branch and generate a filamentous, two-dimensional, network known as protonemal tissue. The stem cell for this network is at the apex of each filament, and each filament grows by polarized growth, or tip growth, secreting necessary cell wall components at the apex. The first cell type to emerge from the spore is the chloronema cells. These cells can be easily recognized as they contain 50-100 fully developed chloroplasts, and cell plates that form between dividing cells are transverse to the axis of the cell. Subsequent tissue differentiation is dependent on phytohormone levels (Decker *et al*., 2006).

As the plant continues to grow, apical cells transition from chloronemata to caulonemata in an auxin-dependent manner (Ashton *et al*., 1979). Caulonemata are faster growing cells that contain fewer less-developed plastids and cell plates that are positioned at an oblique angle to the long axis of the cell. The branching of protonemal tissue occurs at subapical cells, producing another

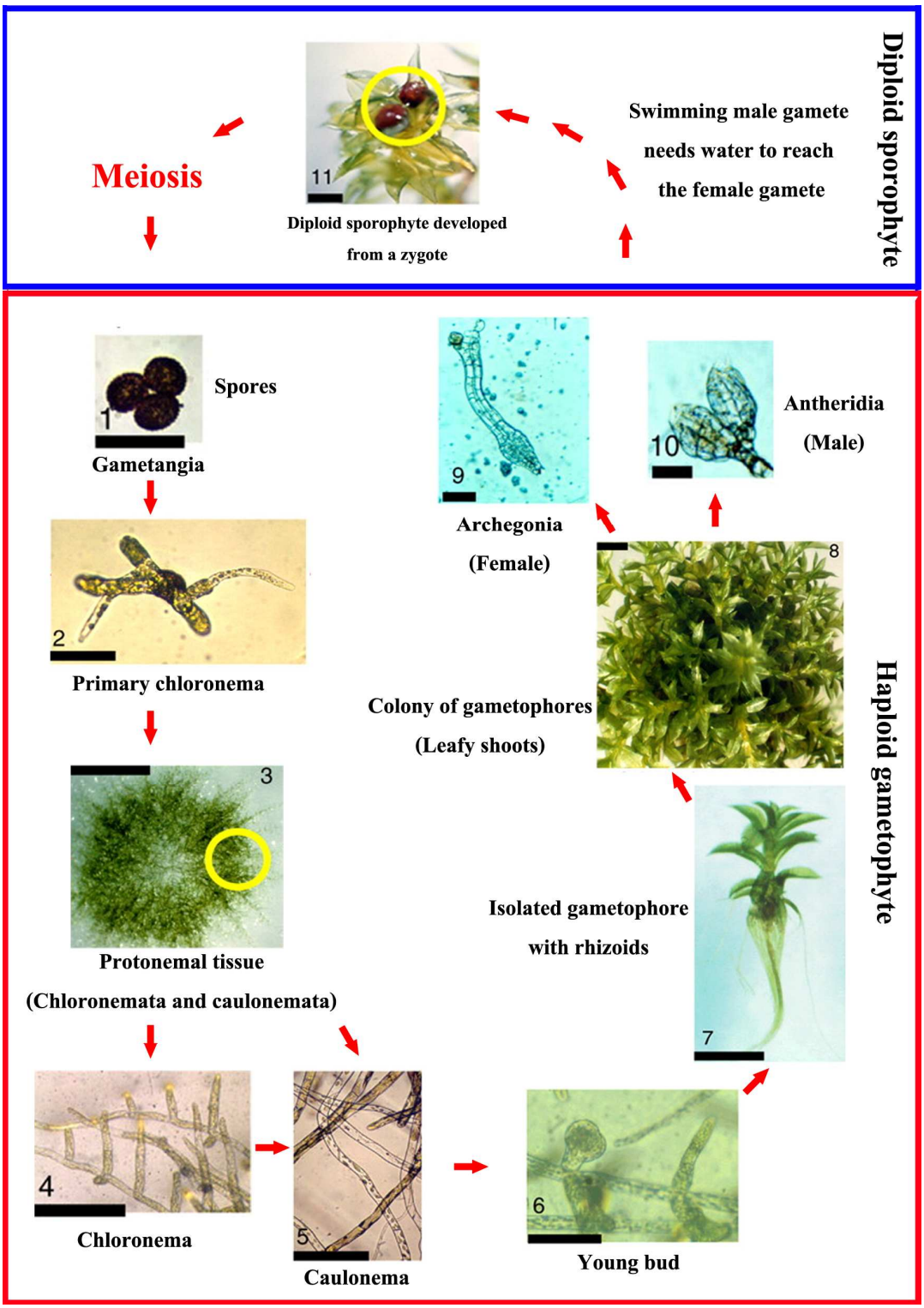

Figure 2.1 The life cycle of *P. patens* (modified from Cove, 1992). Scale of the bars: 50 µm for pictures 1, 2, 9 and 10; 0.5 mm for pictures 4, 5, 6 and 7; 1.0 mm for pictures 8 and 11; 1.0 cm for picture 3.

chloronemal cell. Further development proceeds by the formation of buds which are initially composed of a three-faced apical cell (a transition from two-dimensional filament growth to three-dimensional shoot development). This bud forms the initial meristem for development of the leafy adult gametophyte and then the formation of the sexual organs at the top of a single gametophore. Male gametes, known as spermatozoids are produced in the antheridia and swim to fertilize the female gametes (oogonia or egg cells) within an archegonium.

After fertilization, the zygote develops into the diploid generation, the sporophyte, which is composed of a short seta topped with a spore capsule. Within the capsule, meiosis occurs and at maturity, about 4000 haploid spores are produced and released into the environment (Engel, 1968). The life cycle of *P. patens* can be completed in culture in about 8-12 weeks (Figure 2.1).

2.1.2 Culture conditions of *P. patens* (Cove, 2000; Frank *et al*., 2005)

The nutritional requirements of *P. patens* are simple. It can be cultivated either on solid or in liquid media containing only inorganic salts (Figure 2.2a and 2.2b). It is routinely grown on agar-gelled medium in Petri dishes or in liquid medium in Erlenmeyer flask as well as bioreactor (Figure 2.2c).

Upon cultivation on solid medium, the plant undergoes normal developmental progression resulting in the formation of leafy gametophores. Starting from protonema tissue, gametophore development is initiated by the formation of bud consisting of a three-faced cell. Plant tissue cultures of gametophores can be maintained by sub-culturing the gametophores at monthly intervals.

Liquid cultures can be started either from protonemal tissue or gametophores, by inoculating liquid medium with the respective tissue. However, *P. patens* also shown a high capacity for regeneration and therefore mechanical disruption of the tissue leads to predominant growth of protonemal tissue in liquid medium, providing a routine method for sub-culturing (Grimsley *et al*., 1977). Liquid cultures can be maintained in Erlenmeyer flask in small volumes or plants can be grown in semi-continuous bioreactor cultures for large-scale production of moss material (Hohe and Reski, 2002). At any stage, moss material from liquid cultures can be used to set up cultures on solid medium. Protonema cultures may also be

maintained by inoculating protonemal filaments onto cellophane sheets overlying solid medium. For routine use of *P. patens*, it is recommended that plant cultures are kept on solid medium as a backup system or spores are kept which can be used to initiate new culture lines.

In addition, medium-term storage of *P. patens* can be achieved by cultivating plant on solid medium at low temperatures (4-15^{o}C) and low light conditions (20 µmol/m^{2}/s^{1}). Long-term storage of *P. patens* was shown to be reliably working via cryopreservation (Schulte and Reski, 2004).

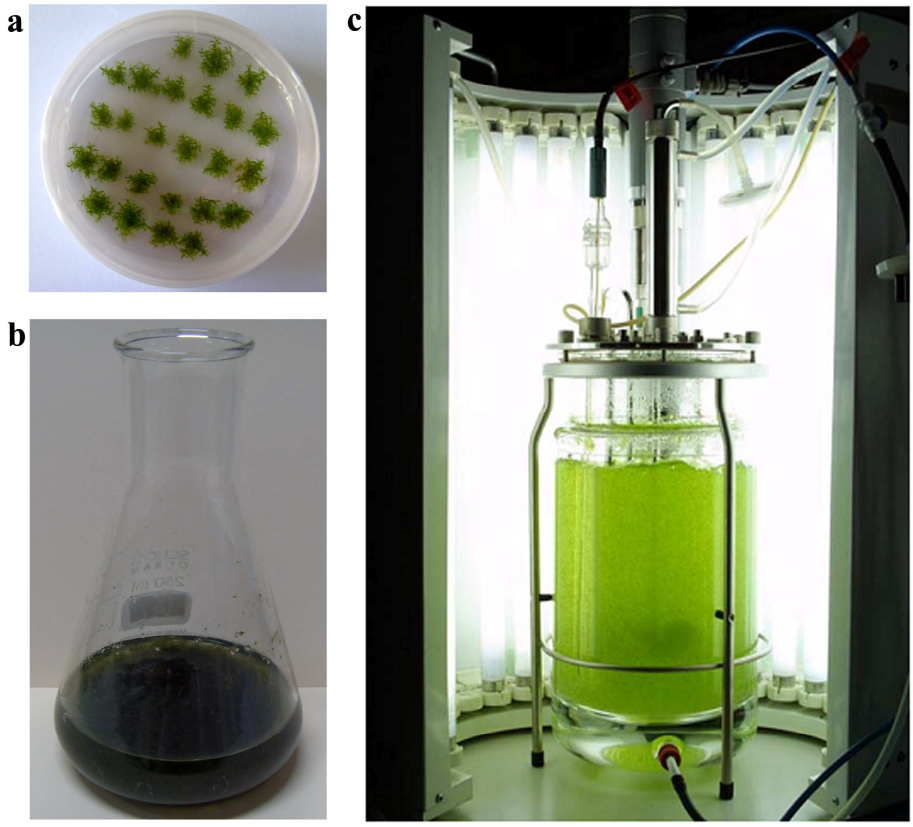

Figure 2.2 *P. patens* is routinely grown on agar-gelled medium in Petri dishes (a) or in liquid medium in Erlenmeyer flask (b) as well as bioreactor (c).

2.1.3 Cultivation of *P. patens* in Petri dishes and Erlenmeyer flask for small-scale production (Frank *et al*., 2005)

P. patens can be grown on agar-containing medium in Petri dishes on basal mineral media devoid of any organic compounds (Figure 2.2a). The media used by different researcher groups only vary in minor constituents. Two media which are most commonly used for standard growth of *P. patens* are BCD medium (Ashton and Cove, 1977) and Knop medium (Reski and Abel, 1985). Solid cultures may be started with inocula from young protonemal tissue or any gametophytic tissue. This obtained tissue can be disrupted with a sterilized blender and inoculated the tissue homogenate into fresh medium. Growth into the agar medium can be prevented by overlaying the medium with cellophane, simplifying the subsequent harvesting of tissue and then the plants are cultured in a growth chamber at 25±1^{o}C under a 16/8 h light/dark photoperiod with a light intensity of 50-70 μmol/m^2/s^1. Tissue obtained in this way and harvested 1 week after inoculation is composed a large number of chloronemal filaments and is excellent moss material for protoplasts, DNA, RNA or proteins isolation. In addition, maintenance of the plant is achieved by monthly sub-culturing of the plant tissue onto fresh medium.

For small-scale propagation of moss material, *P. patens* can be cultivated in liquid medium in Erlenmeyer flask (Figure 2.2b). When initiating a primary liquid culture, a small flask is inoculated with two or three gametophores of *P. patens*, followed by disruption of the plant material using a suitable blender. To promote fast growth of the moss material, 3% (w/v) sucrose can be added (Chodok *et al*., 2010). Cultivation of plant in the presence of sucrose for long time periods should be avoided as the cultures show deviating differentiation compared to growth in basal mineral medium. At regular disintegration of the protonemal filaments, these cultures can be kept as long-term suspension cultures.

2.1.4 Cultivation of *P. patens* in a bioreactor for large-scale production (Frank *et al*., 2005)

P. patens bioreactor cultures are useful for scale-up and to establish highly standardized growth conditions, as environmental parameters may affect growth kinetics, gene expression patterns and differentiation. The cultivation of *P.*

patens in bioreactors has been reported previously (Reutter and Reski, 1996; Cove *et al*., 1997). For long-term cultivation of *P. patens* on a laboratory scale, a semi-continuous bioreactor has also been established for three reasons (Hohe *et al*., 2002a) (Figure 2.2c): (1) Protonema suspensions are used for protoplast isolation for large scale transformation (Hohe *et al*., 2001; Hohe and Reski, 2002a). (2) Bioreactor cultures represent a contained environment for the production of heterologous compounds (Reutter and Reski, 1996) and (3) Bioreactor culture offers a unique possibility for studying the effect of environmental conditions on growth and development (Hohe *et al*., 2002b).

Standard Knop medium is appropriate for the growth of *P. patens* in bioreactors. The cultures are grown in stirred glass tank bioreactors (Figure 2.3c) with working volumes up to 12 l, equipped with a marine impeller. The cultures are aerated and growth at 25^{o}C under a photoperiod regime of 16/8 h light/dark cycle with light supplied at the surface of the vessels. The cultures can be run semi-continuously, i.e., the suspension has to be harvested and replaced by an equal amount of fresh medium daily. The density of the cultures is controlled by determining the dry weight. For long-term cultivation of *P. patens* suspension cultures, the cell density in the bioreactor should be maintained between approximately 150 and 200 mg/l dry cell weight. The growth rate of the suspension cultures can be increased by aeration with air that is enriched with CO_2 (Hohe *et al*., 2002a). Under these conditions, the growth rate can be doubled but, under non-controlled pH conditions, the pH of the culture may decrease markedly. The growth rate of liquid cultures is not affected within a pH ranging from 4.5 to 7.0, while the development of protonemal filaments is influenced by other pH value. Generally, cultures grown at low pH mainly consist of chloronema filaments, while increased pH values favor caulonema development (Hohe *et al*., 2002a).

2.2 Long chain-polyunsaturated fatty acids (LC-PUFAs)

2.2.1 Definition and classification

LC-PUFAs have a carbon backbone of at least 20 carbons in length and contain multiple double-bond desaturations. LC-PUFAs can be grouped into

either an omega-3(ω-3) or an ω-6 category based on the position of the first double bond from the methyl, or ω, fatty acid terminus (Table 2.2) (Petrie and Singh, 2011).

2.2.2 Nomenclature

2.2.2.1 Trivial (common) nomenclature

A PUFA containing *m* carbon atoms and *n* double bonds, in which the final double bond is located X carbon atom from the methyl end of the fatty acid chain is named as Cm ω-x PUFA or *m*:*n* (ω-x) PUFA.

2.2.2.2 Systematic nomenclature

A PUFA containing *m* carbon atoms and *n* double bonds, with superscripts aZ, bZ, etc. indicating the positions of the double bonds (carbon atoms are numbered from the carboxyl end), Z (*cis*) configuration will be named as $m{:}n\Delta^{aZ,bZ,\ldots,dZ:}$.

As an example, 22:4 $\Delta^{7,10,13,16}$ refers to the long-chain ω-6 ADA which contains 22 carbons and four double bonds, or desaturations, at the 7, 10, 13 and 16 carbon positions from the carboxyl terminus. The structure of LC-PUFAs, their trivial (common) and systematic nomenclatures are shown in Table 2.2.

2.3 LC-PUFAs sources

2.3.1 Commercial sources of LC-PUFAs

Currently, the richest sources of ω-3-LC-PUFAs, such as EPA and DHA are oils extracted from marine fish such as mackerel, herring, salmon and sardines. These fish obtain their LC-PUFAs by consuming the LC-PUFA-rich microalgae and phytoplankton. Commercially, fish oils are available in the form of gelatin capsules or oily preparations, which contain 20% to 30% EPA and DHA (Trautwein, 2001) (Table 2.3).

However, the production of ω-3 LC-PUFA from fish oil is hindered by limitation such as the steady declining fish population in oceans, taste, offensive odor, stability problems and high purification cost. In contrast, marine microalgae are the primary producer of ω-3 LC-PUFA in the ocean environment and marine fish usually

Table 2.2 List of ω-3 and ω-6 LC-PUFAs.

Common name	**Systematic name**	**Chemical structure**
ω-3 LC-PUFAs Eicosatetraenoic acid (ETA)	Δ^8, Δ^{11}, Δ^{14}, Δ^{17}- Eicosatetraenoic acid	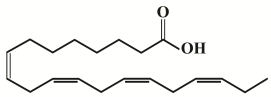
Eicosapentaenoic acid (EPA)	Δ^5, Δ^8, Δ^{11}, Δ^{14}, Δ^{17}- Eicosapentaenoic acid	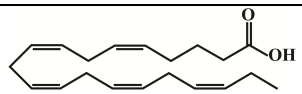
ω-3 docosapentaenoic acid (ω-3 DPA)	Δ^7, Δ^{10}, Δ^{13}, Δ^{16}, Δ^{19}- Docosapentaenoic acid	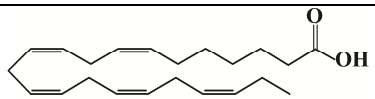
Docosahexaenoic acid (DHA)	Δ^4, Δ^7, Δ^{10}, Δ^{13}, Δ^{16}, Δ^{19}- Docosahexaenoic acid	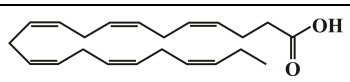
ω-6 LC-PUFAs Di-homo-γ-linolenic acid (DHGLA)	Δ^8, Δ^{11}, Δ^{14}- Eicosatrienoic acid	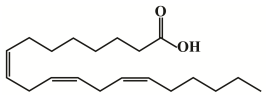
Arachidonic acid (ARA)	Δ^5, Δ^8, Δ^{11}, Δ^{14}- Eicosatetraenoic acid	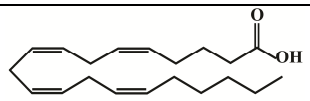
Adrenic acid (ADA)	Δ^7, Δ^{10}, Δ^{13}, Δ^{16}- Docosatetraenoic acid	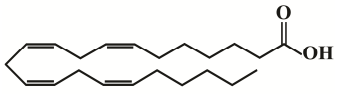
ω-6 docosapentaenoic acid (ω-6 DPA)	Δ^4, Δ^7, Δ^{10}, Δ^{13}, Δ^{16}- Docosapentaenoic acid	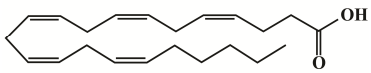

Table 2.3 Commercial sources of ω-3 and ω-6 LC-PUFAs.

LC-PUFA	**Source**	**Product**	**Company**
ARA	Single-cell oil	ROPUFA	Hoffmann-La Roche Ltd, Switzerland
	Fermentation *M. alpina*	ARASCO	Gist-brocades, Holland Martek Biosciences Co.
EPA	Fish oil	Incromega	Croda Oleochemicals, England
		Hi-EPA Oil	Scotia Lipids, Scotland
		Dry n-3®	BASF, Denmark
		EPAX 0626 TG	PRONOVA, Norway
DHA	Tuna	MilkarraTM	Clover Co., Australia
	Fish oil	ROPUFA	Hoffmann-La Roche Ltd., Switzerland
	Fish oil	Incromega	Croda Oleochemicals, England
		Hi-DHA Oil	Scotia Lipids, Scotland
	Crypthecodinium cohnii	DHASCO	Martek Biosciences Co.
	Fish oil	Dry n-3®	BASF, Denmark
	Fish oil	EPAX 0626 TG	PRONOVA, Norway

Source: Alonso and Maroto (2000).

obtain EPA via bioaccumulation in the food chain. EPA and DHA oils can also be obtained from single cell organisms like microalgae and fungi. Diatoms such as *Nitzschia*, are good producers of EPA and dinoflagellates such as *Crypthecodinium cohnii* are used for commercial production of DHA (Barclay *et al*., 1994).

Recently, only a few microalgae species have demonstrated industrial production of ω-3 LC-PUFA due to the low specific growth rate and low cell density of the microalgae grown under conventional photoautotrophic process. This mode is often limited by insufficiency of light caused by mutual shading of cells (Chen, 1996). Marine protists such as the *Thraustochytrids* can also make large amounts of DHA and are a potential source of DHA for human consumption (Barclay *et al*., 1994; Bajpai *et al*., 1991b). While ω-6-LC-PUFAs such as ARA can be found animal viscera, particularly porcine liver, adrenal glands and egg yolk (Gill and Valivety, 1997). However, the ARA yield obtained is very low, and therefore difficult to industrialize. The production of ARA by microorganisms has therefore been gaining more interest. ARA is commercially produced by fermentation of oleaginous fungi such as *Mortierella alpina*, which contains approximately 40% (by wt.) of ARA in their oils (Kendrick and Ratledge, 1992; Streekstra, 1997).

2.3.2 Alternative sources of LC-PUFAs

The increasing demand has raised the interest in obtaining these LC-PUFAs from alternate sources that are more economical and sustainable. Some microorganisms, including bacteria, fungi, and microalgae, are considered alternative sources of LC-PUFAs (Table 2.4).

2.4 Biosynthesis of LC-PUFAs

In aerobic pathway, initial fatty acid biosynthesis in plants is catalyzed by multisubunit fatty acid synthase (FAS) complexes that are present in the plastids. The final product of FAS is palmitoyl (16:0)-acyl carrier protein (ACP). Most of this palmitoyl-ACP is then elongated to stearoyl (18:0)-ACP by successive additions of two carbon atoms from acetyl-CoA. Still in the plastid, most of stearoyl-ACP is desaturated by the soluble plastidial stearoyl-ACP Δ^9 desaturase to oleoyl (18:1 Δ^9)-ACP, which is the main product of the plastidial fatty acid synthesis and is exported

Table 2.4 Alternative sources of ω-3 and ω-6 LC-PUFAs.

Microorganism	LC-PUFA	Reference
Bacteria		
Antarctic bacteria strain 651	ARA, EPA	Nichols *et al*., (1997)
Aureispira maritima TISTR1715	ARA	Saelao *et al*., (2011)
Schizochytrium limacinum OUC88	DHA	Song *et al*., (2007)
Schizochytrium sp. S31	DHA	Wu and Lin, (2003)
Fungi		
Achlya sp. ma-2801	ARA	Aki *et al*., (1998)
Mortierella alpina	ARA	Zhu *et al*., (2003)
M. alpina	ARA	Zhu *et al*., (2006)
M. alpina ATCC32222	ARA, EPA, DHA	Jang *et al*., (2005)
M. alpina I_{49}-N_{18}	ARA	Yuan *et al*., (2002)
M. alpina M_{18}	ARA	Yu *et al*., (2003)
M. alpina ME-1	ARA	Jin *et al*., (2009)
M. alpina 1S-4	ARA	Higashiyama *et al*., (1998)
Pythium irregulare ATCC1095	ARA, EPA	Cheng *et al*., (1999)
P. ultimum strain #144	ARA, EPA	Gandhi and Weet, (1991)
Microalgae		
Chromonas sp.	EPA, DHA	Renaud *et al*., (1999)
Cryptomonas sp.	EPA, DHA	Yongmanitchai and Ward, (1989)
Isochrysis galbana	EPA, DHA	Molina *et al*., (1992)
Monodus subterraneus	EPA	Qiang *et al*., (1997)
Rhodomonas sp.	EPA, DHA	Renaud *et al*., (1999)
Diatom		
Amphora coffeaformis	ARA, EPA, DHA	Renaud *et al*., (1999)
Chaetoceros sp.	ARA, EPA, DHA	Renaud *et al*., (1999)
Fragilaria pinnata	ARA, EPA, DHA	Renaud *et al*., (1999)
Navicula saprophila	ARA, EPA	Kitano *et al*., (1997)
Nitzschia laevis	EPA	Wen and Chen, (2000)
Phaeodactylum tricornutum	EPA	Yongmanitchai and Ward, (1991)
Non-seed lower plant		
Marchantia polymorpha	ARA, EPA	Shinmen *et al*., (1991)
Physcomitrella patens	ARA, EPA	Kaewsuwan *et al*., (2006)

into the cytosol for oil synthesis in the endoplasmic reticulum (ER) (Browse and Somerville, 1991). Subsequently, oleic acid (OA, 18:1 Δ^9) is then incorporated into phosphatidylcholine (PC) by the de novo pathway (Kennedy, 1961) or an acyl exchange mechanism known as "acyl editing" (Bates *et al*., 2009).

OA is first Δ^{12}-fatty acid desaturated to produce LA, which is in turn Δ^{15}-desaturated to produce ALA (Figure 2.3). Essential dietary fatty acids, LA and ALA are the respective substrates for the ω-6 and ω-3 LC-PUFA pathways, with the first committed step in both pathways being a Δ^6-desaturation, which introduces a double bond between carbons sixth and seventh of LA and ALA, to produce GLA and stearidonic acid (SDA), respectively. All of these C_{18}-fatty acids can be found naturally in angiosperms, although GLA and SDA are relatively rare and efforts have been made to engineer these short chain-PUFAs in to oilseed species. The C_{18}-fatty acids GLA and SDA are further Δ^6-elongated to the long-chain (C_{20}) fatty acids DHGLA and ETA, respectively. This elongation normally consists of four consecutive enzymatic steps (condensation, ketoreduction, dehydration and enoylreduction), although the transgenic introduction of the condensing enzyme or 'elongase' is sufficient to confer specificity to the entire elongation with the other elongation reaction components being supplied by the host organism. The products of the Δ^6-elongation, DHGLA and ETA, are then Δ^5-desaturated to ARA and EPA, respectively. ARA marks the end of the traditionally represented ω-6 LC-PUFA pathway, although ARA can be Δ^5-elongated to docosatetraenoic acid or adrenic acid (ADA) which can finally be Δ^4-desaturated to ω-6 docosapentaenoic acid (ω-6 DPA). Similarly, EPA can be Δ^5-elongated to ω-3 DPA which is then Δ^4-desaturated to produce DHA. This Δ^6-pathway is the most commonly found aerobic pathway, however, an alternative Δ^8-pathway also exists. In this pathway, LA and ALA are Δ^9-elongated to eicosadienoic acid (EDA) and eicosatrienoic acid (ETrA), respectively, which are then Δ^8-desaturated to DHGLA and ETA. At this point, the Δ^6- and Δ^8-pathways merge and subsequent desaturations and elongations continue as described above (Petrie and Singh, 2011). However, all these enzymes have been isolated from various organisms (Table 2.5).

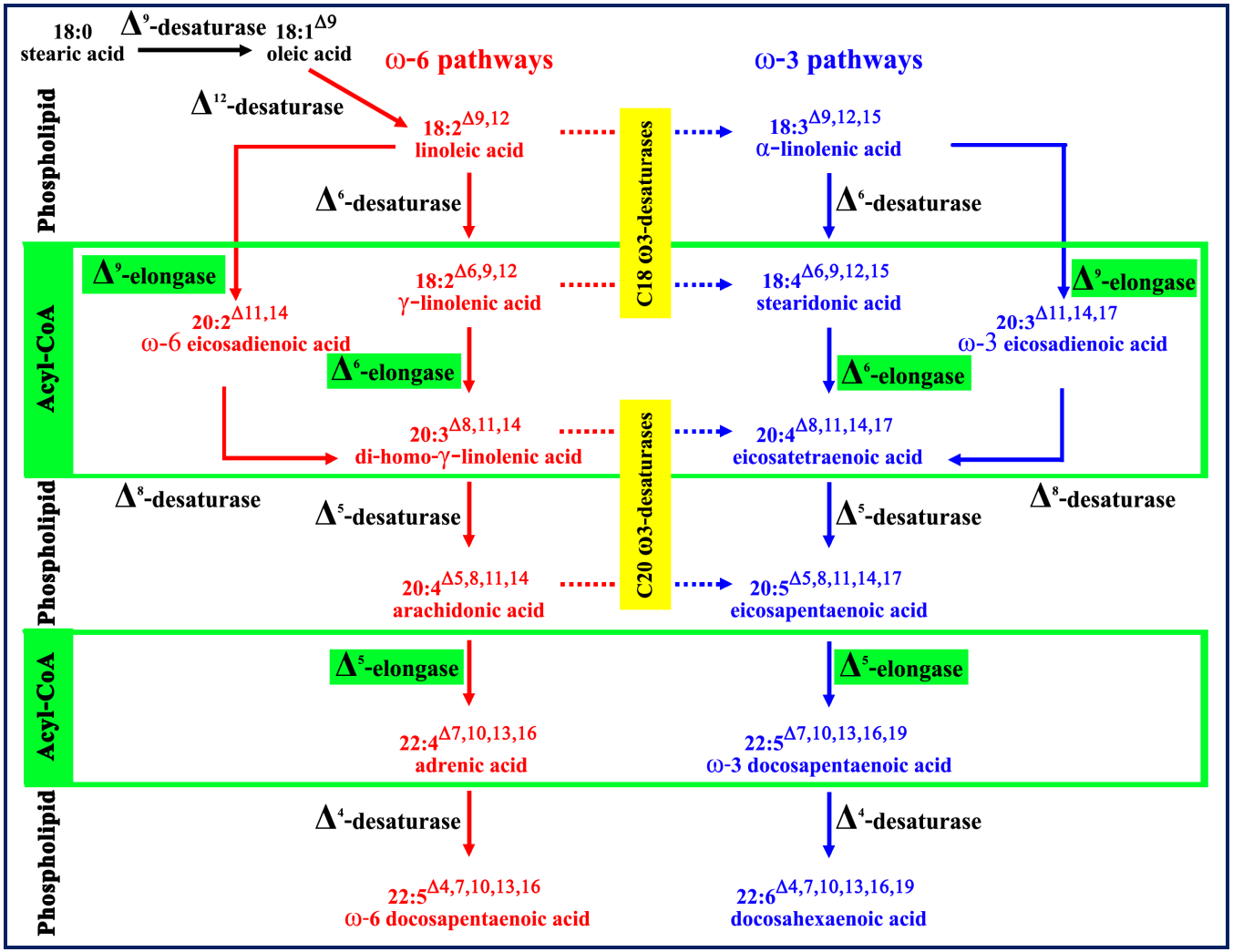

Figure 2.3 A simplified scheme of LC-PUFAs biosynthesis pathways in lower eukaryotes (modified from Truksa *et al*., 2006).

Table 2.5 Functional PUFA biosynthesizing enzymes and their sources.

Enzyme	Type of organism	Specie	Substrate	Product	Reference
Δ^{12}-fatty acid desaturase	Fungi	*Mucor rouxii, Rhizopus arrhizus*	OA	LA	Passorn *et al*., (1999); Wei *et al*., (2004)
	Diatom	*Phaeodactylum tricornutum*	PA, OA	HAD, LA	Domergue *et al*., (2003)
	Plant	*Camelina sativa, Gossypium hirsutum, Olea europaea*	OA	LA	Kang *et al*., (2011); Zhang *et al*., (2009); Hernandez *et al*., (2005)
		Glycin max, G. hirsutum	PA, OA	HDA, LA	Li *et al*., (2007); Pirtle *et al*., (2001)
	Animal	*Caenorhabditis elegans*	PA, OA	HDA, LA	Peyou-Ndi *et al*., (2000)
	Insect	*Acheta domesticus, Tribolium castaneum*	PA, OA	HDA, LA	Zhou *et al*., (2008)
Δ^{6}-desaturase	Fungi	*Conidiobolus obscures, M. rouxii, R. nigricans*	LA, ALA	GLA, SDA	Tan *et al*., (2011); Laoteng *et al*., (2005); Na-Ranong *et al*., (2005); Lu *et al*., (2009)
	Diatom	*Glossomastix chrysoplasta, Parietochloris incise, P. tricornutum, Thalassiosira pseudonana*	LA, ALA	GLA, SDA	Hsiao *et al*., (2007); Iskandarov *et al*., (2010); Domergue *et al*., (2002); Tonon *et al*., (2005)
	Plant	*Marchantia polymorpha, Physcomitrella patens, Ribes nigrum*	LA, ALA	GLA, SDA	Kajikawa *et al*., (2004); Girk *et al*., (1998); Song *et al*., (2010)
	Fish	*Common carp, Gilthead sea bream, Rainbow trout, Turbot*	LA, ALA	GLA, SDA	Zheng *et al*., (2004)

Table 2.5 Functional PUFA biosynthesizing enzymes and their sources (Continued).

Enzyme	Type of organism	Specie	Substrate	Product	Reference
Δ^6-elongase	Fungi	*C. obscures, Mortierella alpina*	GLA, SDA	DHGLA, ETA	Tan *et al*., (2011); Parker-Barnes *et al*., (2000)
	Plant	*M. polymorpha, P. patens*	GLA, SDA	DHGLA, ETA	Kajikawa *et al*., (2004); Zank *et al*., (2002)
	Animal	*C. elegans*	GLA, SDA	DHGLA, ETA	Beaudoin *et al*., (2000)
Δ^5-desaturase	Algae	*Pavlova salina*	DHGLA, ETA	ARA, EPA	Zhou *et al*., (2007)
	Diatom	*P. incise, P. tricornutum, T. pseudonana*	DHGLA, ETA	ARA, EPA	Iskandarov *et al*., (2010); Domergue *et al*., (2002); Tonon *et al*., (2005)
	Phytoplankton	*Emiliania huxleyi*	DHGLA, ETA	ARA, EPA	Sayanova *et al*., (2011)
	Plant	*M. polymorpha, P. patens*	DHGLA, ETA	ARA, EPA	Kajikawa *et al*., (2004); Kaewsuwan *et al*., (2006)
Δ^5-elongase	Algae	*Pavlova* sp.	ARA, EPA	ADA, ω-3 DPA	Pereira *et al*., (2004b)
	Phytoplankton	*E. huxleyi*	ARA, EPA	ADA, ω-3 DPA	Sayanova *et al*., (2011)
	Plant	*M. polymorpha*	ARA, EPA	ADA, ω-3 DPA	Kajikawa *et al*., (2006)
Δ^4-desaturase	Algae	*Isochrysis galbana, P. salina*	ADA, ω-3 DPA	ω-6 DPA, DHA	Pereira *et al*., (2004b); Zhou *et al*., (2007)
	Diatom	*T. pseudonana*	ADA, ω-3 DPA	ω-6 DPA, DHA	Tonon *et al*., (2005)
	Phytoplankton	*E. huxleyi*	ADA, ω-3 DPA	ω-6 DPA, DHA	Sayanova *et al*., (2011)

Table 2.5 Functional PUFA biosynthesizing enzymes and their sources (Continued).

Enzyme	**Type of organism**	**Specie**	**Substrate**	**Product**	**Reference**
Bifunctional Δ^{12},Δ^{15}	Protozoa	*Acanthamoeba Castellanii*	PA, OA, HDA, LA	HDA, LA, 16:3, ALA	Sayanova *et al*., (2006a)
desaturase	Basidiomycetes	*Coprinus cinereus*	PA, OA, HDA, LA	HDA, LA, 16:3, ALA	Zhang *et al*., (2007)
Bifunctional Δ^{12}/ω3-desaturase	Fungi	*Fusarium graminearum, F. moniliforme, Magna porthegrisea*	PA, OA, HDA, LA, GLA, DHGLA	HDA, LA, 16:3, ALA, SDA, ETA	Damude *et al*., (2006)
Δ^{9}-elongase	Phytoplankton	*E. huxleyi*	LA, ALA	EDA, ETrA	Sayanova *et al*., (2011)
Δ^{8}-desaturase	Protozoa	*A. castellanii*	EDA, ETrA	DHGLA, ETA	Sayanova *et al*., (2006b)
	Algae	*P. salina*	EDA, ETrA	DHGLA, ETA	Zhou *et al*., (2007)
	Phytoplankton	*E. huxleyi*	EDA, ETrA	DHGLA, ETA	Sayanova *et al*., (2011)
Δ^{17}-desaturase	Fungi	*Saprolegnia diclina*	ARA	EPA	Pereira *et al*., (2004a)

16:3, Hexadecatrienoic acid.

2.5 Pharmacological activities of LC-PUFAs

2.5.1 ARA and EPA

ARA and EPA are LC-PUFAs that belong to the ω-6 and ω-3, respectively. In recent years, an interest in ARA and EPA has significantly increased due to their recognition as being beneficial for human health. They have been reported to play important functions as not only structural components of membrane phospholipids but also precursors of the eicosanoids of signaling molecules including prostaglandins, thromboxanes and leukotrienes in mammals.

ARA is a biogenetic precursor of eicosanoids which are important modulators and mediators of a variety of essential physiological activities (Gill and Valivety, 1997). Eicosanoids derived from ARA perform a key role in modulating inflammation, cytokine release, immune response, platelet aggregation, vascular reactivity, thrombosis, and allergic phenomenon (Uauy *et al*., 2000). As a component of mature human milk, ARA is necessary for the neurological and neurophysiological development of both term (Carlson *et al*., 1993) and infants (Brick *et al*., 2000). It is therefore served as an important component in infant nutrition (Bougle *et al*., 1999; Nordoy, 1991).

In addition, EPA plays an important role in higher animals and humans as a precursor of a group of eicosanoids which are crucial in regulating developmental and regulatory physiology. The eicosanoids are hormone-like substances including prostaglandins (PG), thromboxanes (TX) and leukotrienes (LT). EPA is precursors of eicosanoid compounds. However, the eicosanoids from these two fatty acids are different both structurally and functionally and are sometimes even antagonistic in their effects. A balanced uptake of EPA/ARA can prevent eicosanoid dysfunctions and may be effective in treating a number of illnesses and metabolic disorders (Gill and Valivety, 1997). There is evidence that EPA is a potential anticachexia and anti-inflammatory agent (Calder, 1997; Babcock *et al*., 2000). EPA also possesses therapeutic activity against cardiovascular diseases. For example, EPA can prevent atherosclerosis by decreasing the level of low density lipoproteins (LDL) (Bonaa *et al*., 1992). EPA appears to affect the electrical behavior, rhythms and chemical responses of the heart and, thus, reduces the likelihood of heart attack and arrhythmias (abnormalities of the heartbeat). EPA is capable of reducing the tendency toward

thrombosis by reducing the level of fibrinogen, an activation factor in the occurrence of thrombosis (Hostmark *et al*., 1988).

2.5.2 ADA

In humans, ADA is the third most abundant fatty acid in the brain and it is particularly enriched in myelin lipid (O'Brien and Sampson, 1965; Martinez, 1992; Wilson and Sargent, 1993). Rapid accumulation of ADA in brain, comparable to ARA accretion levels, occurs during the early postnatal period of brain growth spurt in human infants (Martinez, 1992). Human milk contains a small amount (-3 mg/dl) of ADA (Jensen, 1996). While the specific functions of ADA are not yet clear, it is suggested to play an important role in myelination in neural tissues (O'Brien and Sampson, 1965; Martinez and Mougan, 1998), its abnormality being implicated in the pathogenesis of Alzheimer's disease (Corrigan *et al*., 1998), and evidence from in vitro studies indicates that it serves as a substrate for dihomoeicosanoid formation tissues (Campbell *et al*., 1985; VanRollins *et al*., 1985). In addition, ADA is an abundant fatty acid in the vasculature that causes endothelium-dependent relaxation in bovine coronary arteries (Yi *et al*., 2007). ADA has also been found to significantly enhance tissue factor (TF) activity of thrombin-stimulated endothelial cells, and it is therefore a potential prothrombotic agent (Tardy *et al*., 1992).

2.5.3 DHA

DHA, an ω-3 LC-PUFA, is well known to be a major structural component of photoreceptors. DHA accounts for approximately 50% of the fatty acids found in photoreceptor rod outer segments (Fliesler and Anderson, 1983). This fatty acid is required for the satisfactory development of vision (Uauy *et al*., 2001) and its deficiency causes a loss of visual acuity (Birch *et al*., 1992b). Furthermore, DHA is reported to play a neuroprotective role against oxidative stress in photoreceptors (German *et al*., 2006a, German *et al*., 2006b; Rotstein *et al*., 2003) and to be important both for the maturation of retinal photoreceptors and for preventing photoreceptor apoptosis (Birch *et al*., 1992a) in the developing retina (Rotstein *et al*., 1997). Dietary studies on ω-3 LCPUFAs have demonstrated that DHA deficiency results in delayed retinal development, visual impairment, retinal function

abnormalities, and disruption of rod outer segment membrane renewal in rats (Benolken *et al*., 1973; Rotstein *et al*., 1996; Wheeler *et al*., 1975), monkeys (Neuringer *et al*., 1984; Neuringer *et al*., 1986), and human infants (Birch *et al*., 1992a; Uauy *et al*., 1990). Thus, dietary deficiencies in DHA is well known to have adverse effects on retinal development and photoreceptor function. However, the effects of dietary DHA on inner retinal function have not yet been fully investigated.

2.6 Fatty acid chain elongation enzymes

The terms such as elongase system, elongase, or fatty acid chain elongation system (FACES) all refer to the enzymes that are responsible for the addition of two carbon units to the carboxyl end of a fatty acid chain. Elongation of fatty acid, whether saturated, monounsaturated, or polyunsaturated, involves four enzyme activities: the keto-acyl-CoA synthase, the ketoacyl-CoA reductase, the hydroxyacyl-CoA dehydratase and the enoyl-CoA reductase (Figure 2.4).

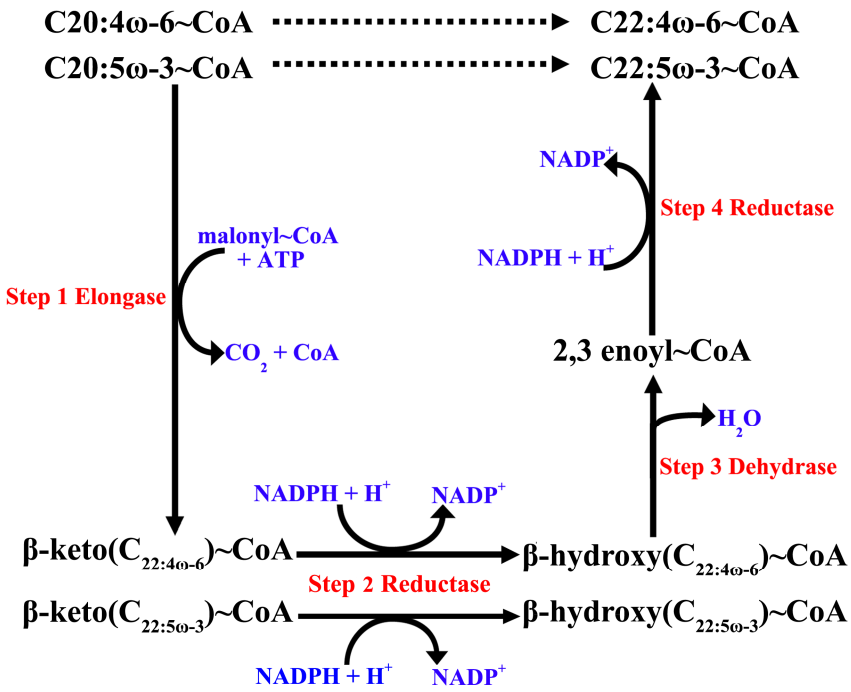

Figure 2.4 Microsomal elongation of PUFAs. PUFA elongation is a multistep process. Step1, which affects chain elongation through the condensation of a fatty acyl-CoA with malonyl-CoA, is rate-limiting and substrate-specific as directed by the elongase polypeptide. Steps 2, 3 and 4 are acyl-reductive processes (Modified from Cinti *et al*., 1992).

Fatty acid elongation is initiated by the condensation of malonyl-CoA with a long chain acyl-CoA, yielding a *β*-ketoacyl-CoA in which the acyl moiety has been elongated by two carbon atoms and it is considered to be rate limiting and specificity controlling with regard to chain length and pattern of double bonds. The formed *β*-ketoacyl-CoA is then reduced by *β*-ketoacyl CoA reductase to the *β*-hydroxyacyl-CoA, which is dehydrated by dehydrase to an enoyl-CoA, and further reduced by enoyl reductase to yield the elongated acyl-CoA (Cinti *et al*., 1992).

Elongase-type sequences involved in LC-PUFA biosynthesis were cloned from several organisms (Table 2.6). The alignment revealed that the predicted amino acid sequence of LC-PUFA elongase included the four conserved motifs KxxExxDT (Box 1), QxxFLHxYHH (Box 2) the extended histidine-rich box, suggested to be functionally important for PUFA elongation (Qi *et al*., 2002), NxxxHxxMYxYY (Box 3), and TxxQxxQ (Box 4), which are commonly of PUFA elongases (Meyer *et al*. 2004; Jakobsson *et al*. 2006).

However, these conserved motifs were not found in other classes of plant microsomal elongases, *β*-ketoacyl CoA synthases, and fatty acid elongases (FAE) involved in extraplastidial elongation of saturated and monounsaturated fatty acids. Jackson *et al*. (1990) reported that the dilysine residues at -2 and -5 positioned from the C-terminus gave these PUFA elongase polypeptypes probable localized in the endplasmic reticulum (ER). However, based on their specificity to substrate fatty acids, elongase-like enzymes can be classified largely into three groups (Mayer *et al*., 2004): one is specific to saturated and monounsaturated fatty acids (SFA and MUFA), another to PUFA of fixed chain-length (single-step), and the other is to PUFA with variable chain-lengths (multi-step) (Table 2.6).

2.7 Gateway cloning for plant transformation (Nakagawa *et al*., 2009)

Gateway cloning technology is an application of the site specific reversible recombination reactions occurring during λ phage integration into and excision from *Escherichia coli* DNA (Figure 2.5) (Walhout *et al*., 2000). In the integration, the *att*P site (242 bp) of λ phage and the *att*B site (25 bp) of *E. coli* recombine and the λ phage genome is integrated into the *E. coli* genome. As a result, λ phage genome is flanked by the *att*L (100 bp) and *att*R (168 bp) sites (the BP

Table 2.6 List of the various members of the ELO family of proteins.

Group	Sources	Protein	Conversion	Reference
SFA and MUFA	*Mortierella alpina* 1S-4	*M. alpina* fatty acid elongase	C_{20}-, C_{22}-, and C_{24}-SFA	Sakuradani *et al*., (2008)
	Saccharomyces cerevisiae	Yeast fatty acid elongase 1	C_{14} to C_{16}	Oh *et al*., (1997); Dittrich *et al*., (1998); Schneiter *et al*., (2000)
		Yeast fatty acid elongase 2	Up to C_{24} SFA/MUFA	
		Yeast fatty acid elongase 3	Broad SFA/MUFA, essential for C_{24} to C_{26}	
	Mouse	Mouse long-chain fatty acid elongase 1	Broad SFA/MUFA up to C_{24}	Tvrdik *et al*., (2000)
	Rat	Rat fatty acid elongase 1	C_{16}–C_{20} MUFA/PUFA	Inagaki *et al*., (2000)
		Rat fatty acid elongase 2	C_{16} and C_{18} SFA/MUFA	
Single-step	*M. alpina*	*M. alpina* γ-linolenic acid elongase	GLA, SDA	Parker-Barnes *et al*., (2000)
	M. alpina 1S-4	*M. alpina* fatty acid elongase	HDA, LA, ALA	Sakuradani *et al*., (2009)
	Conidiobolus obscurus	*C. obscurus* Δ^6-elongase	GLA, SDA	Tan *et al*., (2011)
	Isochrysis galbana	*I. galbana* elongase	LA, ALA	Qi *et al*., (2002)
	I. galbana H29	*I. galbana* Δ^9-elongase	LA, ALA	Li *et al*., (2011)
	Pyramimonas cordata	*P. cordata* Δ^6-elongase	GLA, SDA	Petrie *et al*., (2010a)
		P. cordata Δ^5-elongase	ARA, EPA	
	Pavlova viridis	*P. viridis* Δ^5-elongase	EPA	Niu *et al*., (2009)
	P. salina	*P. salina* Δ^5-fatty acid elongase	EPA	Robert *et al*., (2009)
	Pavlova sp. CCMP459	*Pavlova* sp. Δ^5-fatty acid elongase	ARA, EPA	Pereire *et al*., (2004b)

Table 2.6 List of the various members of the ELO family of proteins (Continued).

Group	Sources	Protein	Conversion	References
Single-step	*Parietochloris incisa*	*P. incisa* Δ^6-elongase	GLA, SDA	Iskandarov *et al*., (2009)
	Physcomitrella patens	*P. patens* elongase	GLA, SDA	Zank *et al*., (2002)
Multi-step	*Thraustochytrium aureum*	*T. aureum* Δ9-elongase	OA, LA, ALA, GLA, EPA	Lee *et al*., (2008)
	T. aureum	*T. aureum* elongase	LA, ALA, GLA, SDA	Kang *et al*., (2008)
	Caenorhabditis elegans	*C. elegans* fatty acid elongase	C_{16} MUFA/C_{18} PUFA	Beaudoin *et al*., (2000)
	Zebrafish (*Danio rerio*)	Zebrafish multifunctional fatty acid elongase	SDA, EPA, ω-3 DPA	Agaba *et al*., (2004)
	Atlantic salmon	Salmon fatty acyl elongase 5a	GLA, SDA, ARA, EPA, ADA, ω-3 DPA	Hastings *et al*., (2005)
	Atlantic salmon	Salmon fatty acyl elongase 5b	GLA, SDA, ARA, EPA, ADA, ω-3 DPA	Morais *et al*., (2009)
		Salmon fatty acyl elongase 2	GLA, SDA, ARA, EPA, ADA, ω-3 DPA	
	Mouse	Mouse long-chain fatty acid elongase 2	C_{20} and C_{22} PUFAs	Tvrdik *et al*., (2000)

reaction). In the reverse reaction, the phage DNA is excised from the *E. coli* genome by recombination between the *att*L and *att*R sites (the LR reaction). The BP reaction needs two proteins, the phage integrase (Int) and the *E. coli* integration host factor (IHF). The mixture of these two proteins is called BP clonase in the Gateway system. In the LR reaction, Int, IHF and one more phage protein, excisionase (Xis) are required, and this mixture is called LR clonase. The Gateway cloning method uses these *att* sites and clonases for construction of plasmid *in vitro* (Hartley *et al*., 2000; Walhout *et al*., 2000).

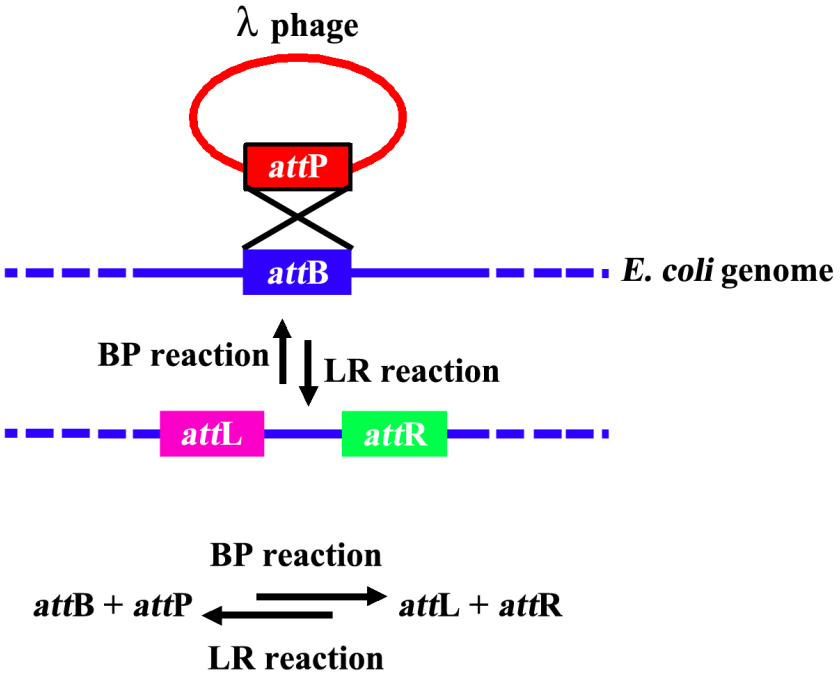

Figure 2.5 Integration and excision of λ phage into and from the *E. coli* genome. The *att*P site (242 bp) of λ phage recombines with the *att*B site (25 bp) of *E. coli* (BP reaction), resulting in generation of *att*L (100 bp) and *att*R (168 bp) located at each end of the λ phage genome. The BP and LR reactions are reversible reactions (Nakagawa *et al*., 2009).

In the early version of the Gateway system, four pairs of modified *att* sites were generated for directional cloning. They are *att*B1 and *att*B2, *att*P1 and *att*P2, *att*L1 and *att*L2, *att*R1 and *att*R2, and a recombination reaction can occur only

in combination of *att*B1 and *att*P1, *att*B2 and *att*P2, *att*L1 and *att*R1, or *att*L2 and *att*R2, since this recombination strictly depends on *att* sequences (Hartley *et al*., 2000; Walhout *et al*., 2000). In addition to these *att* sites, *ccd*B whose protein product inhibits DNA gyrase and a chloramphenicol resistance (Cm^r) marker are used for selection and maintenance of Gateway vectors. Usually, *att*1 is located at the 5'-end of the open reading frame (ORF) and *att*2 is located at the 3'-end. This orientation is maintained in all cloning steps. Figure 2.6 shows the scheme of Gateway cloning. First, the *att*B1 and *att*B2 sequences are added to the 5'- and 3'-ends of the ORF, respectively, by adapter PCR. The product (*att*B1-ORF-*att*B2) is subjected to a BP reaction with a Donor vector, which possess an *att*P1- *ccd*B-Cm^r-*att*P2 cassette. Because of the existence of the negative selection marker *ccd*B between *att*P1 and *att*P2, only the transformants harboring the recombined vectors carrying *att*L1-ORF-*att*L2 (the entry clone) can grow on the selection plate. Once the entry clone is in hand, the ORF is rapidly transferred to a desired destination vector that possesses an *att*R1-Cm^r-*ccd*B-*att*R2 cassette. Since destination vectors also contain *ccd*B between *att*R1 and *att*R2, and have a resistance marker that is different from that carried by the entry clone, only the recombined destination vectors carrying *att*B1-ORF-*att*B2 (the expression clone) will be selected. The Gateway cloning is designed so that the smallest *att* site, *att*B (25 bp), appears in the final product (the expression clone) to minimize the length of cloning junctions after the clonase reaction.

Many destination vectors have been developed for different purposes such as vectors for expression in plants, vectors for fusion with reporter and epitope tags and vectors for RNAi (Curtis and Grossniklaus, 2003; Earley *et al*., 2006). In fusion constructs, the ORF is linked to a tag with eight or more amino acids encoded by the *att*B1 or *att*B2 sites. Because the reading frame of *att*B1 and *att*B2 is unified in the Gateway system, any entry clone incorporated into a destination vector is correctly fused to the tag sequence. As described above, Gateway cloning has great advantages: it is free from the need for restriction digestion, has a simple and uniform protocol, and offers high efficiency and reliability of cloning, easy manipulation of fusion constructs, and the existence of a variety of destination vectors for many purposes. The use of Gateway cloning has expanded in many fields of biological research in recent years.

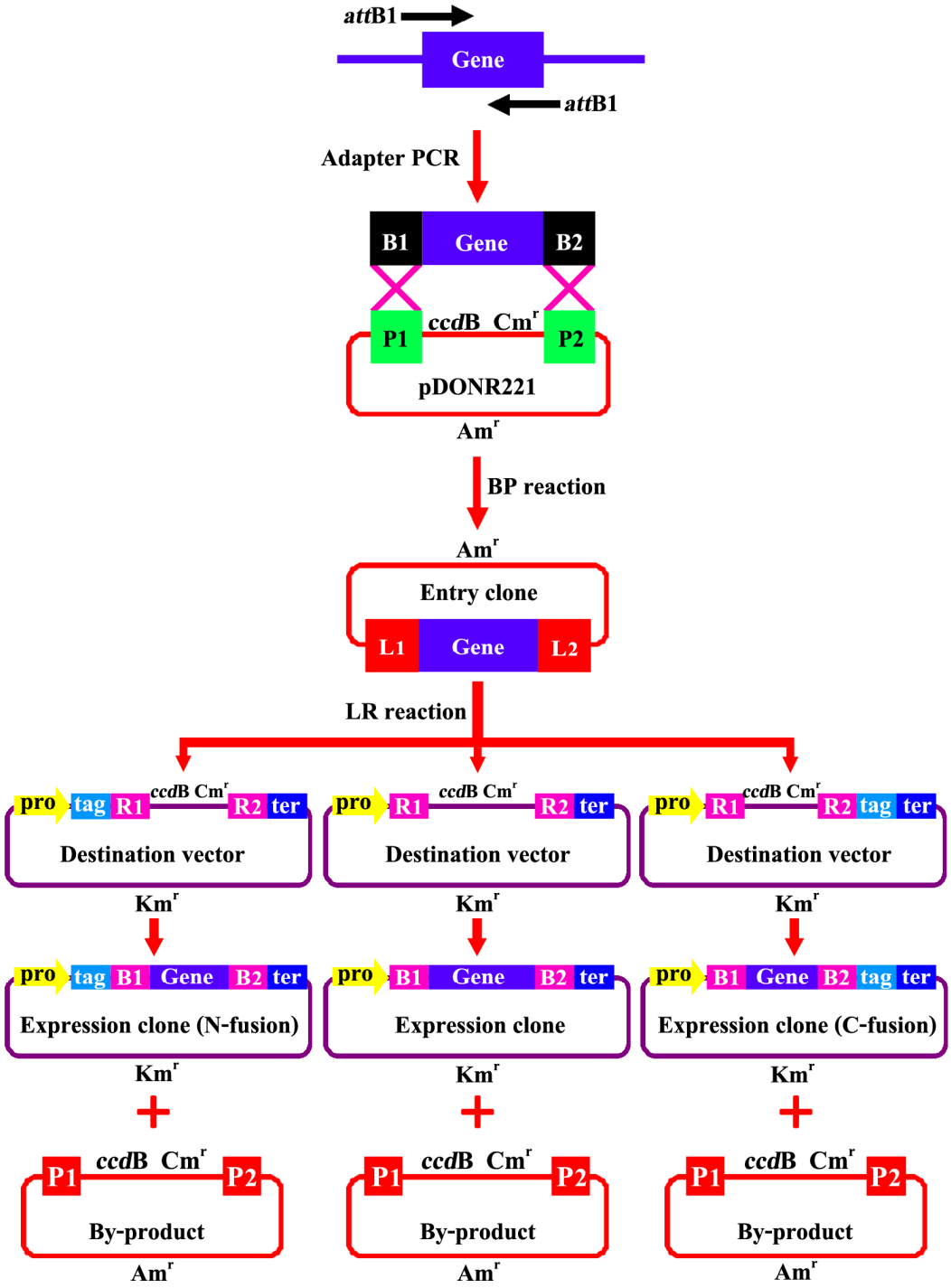

Figure 2.6 Schematic illustration of Gateway cloning. The open reading frame (ORF) region is amplified by adapter PCR and the resulting *att*B1-ORF-*att*B2 fragment is cloned into pDONR221 by a BP reaction to generate an entry clone containing *att*L1-ORF-*att*L2. Subsequently, the ORF is cloned into desired destination vectors by an LR reaction to generate expression clones including tag fusion constructs. B1, *att*B1; B2, *att*B2; P1, *att*P1; P2, *att*P2; L1, *att*L1; L2, *att*L2; R1, *att*R1; R2, *att*R2; Pro, promoter; Ter, terminator (Modified form Nakagawa *et al*., 2009).

2.8 Plant genetic engineering for improved LC-PUFAs production

There are several technical or scientific challenges can be engineered to accumulate adequate levels of LC-PUFAs in oilseed crops. These challenges are mainly focused on increasing the conversion of the native plant fatty acid substrates through to the LC-PUFAs of interest with as few intermediate fatty acids as possible. In theory, this simply requires the use of transgenic enzymes which have high conversion efficiencies. However, in practice, the conversion efficiencies of LC-PUFA biosynthesis enzymes are not affected only by actual enzyme activity but also by factors such as substrate dichotomy, the requirement of some enzymes to use substrates from certain metabolic pools (Petrie and Singh, 2011).

The biosynthesis of ω-6 and ω-3 LC-PUFAs in land plants was first reported in 2004 with publications describing the introduction of both the Δ^8- and Δ^6 pathways. Qi *et al*. (2004) demonstrated the production of 3% EPA and 6.6% ARA in *A. thaliana* leaf tissue by a Δ^8-pathway consisting of the *I. galbana* Δ^9-elongase, *Euglena gracilis* Δ^8-desaturase and *M. alpina* Δ^5-desaturase with constitutive 35S promoters. This study demonstrated that production of LC-PUFAs in land plants was feasible, albeit in leaf tissue.

Shortly after, Abbadi *et al*. (2004) published the production of LC-PUFA in the seeds of tobacco and linseed by the Δ^6-pathway. In this pathway, SDA (11.4%) and GLA (16.8%) were produced in linseed, although these fatty acids were not effectively Δ^6-elongated with only 0.8% EPA and 1.0% ARA being produced. A number of studies that proofed the concept for LC-PUFA production in various plants was achievable and summarized in Table 2.7.

2.9 Response surface methodology (RSM)

Since the production of LC-PUFAs by microorganisms is strongly influenced by various chemical parameters, such as carbon and nitrogen sources, growth factors, and metallic ions and physical parameters such as temperature, culture pH and aeration. It is crucial to search for the key influencing factors among many related ones. There are two ways by which the problem of fermentation parameters may be addressed: classical and statistical methods. The classical method is based on the “one-factor-at-a-time” method in which one independent variable is studied while

Table 2.7 LC-PUFAs production in various transgenic plants.

Plant host	**Target gene**	**New fatty acid production (% of total fatty acid)**	**Reference**
Arabidopsis thaliana	*Isochrysis galbana* Δ^9-elongase, *Euglena gracilis* Δ^8-desaturase, *Mortierella alpina* Δ^5-desaturase	EDA (2.6%), ETrA (4.6%), DHGLA (1.3%), ETA (1.2%), ARA (6.6%), EPA (3.0%)	Qi *et al*., (2004)
A. thaliana	*Danto rerio* Δ^5/ Δ^6-desaturase, *Caenorhabditis elegans* Δ^6-elongase, *Pavlova salina* Δ^5-elongase, *P. salina* Δ^4-desaturase	GLA (0.4%), SDA (1.5%), DHGLA (1.5%), ETA (0.8%), ARA (1.0%), EPA (2.4%), ω-3 DPA (0.1%), DHA (0.5%)	Robert *et al*., (2005)
Brassica juncea	*Pythium irregulare* Δ^6-desaturase, *Thraustochytrium* sp. Δ^5-desaturase, *Physcomitrella patens* Δ^6-elongase, *Calendula officinalis* Δ^{12}-desaturase, *Thraustochytrium* sp. Δ^6-elongase, *P. irregulare* ω3-desaturase, *Thraustochytrium* sp. Δ^4-desaturase, *Oncorhynchus mykiss* elongase, *Thraustochytrium* sp. lysophosphatidyl acyltransferase	GLA (27.3%), SDA (2.2%), DHGLA (1.9%), ETA (1.1%), ARA (4.0%), EPA (8.1%), DPA (0.1%), DHA (0.2%)	Wu *et al*., (2005a)
B. napus	*P. salina* Δ^5-desaturase, *I. galbana* Δ^9-elongase, *P. salina* Δ^8-desaturase	EDA (3.8%), ETrA (0.3%), DHGLA (1.0%), ARA (20.7%), EPA (0.8%)	Petrie *et al*., (2010a)

Table 2.7 LC-PUFAs production in various transgenic plants (Continued).

Plant host	**Target gene**	**New fatty acid production (% of total fatty acid)**	**Reference**
B. carinata line C90-1163 (High erucic acid)	*P. irregulare* Δ^6-desaturase, *Thraustochytrium* sp. Δ^5-desaturase, *Thalassiosira pseudonana* elongase	GLA (18.2%), SDA (3.2%), DHGLA (0.9%), ETA (1.0%), ARA (2.8%), EPA (9.3%), ω-3 DPA (1.4%)	Cheng *et al*., (2010)
B. juncea line 1424 (Zero erucic acid)	*P. irregulare* Δ^6-desaturase, *Thraustochytrium* sp. Δ^5-desaturase, *T. pseudonana* elongase	GLA (19.9%), SDA (2.2%), DHGLA (1.8%), ETA (0.5%), ARA (4.3%), EPA (5.0%), ω-3 DPA (0.4%)	Cheng *et al*., (2010)
B. carinata line 10H3 (Zero erucic acid)	*P. irregulare* Δ^6-desaturase, *Thraustochytrium* sp. Δ^5-desaturase, *T. pseudonana* elongase	GLA (26.9%), SDA (5.4%), DHGLA (2.2%), ETA (2.5%), ARA (5.7%), EPA (20.4%), ω-3 DPA (4.0%)	Cheng *et al*., (2010)
Glycine max	*M. alpina* Δ^5-,Δ^6-desaturases and GLELO elongase	GLA, EDA, DHGLA, ARA (11%) in somatic embryos (8.4%) in mature seeds	Chen *et al*., (2006)
Linum usitatissimum	*Phaeodactylum tricornutum* Δ^6-desaturase, *P. patens* Δ^6-elongase, *P. tricornutum* Δ^5-desaturase	GLA (16.8%), SDA (11.4%), DHGLA (1.2%), ETA (1.0%), ARA (0.9%), EPA (0.8%)	Abbadi *et al*., (2004)

Table 2.7 LC-PUFAs production in various transgenic plants (Continued).

Plant host	**Target gene**	**New fatty acid production (% of total fatty acid)**	**Reference**
Nicotiana benthamiana	*Micromonas pusilla* Δ^6-desaturase, *Pyramimonas cordata* Δ^6-elongase, *P. salina* Δ^5-desaturase	GLA (2.1%), ARA (0.6%), SDA (1.5%), ETA (0.6%), EPA (10.7%), ω-3 DPA (0.3%)	Petrie *et al*., (2010c)
N. benthamiana	*Echium plantagineum* Δ^6-desaturase, *P. cordata* Δ^6-elongase, *P. salina* Δ^5-desaturase	GLA (4.4%), ARA (1.3%), SDA (2.4%), ETA (0.1%), EPA (3.4%), ω-3 DPA (0.2%)	Petrie *et al*., (2010c)
N. benthamiana	*Ostreococcus tauri* Δ^6-desaturase, *P. cordata* Δ^6-elongase, *P. salina* Δ^5-desaturase	GLA (5.8%), ARA (1.2%), SDA (1.1%), ETA (0.4%), EPA (9.6%), ω-3 DPA (0.2%)	Petrie *et al*., (2010c)
N. benthamiana	*P. salina* Δ^9-elongase, Δ^8-desaturase, Δ^5-desaturase, Δ^5-elongase and Δ^4-desaturase	EDA (1.7%), DHGLA (0.5%), ARA (2.4%), ADA (1.2%), ETrA (1.5%), ETA (0.2%), EPA (1.2%), ω-3 DPA (0.6%), DHA (0.7%)	Petrie *et al*., (2010b)

maintaining all the other factors at a fixed level. This method is extremely laborious and time-consuming, especially for large number of variables. Moreover, it does not guarantee the determination of optimal conditions, and is unable to detect the frequent interactions occurring between two or more factors (Choudhari and Singhal, 2008). These limitations of a single factor optimization process can be overcome by using statistical methods. RSM, the statistical based approaches, is a collection of statistical techniques for designing experiments, building models, evaluating the effects of factors and analyzing optimum conditions of factors for desirable responses (Kalil *et al*., 2000).

The main advantage of RSM is the reduced number of experimental runs needed to evaluate multiple factors and their interactions. Also, study of the individual and interactive effects of these factors will be helpful in efforts to find the target value. Hence, RSM provides an effective tool for investigating the aspects affecting desired response if there are many factors and interactions in the experiment (Yin *et al*., 2010). In addition, RSM has been successfully utilized to optimize compositions of fermentation media for production of LC-PUFAs by microorganisms (Table 2.8).

2.10 Factors affecting for LC-PUFAs production

2.10.1 Carbon and nitrogen sources

A variety of carbon sources including mono-, di- and polysaccharides such as glucose, fructose, sucrose, starch, acetate, ethanol and vegetable oils including linseed, corn and canola oils have been reported to affect LC-PUFAs production in various kinds of microorganisms (Table 2.9). These carbon sources are generally metabolized via the Embden–Meyerhoff or Krebs cycle pathways to generate acetyl-CoA used for fatty acids synthesis and provide additional reducing power, NADPH, for the various desaturation enzyme needed to PUFAs production.

For instances, Jin *et al*. (2008) studied the influence of ethanol concentration on ARA production and found that ethanol could be converted directly to acetyl-CoA used for the synthesis of fatty acids and might generate additional reducing power, NADPH, for the Δ^5-desaturases needed to produce ARA in *M. alpina*. Zhu *et al*. (2003) studied the influence of maize starch hydrolysate

Table 2.8 Optimized culture conditions for LC-PUFA production in various microorganisms by RSM.

Microorganism	**Optimized variable**	**LC-PUFA**	**LC-PUFA production (mg/l)**	**Reference**
Aureispira maritima TISTR1715	Tryptone (9 g/l), pH (7.9), agitation speed (170 rpm), temperature (17.8^{o}C)	ARA	43.43	Saelao *et al*., (2011)
Mortierella alpina ME-1	Fermentation time (5.6 days), temperature (13.7^{o}C), ethanol (42.44 g/l), KNO_3 (2.62 g/l)	ARA	1,902	Jin *et al*., (2009)
M. alpina	Glucose (10.0 g/l), corn solids (5.0 g/l), KH_2PO_4 (1.0 g/l), KNO_3 (1.0 g/l)	ARA	1,390	Nisha *et al*., (2011)
Nitzschia laevis	NaCl (14 g/l), $CaCl_2$ (0.1 g/l), pH (8.5), temperature (18^{o}C)	EPA	280	Wen and Chen, (2001a)
Schizochytrium sp. S31	Glucose (27.98 g/l), yeast extraction (4.52 g/l), NaCl (24.82 g/l), pH (6.96), temperature (30^{o}C)	DHA	516	Wu and Li, (2003)
S. limacinum OUC88	Temperature (23^{o}C), aeration rate (1.48 l/min/l), agitation speed (250 rpm), inoculum age (mid-exponential phase)	DHA	4,700	Song *et al*., (2007)
S. limacinum SR21	PI (30 ml/l), NH_4Cl (0.04 g/l), ammonium acetate (1.0 g/l), temperature (19.2^{o}C)	DHA	4,910	Chi *et al*., (2007)

Table 2.9 Effects of carbon sources and concentration on LC-PUFA production in various microorganisms.

Organism	**Carbon source**	**Carbon concentration (g/l)**	**LC-PUFA**	**LC-PUFA production (mg/l)**	**Reference**
Aurantiochytrium limacinum SR21	Glucose	90	DHA	4,200	Yokochi *et al*., (1998)
A. mangrovei KF6	Glucose	60	DHA	3,100	Fan *et al*., (2001)
A. mangrovei SK2	Glucose	75	DHA	4,700	Unagul *et al*., (2005)
A. mangrovei MP2	Glucose	90	DHA	800	Wong *et al*., (2008)
Mortierella alpina ATCC 16266	Glycerol	20	ARA	910	Bajpai *et al*., (1991a)
M. alpine	Glucose (maize starch hydrolysate)	100	ARA	1,470	Zhu *et al*., (2003)
M. alpina ATCC32222	Glucose	60	ARA	2,424.7	Jang *et al*., (2005)
	Starch	100	ARA	2,636.9	
M. alpina NRRL 6302	Glycerol	60	ARA	24.83 (%TFA)	Hou, (2008)
M. alpina CBS528.72	Rhamnose	20	ARA	40.41 (%TFA)	Nischa and Venkateswaran, (2011)
Pythium acanthicum ATCC 18660	Glycerol	20	ω-3 DPA	69.5	Singh and Ward, (1998)
Schizochytrium sp.S31	Glucose	40	DHA (in lipid)	13.64 (%w/w)	Wu *et al*., (2005b)
S. limacinum SR21	Biodiesel-waste glycerol	75	DHA	3,005	Chi *et al*., (2007)
Thraustochytrium roseum ATCC 2821	Starch	25	DHA	650	Li and Ward, (1994)
Thraustochytrium sp. ONC-T18	Soy	100	DHA	4,030	Burja *et al*., (2006)

concentration on ARA production in the culture of *M. alpina* and found that a high initial glucose concentration of starch hydrolysate of 100 g/l led to a high ARA accumulation (1.47 g/l). Wu *et al*. (2005b) indicated that glucose was the most effective carbon source for biomass, lipid and DHA production and demonstrated that the production of DHA increased with an increase in concentration of glucose from 5-10 g/l. Jang *et al*. (2005) revealed that glucose and soluble starch were the best carbon sources for ARA production by *M. alpina*. The production of ARA enhanced with an increase of glucose and soluble starch increased from 0 to 60 g/l and from 0 to 100 g/l, respectively, whereas higher than that ranges diminished ARA production.

Simple nitrogen sources such as nitrate and urea promote ARA and EPA production in *M. alpina* (Jin *et al*., 2009) and *Phaeodactylum tricornutum* (Yongmanitchai and Ward, 1991), respectively (Table 2.10). Potassium nitrate, KNO_3, is essential for the production of LC-PUFAs because it plays a crucial function in maintaining high activity of malic enzyme which plays an important role in the provision of NADPH for fatty acid biosynthesis and thus regulates the extent of LC-PUFAs accumulation in *M. alpina*, especially ARA (Wynn *et al*., 1999). The concentration of nitrogen source must be controlled within a relative low level because a high concentration of nitrogen source leads the flux of carbon to the citric acid cycle with little carbon used for synthesis of fatty acids (Wynn *et al*., 2001). Jang *et al*. (2005) indicated that KNO_3 was the best nitrogen source for ARA production by *M. alpina*. In addition, complex nitrogen sources such as yeast extract, tryptone and corn steep liquor also performed the beneficial effects for LC-PUFA production by individual microorganisms (Table 2.10). Such complex nitrogen sources provide amino acids, vitamins and growth factors (Aasen *et al*., 2000; Wen and Chen, 2001b). Tryptone is widely used as a complex nitrogen source in various cell cultures. It has been reported that the PUFA content of the diatom *Nitzschia laevis* increased when concentration of tryptone was doubled from 0.5 to 1.0 g/l (Wen and Chen, 2001b).

Glutamate was demonstrated to have a role in activating acetyl-CoA carboxylase (ACC; EC 6.4.1.2). ACC catalyzes the formation of malonyl-CoA, an essential substrate for fatty acid synthase and for fatty acyl chain elongation systems (Kowluru *et al*., 2001). Furthermore, glutamate can be utilized for fatty acid synthesis, either directly through the generation of keto acids or acetyl-CoA (Albers *et al*.,

Table 2.10 Effects of nitrogen sources and concentration on LC-PUFA production in various microorganisms.

Organism	**Nitrogen source**	**Nitrogen concentration (g/l)**	**LC-PUFA**	**LC-PUFA production (mg/l)**	**Reference**
Aurantiochytrium limacinum SR21	Corn steep liquor	20	DHA	4,200	Yokochi *et al*., (1998)
A. mangrovei KF6	Yeast extract	10	DHA	3,100	Fan *et al*., (2001)
A. mangrovei SK2	Yeast extract	10	DHA	4,700	Unagul *et al*., (2005)
A. mangrovei MP2	Yeast extract	10	DHA	800	Wong *et al*., (2008)
Mortierella alpina ATCC32222	KNO_3 : yeast extract	1.0 %	ARA	51.62 g/g substrate carbon	Jang *et al*., (2000)
	(2:1, w/w)	7.5%	EPA	16.88 g/g substrate carbon	
M. alpina ZQ9998	Glutamate	0.8	ARA	1,400	Lan *et al*., (2002)
M. alpina M_{18}	Glutamate	0.8	ARA	1,410	Yu *et al*., (2003)
M. alpina ATCC32222	KNO_3 : yeast extract	(2:1, w/w)	ARA	826.3	Jang *et al*., (2005)
M. alpina CBS528.72	Yeast extract	10.0	ARA	35.28 (%TFA)	Nischa and Venkateswaran, (2011)
Phaeodactylum tricornutum	Urea	1.4	EPA	117.5	Yongmanitchai and Ward, (1991)
Pythium acanthicum ATCC 18660	Glutamate	2.0	ω-3 DPA	43.1	Singh and Ward, (1998)
Schizochytrium limacinum SR21	Corn steep liquor	1.0	DHA	1,700	Yokochi *et al*., (1998)
Schizochytrium sp.S31	Yeast extract	4.0	DHA	328	Wu *et al*., (2005b)
Thraustochytrium sp. ONC-T18	Yeast extract	2.0	DHA	4,470	Burja *et al*., (2006)

1996). Yu *et al*. (2003) studied the influence of glutamate concentration on total lipids and ARA production and found that supplementation of less than 0.8 g/l glutamate could increase total lipids and ARA production. However, supplementation of greater than 0.8 g/l glutamate led to a decrease in the total lipids in biomass and ARA production compared with the response to 0.8 g/l glutamate. Similarly, Singh and Ward (1998) suggested that glutamate was the best nitrogen sources for ω-3 DPA production by *P. acanthicum*. Certik *et al*. (1999) reported that glutamate was one of the potentially available nitrogen sources for increasing G6PDH activities and enhancing PUFA biosynthesis. However, when glutamate concentration is too high, glutamate will be converted to proline accompanied by NADPH consumption (Andarwulan and Shetty, 1999), which is necessary for ARA biosynthesis.

2.10.2 Metal ions

$CaCl_2$ and $MgSO_4$ are known to play important roles in various enzyme reactions. For example, in the synthesis of lipids and PUFAs, acetyl-CoA carboxylase catalyzing the initial step of fatty acid synthesis requires bivalent ions as cofactors (Singh and Ward, 1997). One reason for these phenomena is that acetyl-CoA carboxylase, which catalyzes the conversion of acetyl-CoA into malonyl-CoA, requires bivalent metal ions as the cofactors (Guchhait *et al*., 1974). In addition, Mg^{2+} ion has affected to malic enzyme and ATP citrate lyase activity influencing on the production of acetyl-CoA and NADPH for synthesis of fatty acid (Muhid *et al*., 2008). Added minerals may act as cofactors of this enzyme system, which catalyzes the initial step of fatty acid synthesis (Higashiyama *et al*., 1999).

However, the concentrations of the ions in the medium needs to be at appropriate levels for maximizing yields. Chiou *et al*. (2001) found that ferrous (Fe^{2+}) ions increased the production of ARA and EPA in cultures of the bryophyte, *M. polymorpha*, whereas there was no notable change in PUFA production by additional Mg^{2+}, Mn^{2+} and Cu^{2+}. Enhancement of PUFA yield by Fe^{2+} resulted in an increase of intracellular lipid content, rather than selective enhancement of certain fatty acids (Chiou *et al*., 2001). On the other hand, Sajbidor *et al*. (1992) studied the influence of Ca^{2+}, Mg^{2+}, Mn^{2+} and Fe^{2+} on ARA production in the culture of *Mortierella* sp. and indicated that a low concentration (2 mg/l) of Mn^{2+} was beneficial for ARA

production, whereas a higher concentration repressed lipid accumulation. However, these three metal ions (Ca^{2+}, Mg^{2+} and Fe^{2+}) still influenced LA production (Sajbidor *et al*., 1992).

2.10.3 Effect of oil supplementation

Various studies have also indicated that vegetable oil addition was beneficial to enhance LC-PUFAs yield (Table 2.11). Vegetable oils generally contain high levels of C_{18}-fatty acid, precursors for LC-PUFA biosynthesis. For example, LA is the major fatty acid in soybean oil, corn oil, peanut oil and sunflower oil (56–85%), ALA is the major fatty acid in linseed oil (58%) (Jang *et al*., 2005), and OA is rich in palm oil (30–45%) (Mhanhmad *et al*., 2011).

Utilization of oils by microorganisms is accompanied with production of extracellular lipases, which cleave fatty acid residues from glycerol, and the fatty acids produced can either be incorporated to lipid structures or degraded to basic skeletons serving the biomass synthesis (Esfhani *et al*., 1981; Akhtar *et al*., 1983). Shinmen *et al*. (1989) showed that olive oil and soybean oil addition increased the accumulation of ARA in *Mortierella* fungi and supplementation of oils stimulates EPA, DHA and total PUFA production in *M. alpina* (Jang *et al*., 2005). Jareokitmongkol *et al*. (1993) suggested that 3% of linseed oil amendment produced 1 g/l of EPA in *M. alpina* (20% of total fatty acid).

2.10.4 Temperature

Temperature is thought to be one of the most important environmental factors that affect all aspects of the growth and the fatty acid composition of most microorganisms (Table 2.12). It also influence the enzymatic reactions, cell membrane transport system, and some other cellular characters. A low-temperature growth condition will lead to a spontaneous response of strain, which aims at maintaining proper membrane lipid fluidity and functions. This reaction will increase the proportion of unsaturated fatty acids, especially PUFAs. This evidence may cause by the more availability of dissolved oxygen at lower temperatures (Harris and James, 1969) which lead to enhance fatty acid synthesis by aerobic desaturase and elongase enzymes (Singh and Ward, 1997; Higashiyama *et al*., 1999). Jang *et al*. (2005) also

Table 2.11 Effects of oil supplement on LC-PUFA production in various microorganisms.

Organism	**Oil type**	**Oil concentration (%w,w)**	**LC-PUFA**	**LC-PUFA production (mg/l)**	**Reference**
Mortierella alpina ATCC32222	Soybean oil	1.0	ARA	57.02 g/g substrate carbon	Jang *et al*., (2000)
			EPA	29.45 g/g substrate carbon	
M. alpina ATCC32222	Linseed oil	1.0	ARA	1923.3	Jang *et al*., (2005)
			EPA	524.6	
	Sunflower oil	1.0	DHA	36.3	
Pythium acanthicum ATCC 18660	Linseed oil	1.0	ω-3 DPA	110.8	Singh and Ward, (1998)

Table 2.12 Effect of temperature and temperature shift on LC-PUFA production in various microorganisms.

Organism	**Temperature (^{o}C)**	**LC-PUFA**	**LC-PUFA production (mg/l)**	**Reference**
Aurantiochytrium sp. mh0186	15	DHA	~800	Taoka *et al*., (2009)
Crypthecodinium cohnii ATCC 30556	Shift from 25^{o}C (48 h) to 15^{o}C (24 h)	DHA	105.84	Jiang and Chen, (2000a)
Mortierella alpina ATCC32222	Shift from 20^{o}C (5 days) to 12^{o}C (5 days)	ARA	49.78 g/g substrate carbon	Jang *et al*., (2000)
	Shift from 20^{o}C (5 days) to 12^{o}C (5 days)	EPA	26.93 g/g substrate carbon	
M. alpina ATCC32222	12	ARA	882.4	Jang *et al*., (2005)
	12	EPA	34.4	
M. alpina NRRL 6302	30	ARA	23.31 (%TFA)	Hou, (2008)
M. zychae NRRL 2592	20	ARA	22.81 (%TFA)	
M. alpina CBS528.72	25	ARA	38.70 (%TFA)	Nischa and Venkateswaran, (2011)
Phaeodactylum tricornutum	Shift from 25^{o}C (6 days) to 10^{o}C (12 h)	EPA	6.6	Jiang and Gao, (2004)
Pythium acanthicum ATCC 18660	20	ω-3 DPA	40.8	Singh and Ward, (1998)
P. ultimum	25	ARA	220	Gandhi and Weet, (1991)
	25	EPA	170	
Schizochytrium sp. HX-308	Shift from 30 °C (32 h) to 20 °C	DHA	51.98 (%TFA)	Zeng *et al*., (2011)

reported that ARA and EPA production of *M. alpina* ATCC 32222 was the highest at 12^{o}C (Jang *et al*., 2005). Similarly, both ARA and EPA yields of *M. alpina* cultures were enhanced at low culture temperature (12-15^{o}C) (Jang *et al*., 2000).

The two-stage cultivation for PUFA production has been conducted by Yuan *et al*. (2002). The obtained results showed that the higher temperature was favorable for an increase in biomass and lipids, but the lower temperature was more suitable for the accumulation of ARA in *M. alpina* I_{49}-N_{18}. A temperature shift strategy has also employed to enhance the overall PUFA (including ARA, EPA and DHA) production because the optimal temperature for cell growth is often higher than that for PUFAs formation (Jiang and Chen, 2000a).

2.10.5 Initial pH of the culture medium

The media pH is a significant factor that influences the physiology of a microorganism by affecting nutrient solubility and uptake, enzyme activity, cell membrane morphology, by-product formation and oxidative- reductive reactions (Cromwick *et al*., 1996), and therefore it is a parameter that clearly manipulates PUFA production (Table 2.13). However, the effect of pH on production of PUFAs depends on the species of microorganism used.

For example, the yield of EPA by the diatom *P. tricornutum* reaches its maximum when the pH is 7.6 (Yongmanitchai and Ward, 1991). Jiang and Chen (2000b) also found that a neutral pH (7.2) was optimum in terms of degree of fatty acid unsaturation, and the proportion of ω-3PUFAs produced by *Crypthecodinium cohnii*. Whereas the percentage of EPA in the total lipids in the culture of another diatom, *I. galbana*, increased with decreasing the pH from pH 8.0 to 6.0 (Molina *et al*., 1992). Yuan *et al*. (2002) reported that higher pH values (8.0-8.5) were favorable for the production of ARA in lipids and in media by *M. alpine* I_{49}-N_{18}. However, Nuutila *et al*. (1997) reported that lowering the pH to 5.0 caused the ARA concentrations to increase, whereas the optimum pH for EPA production was 7.6 in the cultivation of the red alga *Porphyridium cruentum*.

Table 2.13 Effect of pH on LC-PUFA production in various microorganisms.

Organism	**Intitial pH**	**LC-PUFA**	**LC-PUFA production (mg/l)**	**Reference**
Mortierella alpina ATCC32222	6.0	ARA	54.07 g/g substrate carbon	Jang *et al*., (2000)
	7.0	EPA	18.2 g/g substrate carbon	
M. alpina NRRL 6302	6.0	ARA	21.05 (%TFA)	Hou, (2008)
M. zychae NRRL 2592	6.0	ARA	23.38 (%TFA)	Hou, (2008)
M. alpina CBS528.72	6.5	ARA	34.72 (%TFA)	Nischa and Venkateswaran, (2011)
Phaeodactylum tricornutum	7.6	EPA	93.1	Yongmanitchai and Ward, (1991)
Schizochytrium sp.S31	7.0	DHA	314	Wu *et al*., (2005b)

2.10.6 Agitation speed and aeration (O_2)

Agitation speed level is always an important factor in aerobic biological systems, since when the supply of oxygen is limited, both cell growth and product formation can be severely affected (Wang and Zhong, 2007). Higher agitation rates result in an increase in oxygen supply for growth, and can lead to an increase in the availability of intracellular molecular oxygen. This ensures optimum activities of the oxygen-dependent enzymes in PUFA biosynthesis (Gibbs and Seviour, 1996; Singh and Ward, 1997; Higashiyama *et al*., 1999). However, the optimal dissolved oxygen concentration may vary with different spices.

For example, the fungus *T. aureum* ATCC34304 showed maximum biomass production with an agitation speed of 100 rpm, and the highest PUFA content in total lipids at 150 rpm, under optimal culture conditions. However, agitation speeds higher than 250 rpm physically disrupted the cells, so that the morphology was found to be severely changed and the PUFA content was also greatly reduced (Hur *et al*., 2002). Higashiyama *et al*. (1999) also found that a dissolved oxygen (DO) range of 10-15 ppm was optimum for maximum ARA yield in *M. alpina* cultures, but high levels of oxygen (average DO, 20-50 ppm) decreased ARA production due to cell adaptation by β-oxidation of the fatty acid.

CHAPTER 3

MATERIALS AND METHODS

3.1 Materials

3.1.1 Marine algae and plant materials and culture conditions

Pavlova sp. CCMP459 was purchased from Provasoli-Guillard National Center for Culture of Marine Phytoplankton (CCMP, West Boothbay Harbor, ME, USA). The Gransden strain of *Physcomitrella patens* (Ashton and Cove, 1977) supplied by Prof. Ralph S. Quatrano (Washington University, St. Louis, USA) was used throughout these studies. Protonemata (14-day-old) were grown in liquid BCD basal medium to which di-ammonium tartrate was added to 5 mM and cultured at 25^{o}C under continuous light provided by fluorescent tubes (Knight *et al*., 2002) unless indicated otherwise.

3.1.2 Materials

Materials used for cloning, expression of *Pavlova* sp. Δ^5-elongase and fatty acid analysis were purchased from the following companies.

Materials	Company
- Biodyne® B (0.4 µm)	Pall Life Sciences, Mexico
- 1,000 µl Blue Traditional Shaped Tip	Biotix, Mexico
- 5 ml Castor® Stripette®	Corning, USA
- 10 ml Castor® Stripette®	Corning, USA
- 10 µl Extended Length Tip (Neptune)	Biotix, Mexico
- 0.2 ml Flat Cap PCR Tubes	Axygen, Mexico
- GC vial (1.5 ml)	Agilent Technologies, USA
- Glass Insert (0.1 ml)	Agilent Technologies, USA
- 0.25 mm x 30 m x 0.25 µm HP-INNOWax capillary column	Agilent Technologies, USA

- 1.5 ml Microcentrifuge Tube	Biomed, Thailand
- Omni Tip™ Plastic Probes	Omni International, USA
- Pipet Aid (ROTA-Filler 3000®)	Heathrow Scienctific, China
- 14 ml Polypropylene Round-Bottom Tube	BD Biosciences, USA
- 15 ml Screw Cap Conical Bottom Centrifuge Tubes	Corning, USA
- 50 ml Screw Cap Conical Bottom Centrifuge Tubes	Corning, USA
- Sterilized-Disposable Plastic Petri-dishes (90x15 mm)	Biomed, Thailand
- 0.2 µm Syringe filter	Sartorius Stedim Biotech, Germany
- 200 µl Universal Tip	Biotix, Mexico

3.1.3 Chemicals

3.1.3.1 Chemicals used for cloning and expression of *Pavlova* sp. Δ^5-elongase were purchased from the following companies.

Chemicals	Company
- Agarose	Bio Basic, Canada
- Ammonium tartrate	Fluka, Germany
- Ampicillin	Bio Basic, Canada
- Anti-digoxigenin-AP Fab Fragments	Roche Applied Sciences, Germany
- Blocking reagent	Roche Applied Sciences, Germany
-5-Bromo-4-chloro-3-indolyl-beta-D-galactopyranoside (X-Gal)	Sigma-Aldrich, USA
- Casein Enzyme Hydrolysate, Type-1	Himedia, India
- Chemi-luminescent substrate (CSPD)	Roche Applied Sciences, Germany
- DIG Easy Hyb	Roche Applied Sciences, Germany

- DL-maleic acid	Bio Basic, Canada
- DNA Molecular Weight Marker II DIG labeled 0.12-23.1 kbp	Roche Applied Sciences, Germany
- Ethanol, AR grade	RCI Labscan, Thailand
- Ethylenediaminetetraacetic acid tetrasodium salt dihydrate	Fluka, Germany
- Geneaid Plasmid Maxi Kit	Geneaid Biotech, Taiwan
- Glutamic acid	Univar, New Zealand
- High-Speed Plasmid Mini Kit	Geneaid Biotech, Taiwan
- Hygromycin B	Sigma-Aldrich, Germany
- Isopropyl thiogalactoside (IPTG)	Sigma-Aldrich, USA
- Kanamycin	Bio Basic, Canada
- 1 kb DNA Ladder	Promega, Germany
- Lithium chloride	Ajax Finechem, New Zealand
- Manganess (II) chloride	Univar, New Zealand
- Mannitol	Univar, New Zealand
- MES monohydrate	Fluka, Germany
- Nickel chloride	Univar, New Zealand
- Nucleon™ PhytoPure™ Genomic DNA Extraction Kit	GE Healthcare, USA
- Orange G (molecular biology tested)	Sigma-Aldrich, Germany
- PCR Dig Probe Synthesis Kit	Roche Applied Sciences, Germany
- Polyethylene glycol 6000	Fluka, Germany
- Potassium nitrate	Univar, New Zealand
- Potassium phosphate	J.T. Baker, USA
- Propan-2-ol, AR grade	RCI Labscan, Thailand
- QIAquick Gel Extraction Kit	Qiagen, USA
- RNeasy Plant Mini Kit	Qiagen, USA
- Seakem® LE agarose gel	Cambrex Bio Science Rockland, USA

- Sodium chloride	RCI Labscan, Thailand
- Sodium dodecyl sulphate	Ajax Finechem, New Zealand
- Spectinomycin	Bio Basic, Canada
- SYBR® Safe DNA gel stain	Invitrogen, USA
- Tris-hydrochloride	Bio Basic, Canada
-Tris (hydroxymethyl) aminomethane (molecular biology grade)	Research Organics, USA
- Tri-sodium citrate	Ajax Finechem, New Zealand
- Yeast extract	Himedia, India

3.1.3.2 Chemicals used for fatty acid analysis were purchased from the following companies.

Chemicals	**Company**
- Fatty acid standard	Nu-Check-Prep, USA
- Heptane, AR grade	Lab Scan, Thailand
- Methanol, AR grade	Lab Scan, Thailand
- Sulfuric acid, AR grade	Lab Scan, Thailand

3.1.4 Bacterial strains

Two strains of *E. coli* were used in this study were purchased from the Invitrogen.

Strain	**Genotype**
E. coli DB3.1	F^- *gyr*A462 *end*A1 D(*sr*1-*rec*A) *mcr*B *mrr hsd*S20(r_B^-, m_B^-) *sup*E44 *ara*-14 *gal*K2 *lac*Y1 *pro*A2 *rps*L20(Sm^r) *xyl*-5 λ^- *leu mtl*$^-$1
E. coli TOP10	F^- *mcr*A Δ(*mrr-hsd*RMS-*mcr*BC) Φ80*lac*ZΔM15 Δ*lac*X74 *rec*A1 *ara*D139 Δ(*ara-leu*)7697 *gal*U *gal*K *rps*L (Str^R) *end*A1 *nup*G

3.1.5 Enzymes

Restriction enzymes, polymerases and DNA modifying enzymes were purchased from the following companies.

Enzyme	Company
- *Apa*I	TaKaRa Bio, Japan
- Driselase from *Basidiomycetes* sp.	Sigma-Aldrich, Japan
- *Eco*RI	TaKaRa Bio, Japan
- *Eco*RV	TaKaRa Bio, Japan
- Gateway® LR Clonase™ II Enzyme Mix	Invitrogen, USA
- *Hin*dIII	TaKaRa Bio, Japan
- *Nco*I	TaKaRa Bio, Japan
- *Taq* DNA Polymerase	Invitrogen, USA
- ThermoScript™ RT-PCR System	Invitrogen, USA

3.1.6 Plasmid vectors

Cloning vector (pCR®2.1-TOPO®), gateway entry vector (pCR®8/GW/TOPO) were purchased from Invitrogen (Carlsbad, CA, USA) and plant gateway destination vectors (pMDC32 and pMDC43) were purchased from Arabidopsis Biological Resource Center (ABRC) (Column, OH, USA). The maps of the vectors pCR®2.1-TOPO®, pCR®8/GW/TOPO, pMDC32 and pMDC43 are shown in Figures 3.1, 3.2, 3.3 and 3.4, respectively.

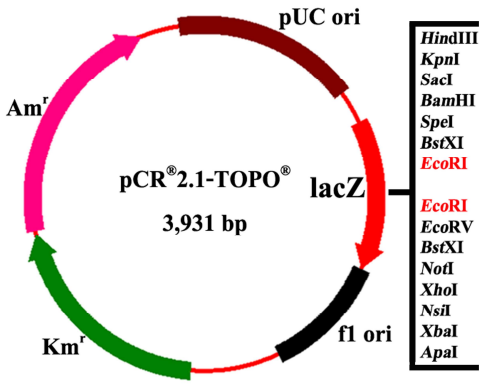

Figure 3.1 Map of cloning vector pCR®2.1-TOPO® (Invitrogen).

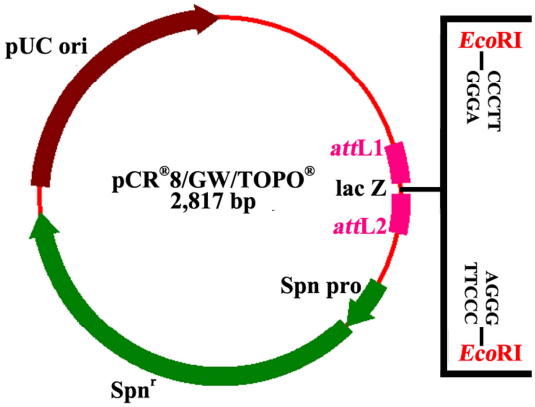

Figure 3.2 Map of gateway cloning vector pCR8®/GW/TOPO® (Invitrogen).

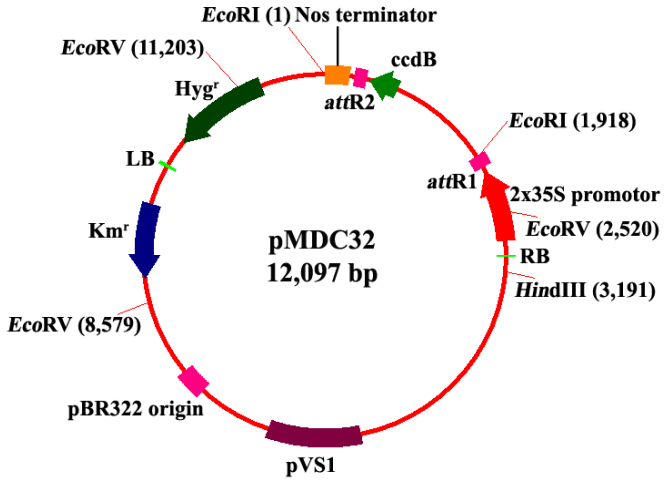

Figure 3.3 Map of gateway plant destination vector pMDC32 (ABRC).

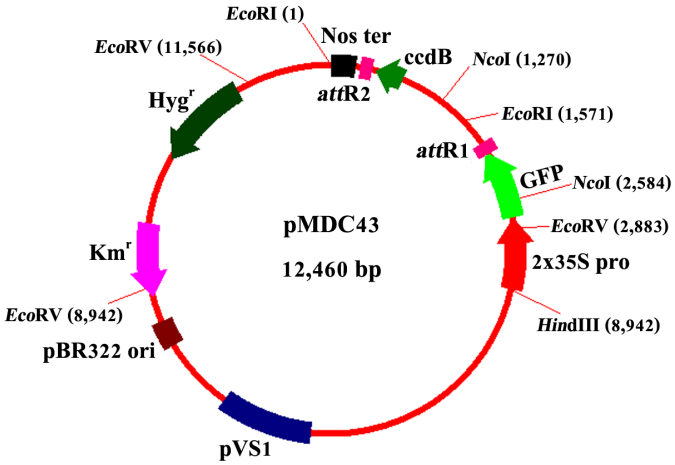

Figure 3.4 Map of gateway plant destination vector pMDC43 (ABRC).

3.1.7 Apparatuses used for cloning, expression of *Pavlova* sp. Δ^5-elongase and fatty acid analysis

Apparatus	Company
- Agilent 6890N Gas chromatograph (GC)	Agilent technologies, USA
- Bioharzard Safety Cabinet Class II (Safe 2010)	Thermo electron, USA
- Freezer (-20^{o}C)	Sanyo, Japan
- Gas chromatograph-Mass spectrometry (GC-MS)	
- GC: Hewlett Packard 5890 Series II	Hewlett Packard, USA
- MS: Hewlett Packard 5972A	Hewlett Packard, USA
- Gel documentation (Bio-Rad Gel Doc 1000)	Bio-Rad, USA
- GyroSpin Centrifuge	Gyrozen, Korea
- Hermle Z323K universal refrigerated centrifuge	Hermle Labortechnik, Germany
- Hot air oven	Memmert, Germany
- New Brunswick Scientific Innova 2100 Platform Shaker	New Brunswick Scientific, USA
- New Brunswick Scientific Innova 4230 Refrigerated Benchtop Incubator Shaker	New Brunswick Scientific, USA
- Omni THQ - Digital Tissue Homogenizer	Omni International, USA
- pH meter (420A)	Orion Research, USA
- Refrigerator	Toshiba, Japan
- SL SHEL LAB Laboratory Incubators	Sheldon Manufacturing, USA
- TaKaRa PCR Thermal Cycler Dice TP600	TaKaRa Bio, Japan
- Thermomixer Comfort	Lab Mark, Czech Republic
- Ultra Low Temperature Freezer (-86^{o}C Freezer)	Shenyang Faith Trading, China
- UV-spectrophotometer Gensys 6	Thermo Scientific, USA
- Water bath	Memmert, Germany

3.2 Methods

3.2.1 Cloning of *Pavlova* sp. Δ^5-elongase gene

3.2.1.1 RNA extraction

Approximately 20 mg fresh weight of *Pavlova* sp. CCMP 459 was ground to a fine powder under liquid nitrogen using a pre-cooled mortar and pestle. Total RNA was extracted from *Pavlova* sp. CCMP 459 using the RNeasy Plant Mini Kit (Qiagen) and determine the total RNA concentration using UV-spectrophotometer (Table 3.1).

Table 3.1 Total RNA extraction (RNeasy Plant Mini Kit, Qiagen).

Step	Action
1. Breaking the cell wall	- Approximately 20 mg fresh weight of *Pavlova* sp. - Grind to a fine powder using liq. N_2 in a mortar and pestle - Transfer the powder to RNase-free, liq.N_2 in 1.5 ml microcentrifuge tube
2. Cell lysis	- Add 450 µl of buffer RTL - Mix vigorously - Incubate at 56^{o}C for 30 min
3. Centrifugation	- Pipet the lysate onto a QIA shredder spin column placed in 2 ml collection tube - Centrifuge at 12,500 rpm - Transfer the supernatant of the flow-through to a new microcentrifuge tube
4. Wash	- Add 0.5 volumn of 100% ethanol - Mix immediately - Apply all sample to an RNeasy mini column placed in a 2 ml microcentrifuge tube

Table 3.1 Total RNA extraction (RNeasy Plant Mini Kit, Qiagen) (continued).

Step	Action
4. Wash (continued)	- Centrifuge at 12,500 rpm for 30 sec - Discard the flow-through liquid
5. Wash	- Add 700 µl of buffer RW1 to the RNeasy column - Centrifuge at 12,500 rpm for 30 sec - Discard the flow-through liquid - Transfer the RNeasy column into a new 2 ml microcentrifuge tube
6. Wash	- Add 700 µl of buffer RPE to the RNeasy column - Centrifuge at 12,500 rpm for 30 sec - Discard the flow-through liquid
7. Wash	- Add another 500 µl of buffer RPE to the RNeasy column - Centrifuge at 12,500 rpm for 5 min - Discard the flow-through liquid - Transfer the RNeasy column into a new 1.5 ml collection tube
8. Elution	- Add 50 µl of RNase-free water directly onto the RNeasy silica gel membrane - Centrifuge at 12,500 rpm for 2 min - Collect the flow-through liquid
9. Determination	- Determine the total RNA concentration using UV-spectrophotometer

3.2.1.2 cDNA synthesis

One µl of Oligo $(dT)_{14}$ primer (RACE 32: 5'-GAC TCG AGT CGA CAT CGA TTT TTT TTT TTT TT-3') (Frohman *et al*., 1988) and 2 µl of 10 mM dNTPs were added to 5 µg of total RNA in a 12 µl volume reaction, incubated at 65^{o}C for 5 min and placed on ice. The cDNA synthesis mix containing 4 µl of 5x first strand buffer, 1 µl of 0.1 M DTT and 15 units/µl ThermoScript^{TM} III Reverse

Transcriptase (Invitrogen) was then added to the previous reaction on ice. After incubation at 4°C for 10 min, followed by 60 min at 50°C and finally, the reaction was terminated by incubating at 75°C for 5 min. The cDNA was subsequently used as a template for PCR amplification with primers.

3.2.1.3 DNA cloning

Single strand cDNA of *Pavlova* sp. CCMP459 was used as a template for PCR amplification with specific primers. The forward and reverse primers were PsELO5-For, 5'-ATG ATG TTG GCC GCA G-3' (underlined sequence is a start codon) and PsELO5-Rev, 5'-TTA CTC CGC CTT GAC CG-3' (underlined sequence is a stop codon), respectively (Pereira *et al*., 2004b).

The PCR was carried out in a total volume of 50 µl containing 2 µl of 10 µM each primers, 5 µl of 10x PCR buffer, 1 µl of10 mM dNTPs, 1 µl of cDNA as a template, 1.5 µl of 50 mM $MgCl_2$, and 0.5 µl of 5 U/µl *Taq* DNA polymerase (Invitrogen). After initial denaturation at 94°C for 4 min, amplification was performed in 35 cycles of 1 min at 94°C, 0.5 min at 49°C and 2.5 min at 72°C, followed by a final extension at 72°C for another 10 min. The amplified products were separated on 1.0% (w/v) agarose gels and purified by QIAquick Gel Extraction (Table 3.2).

Aliquot of 1 µl was directly cloned into pCR® 2.1-TOPO® (Invitrogen) (Figure 3.1) in a total volume of 6 µl at 4°C overnight. Three microliters of the ligation reaction were then transformed into One Shot® TOP10 Chemically competent *E. coli* cells (Invitrogen) and cultured on solid Luria-Bertani (LB) medium containing 100 µg/ml ampicillin, surface spread by 50 µl of 100 mM IPTG and 50 mg/ml X-Gal. Plasmids DNA were purified from transformed *E. coli* cultures by High-Speed Plasmid Mini Kit (Geneaid) (Table 3.3).

The resulting plasmids were verified by digestion with *Eco*RI for 60 min at 37°C and analyzed by 1.0% agarose gel electrophoresis. Plasmid DNA was purified and sequenced in both directions with M13 forward and reverse primers, resulting in the plasmid named pCR®2.1-TOPO®-PsELO5.

Table 3.2 DNA gel purification (QIAquick Gel Extraction, Qiagen).

Step	Action
1. Excise	- Excise the DNA fragment form the agarose gel - Weigh the gel slice in a 1.5 ml microcentrifuge tube
2. Dissolve gel	- Add 3 volumes of buffer QG to 1 volume of gel - Incubate at 50^{o}C for 15 min and mix
3. Centrifugation	- Pipet the sample onto the QIAquick column - Centrifuge at 12,500 rpm for 1 min - Discard the flow-through
4. Binding DNA	- Add 500 µl of buffer QG to QIAquick column - Centrifuge at 12,500 rpm for 1 min - Discard the flow-through
5. Wash the DNA pellet	- Add 750 µl of Buffer PE to QIAquick column - Stand for 2 min - Centrifuge at 12,500 rpm for 1 min twice - Discard the flow-through
6. Elution	- Place QIAquick column to a clean 1.5 ml microcentrifuge tube - Add 32 µl of Buffer EB to QIAquick membrane - Centrifuge at 12,500 rpm for 1 min twice - Collect the purified DNA - Store at -20^{o}C until used

Table 3.3 Plasmid DNA isolation (High-Speed Plasmid Mini Kit, Geneaid).

Step	Action
1. Harvesting	- Harvest 5 ml of bacterial culture by centrifugation at 12,500 rpm for 6 min - Pour off supernatant
2. Cell lysis	- Add 200 µl of Cell Resuspension Solution containing 50 µg/ml RNase - Mix with vortex - Add 200 µl of Cell Lysis Solution - Inverting mix
3. Cell debris precipitation	- Add 300 µl of PD3 - Inverting mix immediately - Centrifuge at 12,500 rpm for 15 min
4. Binding DNA	- Decant the clear lysate into the Spin column placed in a 2 ml collection tube - Centrifuge at 12,500 rpm for 1 min - Discard the flow-through
5. Wash the DNA pellet	- Add 400 µl of PW - Centrifuge at 12,500 rpm for 1 min - Discard the flow-through
6. Wash the DNA pellet	- Add 600 µl of Wash Buffer - Centrifuge at 12,500 rpm for 1 min twice - Discard the flow-through
7. Elution	- transfer the Spin column to a new 1.5 ml microcentrifuge tube - Add 50 µl of TE buffer - Stand for 2 min - Centrifuge at 12,500 rpm for 2 min - Collect the plasmid DNA - Store at -20^{o}C until used

3.2.2 Functional analysis of *Pavlova* sp. Δ^5-elongase in *P. patens*

3.2.2.1 Construction of entry clone

The primers PsELO5-For and PsELO5-Rev were used for PCR amplification of the pCR®2.1-TOPO®-PsELO5 with *Taq* DNA polymerase (Invitrogen). PCR was carried out in a total volume of 50 µl containing 2 µl of 10 µM of each primer, 5 µl of 10x PCR buffer, 1 µl of 10 mM dNTPs, 1.5 µl of 50 mM $MgCl_2$, 1 µl of 1/50 diluted pCR®2.1-TOPO®-PsELO5 as a template, and 0.5 µl of 5 U/µl *Taq* DNA polymerase (Invitrogen). The PCR conditions were conducted as following; initial denaturation for 4 min at 94°C, followed by 28 cycles of 1 min at 94°C, 0.5 min at 49°C, 2.5 min at 72°C, followed by a final extension at 72°C for another 10 min (Table 3.4).

One microliter of amplification product was incorporated directly into 1 µl of entry vector, pCR® 8/GW/TOPO® vector (Invitrogen) (Figure 3.2) in a total 6 µl solution containing 1 µl of salt solution. The mixture was incubated at room temperature for 60 min and transformed into One Shot® TOP10 Chemically competent *E. coli* cells (Invitrogen). The transformants were cultured on LB medium containing 100 µg/ml spectinomycin. Plasmids DNA were purified from transformed *E. coli* cultures by High-Speed Plasmid Mini Kit (Geneaid) (Table 3.3). The resulting plasmids were verified by digestion with *Eco*RI for 60 min and analyzed by 1.0% agarose gel electrophoresis.

The corresponding plasmid was sequenced with M13 forward and reverse primers, yielding the plasmid *att*L1-PsELO5-*att*L2. The obtained plasmid containing PsELO5 sequence flanked by *att*L recombination sequences was then recombined with *att*R sites of destination vectors using the Gateway® LR Clonase™ II Enzyme Mix (Invitrogen).

Table 3.4 Construction of pCR® 8/GW/TOPO® vector containing *Pavlova* sp. Δ^5-elongase gene (the plasmid *att*L1-PsELO5-*att*L2).

Step	Action	
1. PCR mixtures	- 0.5 µl of *Taq* DNA polymerase (Invitrogen) - 5.0 µl of 10X PCR buffer - 4.0 µl of 2.5 mM dNTPs - 1.5 µl of 50 mM $MgCl_2$ - 2.0 µl of 10 µM Primer PsELO5-For - 2.0 µl of 10 µM Primer PsELO5-Rev - 35 µl of sterile water	
2. PCR conditions	- Pre-denaturation at 94°C for 4 min - Denaturation at 94°C for 1 min - Anneling at 49°C for 0.5 min - Extension at 72°C for 2.5 min - Final extension at 72°C for 10 min	- 1 cycle - 28 cycles - 1 cycle
3. DNA purification	- Separate on 1.0% agarose gel electrophoresis - Gel purify by QIA Gel Extraction Kit (See Table 3.2)	
4. Ligation mixture	- 1.0 µl of pCR® 8/GW/TOPO® vector - 1.0 µl of PCR product - 1.0 µl of salt solution - 3.0 µl of sterile water - Incubate at 4°C, overnight	
5. Transformation	- Add 3 µl of mixed into 50 µl of *E. coli* competent cells - Keep on ice for 30 min and heat at 42°C for 1 min - Keep on ice for 5 min and add 300 µl of SOC medium - Incubate with shaking incubator at 37°C for 60 min - Spread plates on LB medium containing 100 µg/ml spectinomycin	
6. DNA extraction	- Plasmid isolation by High-Speed Plasmid Mini Kit (Geneaid) (See Table 3.3)	

3.2.2.2 Construction of *P. patens* expression vector

This reaction separately transferred 150 ng (2 µl) of PsELO5 coding sequence of the plasmid *att*L1-PsELO5-*att*L2 into 100 ng (3 µl) of desired destination vector, pMDC32 (a tandemly duplicated cauliflower mosaic virus 35S (CaMV35S) promoter) (Figure 3.3) or pMDC43 (a tandemly duplicated CaMV35S promoter together with green fluorescence protein (GFP6) region) (Figure 3.4) (ABRC) (Columbus, OH, USA) (Curtis and Grossniklaus, 2003) in a total volume of 10 µl solution containing 3 µl of TE buffer (pH 8.0), and 2 µl of LR Clonase™ II Enzyme Mix (Invitrogen) at 4°C for 2 days (Table 3.5).

The mixtures are further incubated with 1 µl of Proteinase K at 37 °C for 15 min. An aliquot of 3 µl was introduced into One Shot® TOP10 Chemically Competent *E. coli* cells (Invitrogen). The transformants were cultured on LB medium containing 50 µg/ml kanamycin. Plasmids DNA were further purified from transformed *E. coli* cultures by High-Speed Plasmid Mini Kid (Geneaid) (Table 3.3). The resulting plasmids were verified by digestion with *Eco*RI at 37°C for 60 min and analyzed by 1.0% agarose gel electrophoresis. This resulted in the generation of recombinant plasmids, pMDC32-PsELO5 carrying a gene PsELO5 and pMDC43-PsELO5 carrying a gene PsELO5 fused to C-terminus of GFP6, driven by a tandemly duplicated CaMV35S promoter and nos terminator, and containing hygromycin resistance (Hyg^r) gene as a selection marker.

Table 3.5 Construction of *P. patens* expression vector.

Step	Action
1. Recombination	- 2.0 µl of pMDC32 or pMDC43 (150 ng) (ABRC) - 3.0 µl of pCR® 8/GW/TOPO® vector containing *Pavlova* sp. Δ^5-elongase gene (the plasmid *att*L1-PsELO5-*att*L2) - 2.0 µl of TE buffer (pH 8.0) - 2.0 µl of LR Clonase™ Enzyme Mix (Invitrogen) - Incubate at 4°C, overnight

Table 3.5 Construction of *P. patens* expression vector (continued).

Step	Action
2. Digestion	- Add 1 µl of Proteinase K (Invitrogen) - Incubate at 37^{o}C for 15 min
3. Transformation	- Add 5.0 µl of recombination reaction into *E. coli* competent cells (See Table 3.4)
4. DNA extraction	- Plasmid isolation by High-Speed Plasmid Mini Kit (Geneaid) (See Table 3.3)

3.2.2.3 Large scale plasmid DNA purification

An aliquot of 0.5 µl of recombinant plasmids, pMDC32-PsELO5 or pMDC43-PsELO5, was introduced into One Shot® TOP10 Chemically Competent *E. coli* cells (Invitrogen) (Table 3.4). The transformants were cultured on solid LB medium containing 50 µg/ml kanamycin and a single colony was then transferred into 500 ml Erlenmeyer flasks containing 250 ml of liquid LB medium containing 50 µg/ml kanamycin. Plasmids DNA were further purified from transformed *E. coli* cultures by Geneaid Plasmid Maxi Kit (Geneaid) (Table 3.6). The resulting plasmids were verified by digestion with *Eco*RI for 60 min at 37^{o}C and analyzed by 1.0% agarose gel electrophoresis and determined the DNA concentration using UV-spectrophotometry.

Table 3.6 Large scale plasmid DNA purification (Geneaid Plasmid Maxi Kit, Geneaid).

Step	Action
1. Cell harvesting	- Transfer 50 ml of cells to a 50 ml centrifuge tube - Centrifuge at 13,000 rpm for 15 minutes - Discard the supernatant completely - Repeat as required for samples >50 ml using the same centrifuge tube

Table 3.6 Large scale plasmid DNA purification (Geneaid Plasmid Maxi Kit, Geneaid) (continued).

Step	Action
2. Re-suspension	- Add 10 ml of PM1 Buffer (RNase A added) to re-suspend the cell pellet completely by vortex or pipette
3. Cell lysis	- Add 10 ml of PM2 Buffer and mix gently by inverting the tube 10 times (be sure and mix completely) - Do not vortex, to avoid shearing the genomic DNA - Let stand at room temperature for at least 2 minutes to ensure the lysate is clear
4. Neutralization	- Add 10 ml of PM3 Buffer - Immediately shake vigorously for 10 seconds - Do not vortex - Centrifuge at 13,000 rpm for 30 minutes at $4^{o}C$
5. DNA binding	- Transfer the supernatant to the equilibrated Plasmid Maxi Column and allow the column to empty completely by gravity flow - Discard the flow-through and place the Plasmid Maxi Column back in the 50 ml centrifuge tube
6. Wash	- Wash the Plasmid Maxi Column by adding 30 ml of PW Buffer - Allow the column to empty completely by gravity flow then discard the filtrate
7. DNA elution	- Place the Plasmid Maxi Column in a clean 50 ml centrifuge tube - Add 12 ml of PEL Buffer to elute the DNA by gravity flow - Discard the Plasmid Maxi Column once it has emptied completely

Table 3.6 Large scale plasmid DNA purification (Geneaid Plasmid Maxi Kit, Geneaid) (continued).

Step	Action
8. DNA precipitation	- Add 9 ml (0.75 volumes) of isopropanol to the eluted DNA from Step 7 - Mix the tube completely then centrifuge at 13,000 rpm for 60 minutes at 4ºC - Carefully remove the supernatant and wash the DNA pellet with 5 ml of 75% ethanol - Centrifuge at 13,000 rpm for 30 minutes at 4ºC. - Carefully remove the supernatant - Air-dry the DNA pellet for 10 minutes - Dissolve the DNA pellet in 0.5 ml (or suitable volume) of TE
9. Determination	- Determine the DNA concentration using UV-spectrophotometry

3.2.2.4 Protoplast transformation and regeneration

3.2.2.4.1 Protoplast isolation

Protoplasts were isolated from 5 plates (1 g fresh weight) of 14-day-old protonemal wild type *P. patens* cultures by digestion with 20 ml of 0.5% Driselase enzyme suspension dissolved in 8% D-mannitol for 45 min. The digested moss material was successively passed through sieve with a pore size of 100 µm, centrifuged at 250g and washed in 20 ml of 8% D-mannitol twice. Subsequently, the protoplast pellets were resuspended in 10 ml of calcium protoplast wash (CaPW) solution and estimated the protoplast density using a haemocytometer (Grimsley *et al*., 1977) (Table 3.7).

Table 3.7 Protoplast isolation.

Step	Action
1. Cell Harvesting and digestion	- Approximately 1g fresh weight of 14-day-old protonemata wild type *P. patens* tissue - Digested with 20 ml of 0.5% Driselase (Sigma) for 45 min
2. Centrifugation	- Digested moss material is successively passed through sieve with a pore size of 100 µm - Centrifuge at 250g for 5 min - Discard the supernatant
3. Wash	- Add 20 ml of 8% mannitol twice - Centrifuge at 250g for 5 min - Remove the supernatant - Yielding isolated moss protoplasts pellet
4. Resuspend	- Resuspend the protoplast pellet in 10 ml of CaPW
5. Estimate	- Estimate the protoplast density using a haemocytometer

3.2.2.4.2 Polyethylene-glycol (PEG)-mediated transformation of protoplasts and *P. patens* regeneration

Three hundred microliters of the expression construct, pMDC32-PsELO5 and pMDC43-PsELO5 from section 3.2.2.3 were separately digested with *Hin*dIII in a total volume of 400 µl at 37^{o}C for 5 hr. The linear DNA was then subsequently precipitated. Fiveteen micrograms of the linear plasmids were separately transformed into 5x10^{5} protoplasts of the wild type *P. patens* by PEG-method (Schaefer *et al*., 1991 with modification) (Table 3.10).

Transformation experiments were performed by polyethylene glycol (PEG) 6,000 with 300 µl of D-mannitol/$MgCl_2$/MES (MMM) solution (See Appendix A) of a WT protoplast suspension (5x10^{5} protoplasts) added to 15 µg linear plasmids. After transformation, the transformed protoplasts were resuspended in the 1 ml of sterile 8% D-mannitol and added with 7 ml of molten PRMT (protoplast

regeneration medium-top) medium (See Appendix A), 2 ml of mixtures were plated onto each 90x15 mm Petri dishes containing solidified protoplast regeneration medium-bottom (PRMB) medium (See Appendix A) and cultured at 25^{o}C under continuous light provided by fluorescent tubes. The medium was covered with a sterile cellophane sheet which facilitates the transfer of the regenerating plant at subsequent stages.

After regeneration of protoplasts on PRMB/PRMT medium for 14 days, the cellophanes with the culture were transferred to the solid BCD medium (Knight *et al*., 2002) containing hygromycin B (25 µg/ml) and cultured for 14 days, followed by 14 days release period on medium without antibiotic and retransferred to selective medium for a further 14 days. Transformed plants that survived this selection regime were defined as stable transformants.

Table 3.8 Protoplast transformation and regeneration.

Step	Action	
1. Protoplast harvesting	- Aliquot 5x10^{5} protoplasts into the sterile tube - Centrifuge at 250g for 5 min and discard the supernatant - The protoplast pellet	
2. Resuspend	- Add 300 µl of MMM solution and add 15 µg of expression vector DNA into the protoplast suspension	
3. Transformation	Time in minutes	
	0	- Add 300 µl of PEG solution
	5	- Heat at 45^{o}C for 5 min
	10	- Keep on ice for 10 min
	20	- Add 1 ml of CaPW and mix gently
	25	- Add 2 ml of CaPW and mix gently
	30	- Add 4 ml of CaPW and mix gently
	35	- Add 4 ml of CaPW and mix gently
	40	- Centrifuge at 250g for 5 min

Table 3.8 Protoplast transformation and regeneration (continued).

Step	Action
4. Resuspend and dispense	- Resuspend the protoplast pellet in 1 ml of sterile 8% mannitol - Add 7 ml of molten PRMT medium - Dispense onto 90x15 mm plates of PRMB overlayed with cellophane (2 ml/plate) - Incubate at 25^{o}C under continuous light for 14 days

3.2.3 Fatty acid analysis of *P. patens* by GC-MS

Total fatty acids from 14-day-old protonemata of moss were analyzed by GC and fatty acid methyl esters (FAMEs) prepared according to Kaewsuwan *et al*., (2006). Briefly, total fatty acids of moss tissues from wild type and individual transgenic *P. patens* plants were transmethylated with 2.5% sulfuric acid dissolved in methanol at 85°C for 30 min, a total of 1 ml of water and 1 ml of heptane were added to the extracts and well mixed. The top organic layers with the FAMEs were collected and dried under nitrogen gas.

GC analysis of FAMEs was conducted using an Agilent 6890N (USA) equipped with an HP-INNOWax capillary column (0.25 mm x 30 m x 0.25 µm), a flame ionization detector, using helium as the carrier gas. An aliquot (2 µl) of each sample extract was injected onto the GC column using the injector in the split mode. The initial column temperature was 185^{o}C (0.5 min) and was increased at a rate of 3.5^{o}C/min to 235^{o}C (14.3 min), and then maintained at 235^{o}Cfor 1.0 min. Fatty acids were identified by comparison with the retention times of standards and were expressed as mg/l.

The amounts of fatty acids were estimated from the peak areas extrapolated with the calibration curves of known fatty acid standards. The corresponding fatty acids were further verified with the same condition by GC–MS using the HP 5972A Series operating at an ionization voltage of 70 eV with a scan range of 50-500 Da.

3.2.4 Molecular analysis by PCR and Southern blotting

3.2.4.1 Genomic DNA extraction for PCR analysis

Approximately 50 mg fresh weight of 14-day-old protonemal wild type and stable transgenic *P. patens* were frozen using liquid nitrogen and pulverized in a microcentrifuge tube. The powdered tissues were blended with 250 µl of shortly extraction buffer (See Appendix A) twice, incubated on ice for 5 min, and centrifuged at 13,000 rpm for 5 min. A volume of 350 µl of supernatant was mixed with 350 µl of isopropanol and centrifuged at 13,000 rpm for an additional 15 min. Genomic DNA pellet was washed with 250 µl of 70% ethanol, followed by resuspending dried genomic DNA with 400 µl TE buffer before PCR analysis (Table 3.9).

Table 3.9 Genomic DNA extraction for PCR analysis.

Step	Action
1. Breaking of the cell wall	- Approximately 50 mg fresh weight of wild type and stable transgenic *P. patens*. - Grind to a fine powder using liq. N_2 in a mortar and pestle - Transfer the powder to RNase-free, liq.N_2 in 1.5 ml microcentrifuge tube
2. Cell lysis	- Add 500 µl of shortly extraction buffer - Mix vigorously - Centrifuge at 13,000 rpm for 10 min
3. DNA precipitation	- Add 350 µl of isopropanol to 350 µl of supernatant - Mix with vortex - Centrifuge at 13,000 rpm for 15 min - Discard the supernatant - Yielding the DNA pellet
4. DNA washing	- Add 250 µl of 70% ethanol and mix vigorously - Centrifuge at 13,000 rpm for 15 min

Table 3.9 Genomic DNA extraction for PCR analysis (continued).

Step	Action
5 DNA drying	- Dry the DNA by speed vacuum for 10 min
6. DNA dissolving	- Resuspend the genomic DNA with 400 µl of TE buffer - Keep at 4^{o}C, overnight
7. Storage	- Store at -20^{o}C, overnight until used

3.2.4.2 PCR analysis

DNA integration event of PsELO5 was verified by PCR experiments with specific primers, PsELO5-For, 5'-ATG ATG TTG GCC GCA G-3' and PsELO5-Rev, 5'-TTA CTC CGC CTT GAC CG-3' corresponded to the start and stop regions of PsELO5 (Pereira *et al*., 2004b). The hygromycin resistance (Hyg^{r}) gene was also confirmed by PCR with primers, Hygro-For, 5'-ATG AAA AAG CCT GAA CTA CCG-3' and Hygro-Rev, 5'-CTA TTT CTT TGC CCT CGG A-3' derived from 5'- and 3'- Hyg^{r} coding region.

The PCRs were carried out in a total volume of 50 µl containing 2 µl of 10 µM each primers, 5 µl of 10x PCR buffer, 1 µlof 10 mM dNTPs, 1 µl of 1/50 genomic DNA as a template, 1.5 µl of 50 mM $MgCl_2$, and 0.5 µl of 5 U/µl *Taq* DNA Polymerase (Invitrogen). After initial denaturation at 94^{o}C for 4 min, amplification was performed in 35 cycles of 1 min at 94^{o}C, 0.5 min at 49^{o}C and 2.5 min at 72^{o}C, followed by a final extension at 72^{o}C for another 10 min and amplification product was analyzed on 1.0% agarose gel electrophoresis.

3.2.4.3 Genomic DNA extraction for Southern blotting

Genomic DNA was extracted from approximately 1 g fresh weight of 14-day-old protonemal wild type and stable transgenic *P. patens* tissues using the Nucleon^{TM} PhytoPure^{TM} Genomic DNA Extraction Kit (Amersham Biosciences) (Table 3.10). DNA was recovered by ethanol precipitation and dissolved in 250 µl of TE buffer.

Table 3.10 Genomic DNA extraction (Nucleon™ PhytoPure™ Genomic DNA Extraction Kit, Amersham Biosciences).

Step	Action
1. Breaking of the cell wall	- Approximately 1g fresh weight of 14-day-old protonemata *P. patens* - Grind to a fine powder using liq. N_2 in a mortar and pestle - Transfer the powder to RNase-free, liq.N_2 in 1.5 ml microcentrifuge tube
2. Cell lysis	- Add 4.6 ml of Reagent 1 containing 20 μg/ml RNase and mix thoroughly with vortex mixer - Add 1.5 ml of Reagent 2 - Invert several times to gel homogeneous mixture - Incubate at 56^{o}C in water bath for 10 min - Place sample on ice for 20 min
3. DNA extraction	- Remove sample from ice - Add 2 ml of $CHCl_3$ (-20^{o}C) and mix gently - Add 200 μl of Nucleon PhytoPure DNA extraction resin suspension - Centrifuge at 13,000 rpm for 30 min - Transfer the upper DNA containing phase into a fresh tube (~ 7 ml)
4. DNA precipitation	- Add an equal volume of cold isopropanol (~ 7 ml) - Gently invert the tube until DNA precipitates - Centrifuge at 13,000 rpm for 30 min
5. DNA washing	- Add 10 ml of cold 70% ethanol - Centrifuge at 13,000 rpm for 30 min - Discard the supernatant

Table 3.10 Genomic DNA extraction (Nucleon™ PhytoPure™ Genomic DNA Extraction Kit, Amersham Biosciences) (continued).

Step	Action
6. DNA dry and dissolving	- Dry the DNA pellet by speed vacuum for 30 min - Add 250 µl of sterile TE buffer and keep at 4°C, overnight
7. Determination	- Determine the DNA concentration by UV-spectrophotometry

3.2.4.4 Southern blotting

One microgram aliquots of genomic DNA from wild type and stable transgenic lines (C6, N15 and N64) were completely digested with *Eco*RV, *Eco*RI or *Nco*I for 6 h, separated on a 0.6% (w/v) Seakem LE agarose gel (Cambrex Bio Science Rockland, Rockland, ME, USA). The DNA was then transferred to a Biodyne B positively charged 0.45 nylon membrane (Pall Life Sciences, Ann Arbor, MI, USA) in 10x saline sodium citrate (SSC) for 4 h. To improve transfer of the larger DNA fragments, the gel was soaked in 0.25 M HCl for 10 min to partially depurinate the DNA, followed by denaturation with 0.5 M NaOH/1.5 M HCl for 15 min and neutralization with 0.5 M Tris base/1.5 M NaCl pH 7.0 for an additional 15 min. After prehybridization with DIG Easy Hyb (Roche Applied Science, USA) at 40°C for 45 min, the membrane filter was separately probed with specific fragments amplified from the expression constructs used for transformation which were corresponded to PsELO5 and Hyg^r coding region. The probes were labeled with PCR DIG Probe Synthesis Kit (Roche Applied Science, USA) and the hybridization was performed overnight at 40°C in DIG Easy Hyb (Roche Applied Science, USA). The membrane was washed twice with 2x SSC, 0.1% sodium dodecyl sulfate (SDS) at room temperature for 5 min and then wash twice with 0.1x SSC, 0.1% SDS at 65°C for 30 min. Detection was accomplished with a chemi-luminescent substrate (CSPD, Roche Applied Science, USA) and exposed to CL-XPosure Film (Thermo Scientific Inc., Rockford, IL, USA).

3.2.5 Optimization of biomass and ADA production in transgenic *P. patens* culture

3.2.5.1 Starter culture preparation and cultivation conditions

Protonemata tissues (14-day-old, 1 g) of transgenic *P. patens* C6 were blended with 100 ml of modified liquid BCD basal medium with a homogenizer (OMNI TH_Q, USA) at a speed of 30,000 rpm for 1 min yielding 1.0% (w/v) starter inoculum. Then 10 ml of cell suspension was inoculated in 250 ml Erlenmeyer flasks containing 90 ml of modified liquid BCD basal medium and further cultivated on an orbital shaker (New Brunswick Scientific Innova 2100, USA) at 125 rpm with continuous light conditions provided by fluorescent tubes (126 μmol/m^2/s^1) at 25^{o}C for 14 days.

The obtained protonemata tissues (14-day-old, 4 g) were transferred into 250 ml Erlenmeyer flasks containing 100 ml of liquid BCD basal medium formulated by central composite design (CCD) and further cultivated on an orbital shaker (New Brunswick Scientific Innova 2100, USA) at 125 rpm with a continuous light condition provided by fluorescent tubes (126 μmol/m^2/s^1) at 25^{o}C for 14 days.

3.2.5.2 Optimization of culture medium for biomass and ADA production using RSM

The optimization of medium constituents to improve biomass and ADA production in transgenic *P. patens* C6 was carried out based on BCD medium (Knight *et al*., 2002) using RSM (Rao *et al*., 2000). The effects of sucrose (A), potassium nitrate (B) and glutamate (C) were studied by CCD method with five settings (2, 1, 0, +1, +2) of each three factor levels (Table 3.11). Sucrose could be converted directly to acetyl-CoA used for fatty acids synthesis and provided additional reducing power, NADPH, for the various desaturation enzymes needed to produce ARA (Jin *et al*., 2008; Jin *et al*., 2009), which is precursor of ADA biosynthesis. Potassium nitrate is essential for the production of LC-PUFAs because it plays a crucial function in maintaining high activity of malic enzyme which plays an important role in the provision of NADPH for fatty acid biosynthesis and thus regulates the extent of LC-PUFAs accumulation in *M. alpina*, especially ARA (Wynn

et al., 1999) and glutamate was demonstrated to have a role in activating acetyl-CoA carboxylase (ACC; EC 6.4.1.2). ACC catalyzes the formation of malonyl-CoA, an essential substrate for fatty-acid synthase and for fatty acyl chain elongation systems (Kowluru *et al*., 2001).

The relationship of the independent variables and the responses (biomass or ADA production) was calculated by the second-order polynomial equation:

$$Y_i = \beta_0 + \beta_1 A + \beta_2 B + \beta_3 C + \beta_{11} A^2 + \beta_{22} B^2 + \beta_{33} C^2 + \beta_{12} AB + \beta_{13} AC + \beta_{23} BC \qquad (1)$$

where Y_i is the predicted response, *A, B, C, D, and E* are the independent variables, β_1, β_2 and β_3 are the linear effects, β_{11}, β_{22} and β_{33} are the squared effects, and β_{12}, β_{13} and β_{23} are the interaction terms.

The analysis of variance (ANOVA) for the experimental data and the model coefficients were calculated using the software, Design-Expert® v.7.1.5. (Stat Ease Inc., MN). In addition, two-dimension contour plots were constructed for visual observation of the trend of maximum responses and the interactive effects of the significant variables on the responses.

Table 3.11 Levels of variables used in the central composite experimental design used for studying the effects of sucrose (A), potassium nitrate (B) and glutamate (C) concentrations on biomass and ADA production by transgenic *P. patens* C6.

Runs	Sucrose concentration (A) (g/l)	Potassium nitrate concentration (B) (g/l)	Glutamate concentration (C) (g/l)
1	40 (-1)	0.6 (-1)	1.0 (-1)
2	80 (1)	0.6 (-1)	1.0 (-1)
3	40 (-1)	1.0 (1)	1.0 (-1)
4	80 (1)	1.0 (1)	1.0 (-1)
5	40 (-1)	0.6 (-1)	2.0 (1)

Table 3.11 Levels of variables used in the central composite experimental design used for studying the effects of sucrose (A), potassium nitrate (B) and glutamate (C) concentrations on biomass and ADA production by transgenic *P. patens* C6 (continued).

Runs	Sucrose concentration (A) (g/l)	Potassium nitrate concentration (B) (g/l)	Glutamate concentration (C) (g/l)
6	80 (1)	0.6 (-1)	2.0 (1)
7	40 (-1)	1.0 (1)	2.0 (1)
8	80 (1)	1.0 (1)	2.0 (1)
9	20 (-2)	0.8 (0)	1.5 (0)
10	100 (2)	0.8 (0)	1.5 (0)
11	60 (0)	0.4 (-2)	1.5 (0)
12	60 (0)	1.2 (2)	1.5 (0)
13	60 (0)	0.8 (0)	0.5 (-2)
14	60 (0)	0.8 (0)	2.5 (2)
15	60 (0)	0.8 (0)	1.5 (0)
16	60 (0)	0.8 (0)	1.5 (0)
17	60 (0)	0.8 (0)	1.5 (0)
18	60 (0)	0.8 (0)	1.5 (0)
19	60 (0)	0.8 (0)	1.5 (0)
20	60 (0)	0.8 (0)	1.5 (0)

3.2.5.3 Experimental validation of the optimized conditions

Two selected experiments were conducted in 250 ml shake-flasks containing the total volume of 100 ml final production liquid medium with 4 g of 14-day old protonemata as described above to verify the validity of the optimal conditions for maximum biomass and ADA production. Each of these experiments was carried out in triplicate and the data calculated as mean ± S.E. (n=3).

3.2.5.4 Effects of EPA and oil supplementation on biomass, ADA and ω-3 DPA production in transgenic *P. patens* culture

Oil supplementation was applied to improve C_{22}-PUFA production in transgenic *P. patens* C6 based on the optimized liquid BCD medium from section 3.2.5.3. The basal medium supplemented with 0.1 mM EPA or 0.2% (v/v) each of oils including linseed oil, soybean oil, sunflower oil, corn oil and palm oil was used for oil amendment test. Tween 80 at 0.25% (w/v) was used as an emulsifier.

The cultivation of the transgenic *P. patens* C6 was performed by inoculation of 14 day-old protonemata (4% w/v) in 250 mL sterile shake-flasks containing the total volume of 100 ml optimized liquid BCD with oil supplementation. The liquid BCD basal medium was used as the control experiment. After 14 days of cultivation in a growth room at 25^{o}C in an orbital shaker set at 125 rpm under continuous light provided by fluorescent tubes (126 μmol/m^{2}/s^{1}), DCW and production of PUFAs in the cells were estimated in triplicate.

3.2.5.5 Dry cell weight determination (Biomass production)

After 14 days of culture, the cells were separated from the media by filtration through a sieve and then washed three times with a large amount of distilled water to remove residual medium. The cells were filtered again under vacuum condition, subsequently frozen at -20°C and freeze-dried for 3-4 days. Finally, the biomass production was calculated in term of dry cell weight and expressed as g/l of DCW. Each treatment was conducted in triplicate.

CHAPTER 4

RESULTS AND DISCUSSION

4.1 Cloning of Δ^5-elongase gene from *Pavlova* sp.

The *P. patens* produces several PUFAs, especially ARA and EPA (Grimsley *et al*., 1981; Kaewsuwan *et al*., 2006) which are C_{20}-PUFAs required for the synthesis of the C_{22}-PUFAs, ADA and ω-3 DPA, respectively by a Δ^5-elongase (Pereira *et al*., 2004b). However, *P. patens* lacks this C_{22} PUFA synthesizing enzyme, whereas the algae accumulates large amounts of DHA in the cells (Medina *et al*., 1998; Meireles *et al*., 2003; Zhou *et al*., 2007). Accumulation of C_{22}-PUFA in the algae indicates high activities of very long-chain PUFA synthesizing enzymes. Previously gene encoding for Δ^5-elongase was isolated from the marine microalgae *Pavlova* sp. CCMP459 (Pereira *et al*., 2004b). This expressed enzyme displayed unique substrate specificity for both ω-6 and ω-3 C_{20} PUFA substrates, with no activity toward any C_{18} or C_{22} PUFA substrates (Pereira *et al*., 2004b). This study is therefore interested in the production of C_{22}-PUFA substrates in *P. patens* for further ω-6 DPA and DHA productions.

To identify a gene coding for the Δ^5-elongation enzyme involved in the final step of ADA and ω-3 DPA biosynthesis, which are the precursors of ω-6 DPA and DHA, respectively, cDNA reverse-transcribed from *Pavlova* sp. mRNA was PCR amplified with PsELO5-forward and PsELO5-reverse primers based on NCBI sequence data (accession number AY630573) (Pereira *et al*., 2004b) and *Taq* DNA polymerase (Invitrogen) which performs a nontemplate-dependent terminal transferase activity by adding a single deoxyadenosine (A) to the 3´ ends of PCR products. An amplification product contained the expected length (approximately 836 bp indicated by arrow) (Figure 4.1 and 4.2b) was cloned into pCR®2.1-TOPO® vector (Invitrogen) containing a single overhanging 3´ deoxythymidine (T) residues (Figure 4.2a). Topoisomerase I from *Vaccinia* virus binds to duplex DNA at specific sites and cleaves the phosphodiester backbone after 5′-CCCTT in one strand (Shuman, 1991) (Figure 4.2c). The energy from the broken phosphodiester backbone is conserved by formation of a covalent bond between the 3′ phosphate of the cleaved strand and

a tyrosyl residue (Tyr-274) of topoisomerase I. The phospho-tyrosyl bond between the DNA and enzyme can subsequently be attacked by the 5′ hydroxyl of the original cleaved strand, reversing the reaction and releasing topoisomerase (Shuman, 1994) (Figure 4.2c), yielding plasmid named pCR®2.1-TOPO®-PsELO5 (approximately 3,931 bp) (Figure 4.2d).

The resulting plasmids were verified by digestion with *Eco*RI (Figure 4.2e). After screening the five plasmid DNA (P1-P5), two (P1 and P2) of those plasmids were released the approximately 852 bp sized gene of interest (B) from the approximately 3,913 bp sized of vector (A) (Figure 4.2f) and clone P2 was selected for sequencing with M13 forward and reverse primers.

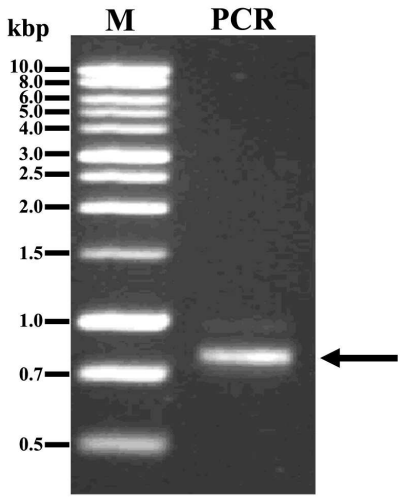

Figure 4.1 PCR amplification products from *Pavlova* sp. cDNA with PsELO5-For and PsELO5 Rev primers and analyzed on 1.0% agarose gel electrophoresis. The DNA sizes in kbp are indicated on the left. The arrow indicates the expected DNA size.

M : 1 kbp DNA Ladder (Promega)

PCR : PCR amplification product

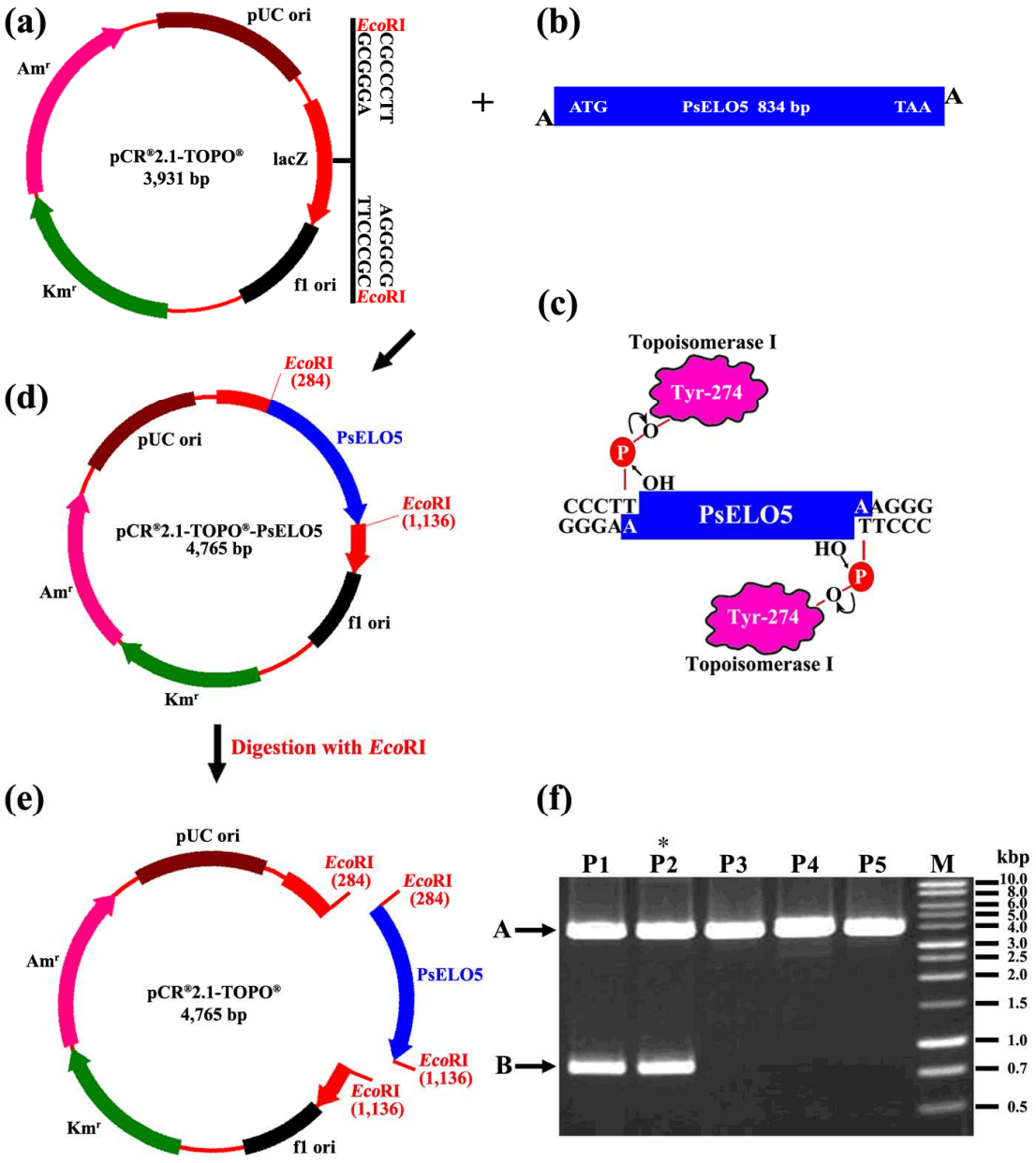

Figure 4.2 Construction of the plasmid pCR®2.1-TOPO®-PsELO5. (a) pCR®2.1-TOPO® vector (Invitrogen). (b) PCR products. (c) Topoisomerase reaction. (d) Recombinant plasmid pCR®2.1-TOPO®-PsELO5. (e and f) Plasmid DNA isolated from *E. coli* cultures and digested with *Eco*RI. The DNA sizes in kbp are indicated on the right.

M : 1 kbp DNA Ladder (Promega)

P1-5 : Plasmid DNA from clone No. 1-5

A : Approximately 3,913 bp sized pCR2.1®-TOPO vector (Invitrogen)

B : Approximately 852 bp sized of *Pavlova* sp. Δ^5-elongase

* : Selected plasmid DNA for sequencing

The open reading frame (ORF) of the clone PsELO5 cDNA (clone P2) is 834 bp from an ATG start to a TAA stop codons and codes for 277 amino acids with 100% identity to a cloned *Pavlova* sp. Δ^5-elongase (accession number AY630573) from previously reported (Pereira *et al*., 2004b) (Figure 4.3). This amino acid polypeptide contained a C-terminal lysine-rich motif, typical characteristic for the endoplasmic reticulum (ER) targeting (Jackson *et al*., 1990) as well as four conserved motifs including KxxExxDT (Box 1), QxxFLHxYHH (Box 2) the extended histidine-rich box which is suggested to be functionally important for PUFA elongation (Qi *et al*., 2002), NxxxHxxMYxYY (Box 3), and TxxQxxQ (Box 4), which are commonly of PUFA elongases (Meyer *et al*. 2004; Jakobsson *et al*. 2006) (Figure 4.3). However, these conserved motifs were not found in other classes of plant microsomal elongases, *β*-ketoacyl CoA synthases, and fatty acid elongases (FAE) involved in extraplastidial elongation of saturated and monounsaturated fatty acids. The secondary structure analysis revealed that PsELO5 is highly hydrophobic and predicted to contain six transmembrane domains (Pereira *et al*., 2004b) (Figure 4.4).

4.2 Functional analysis of *Pavlova* sp. Δ^5-elongase in *P. patens*

4.2.1 Construction of entry clone

In this approach, PCR was used to amplify the PsELO5 sequence from plasmid pCR®2.1-TOPO®-PsELO5 (Figure 4.2d) with two specific primers, PsELO5-For and PsELO5-Rev and *Taq* DNA polymerase (Invitrogen) which performs a non-template-dependent terminal transferase activity by adding a single deoxyadenosine (A) to the 3′ ends of PCR products.

An amplification product containing an approximately 836 bp size of *Pavlova* sp. Δ^5-elongase (Figure 4.5b) was directly ligated into pCR8®/GW/TOPO® entry vector (Invitrogen) containing a single overhanging 3′ deoxythymidine (T) residues (Figure 4.5a). Topoisomerase I from *Vaccinia* virus binds to duplex DNA at specific sites (CCCTT) and cleaves the phosphodiester backbone in one strand (Figure 4.5c) (Shuman, 1991). The energy from the broken phosphodiester backbone is conserved by formation of a covalent bond between the 3′ phosphate of the cleaved strand and a tyrosyl residue (Tyr-274) of topoisomerase I. The phospho-tyrosyl bond

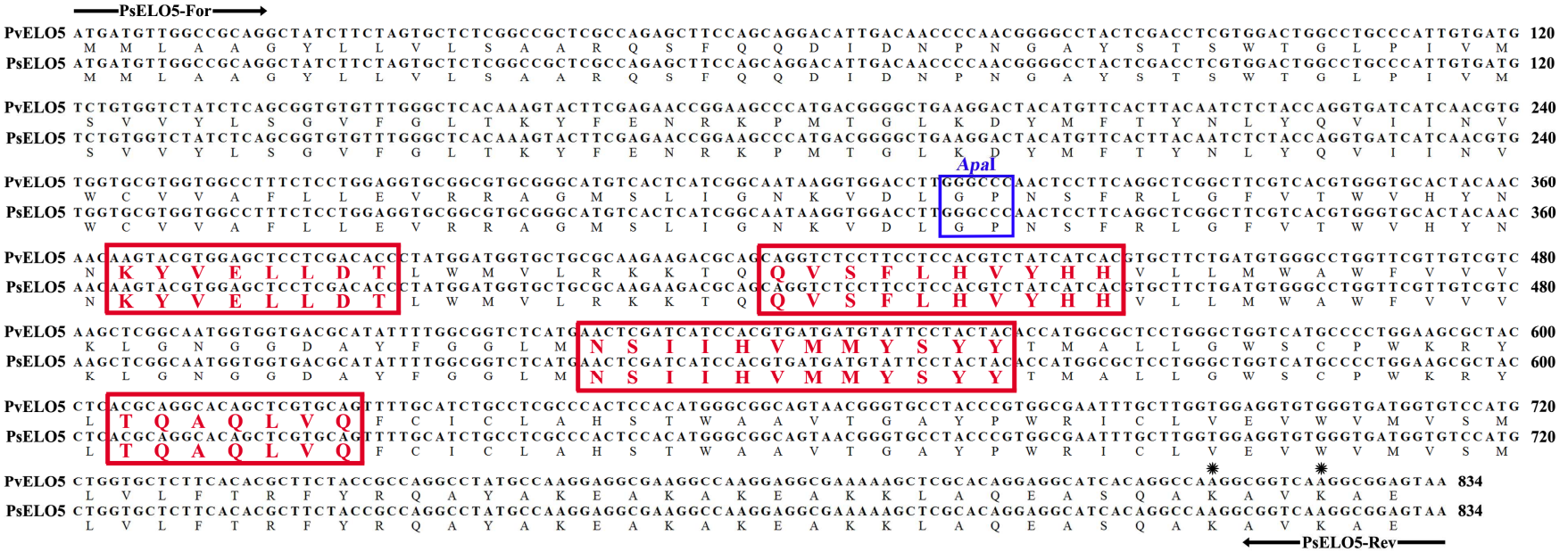

Figure 4.3 Nucleotide and amino acid polypeptide sequences of *Pavlova* sp. Δ^5-elongase characterized in the present study. The alignment was obtained using the Clustal X program. Conserved amino acid motifs are shown in a red box and the restriction enzyme *Apa*I site is shown in a blue box.

PvELO5 : A cloned *Pavlova* sp. Δ^5-elongase (accession number AY630573) from previously reported (Pereira *et al*., 2004b)

PsELO5 : A clone *Pavlova* sp. Δ^5-elongase (In the present study)

* : The dilysine residues at -3 and -6 positioned from the C-terminus gave this gene probable localized in the endoplasmic reticulum (ER)

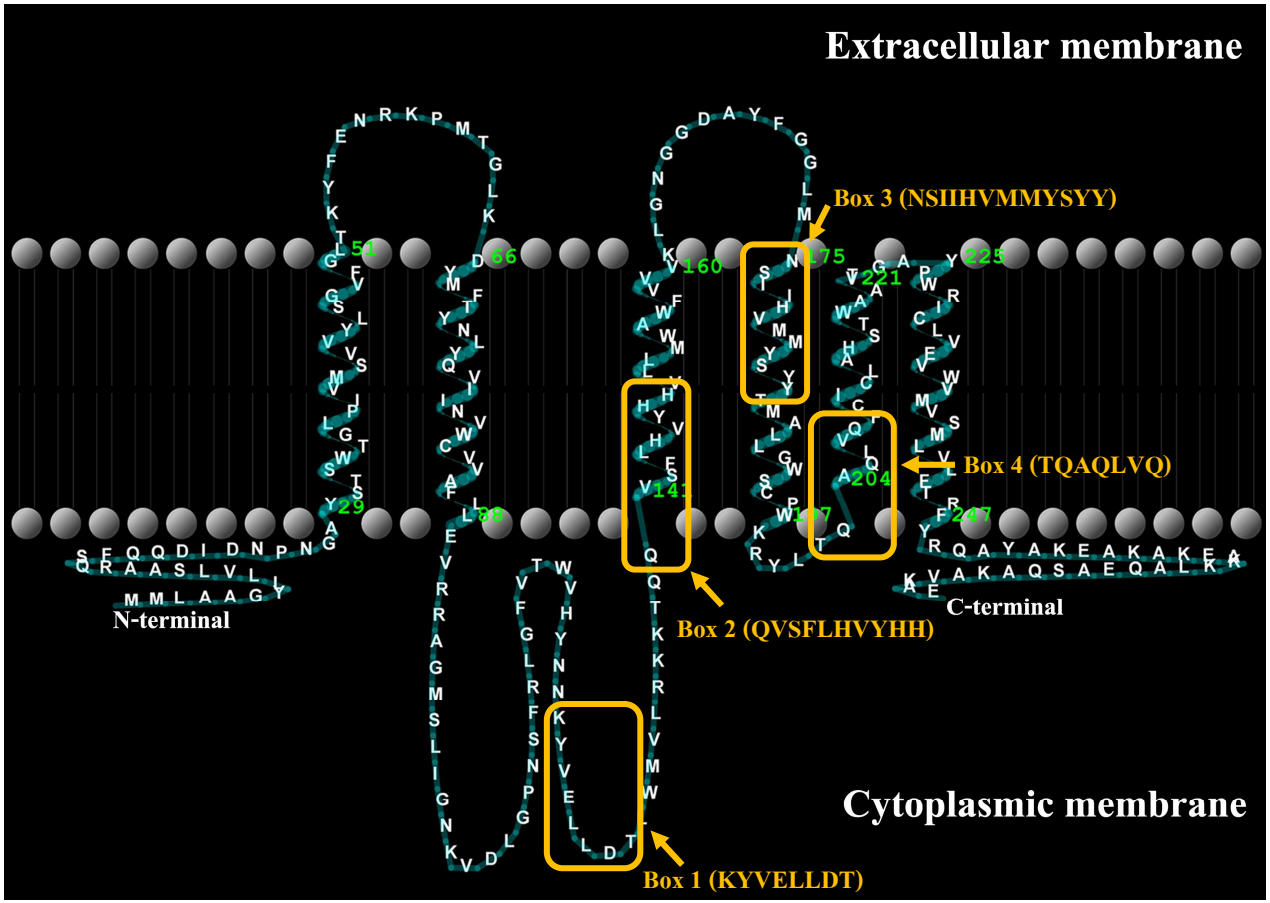

Figure 4.4 Analysis of *Pavlova* sp. Δ^5-elongase using the TMHMM Server v. 2.0 predicts the existence of six transmembrane segments. Using that data the TMRPres2D tool generated two-dimensional rendering of *Pavlova* sp. Δ^5-elongase. The TMHMM analysis predicts that N- and C-terminus are located on the inside of the cytoplasmic membrane. Conserved amino acid motifs are shown in the yellow box.

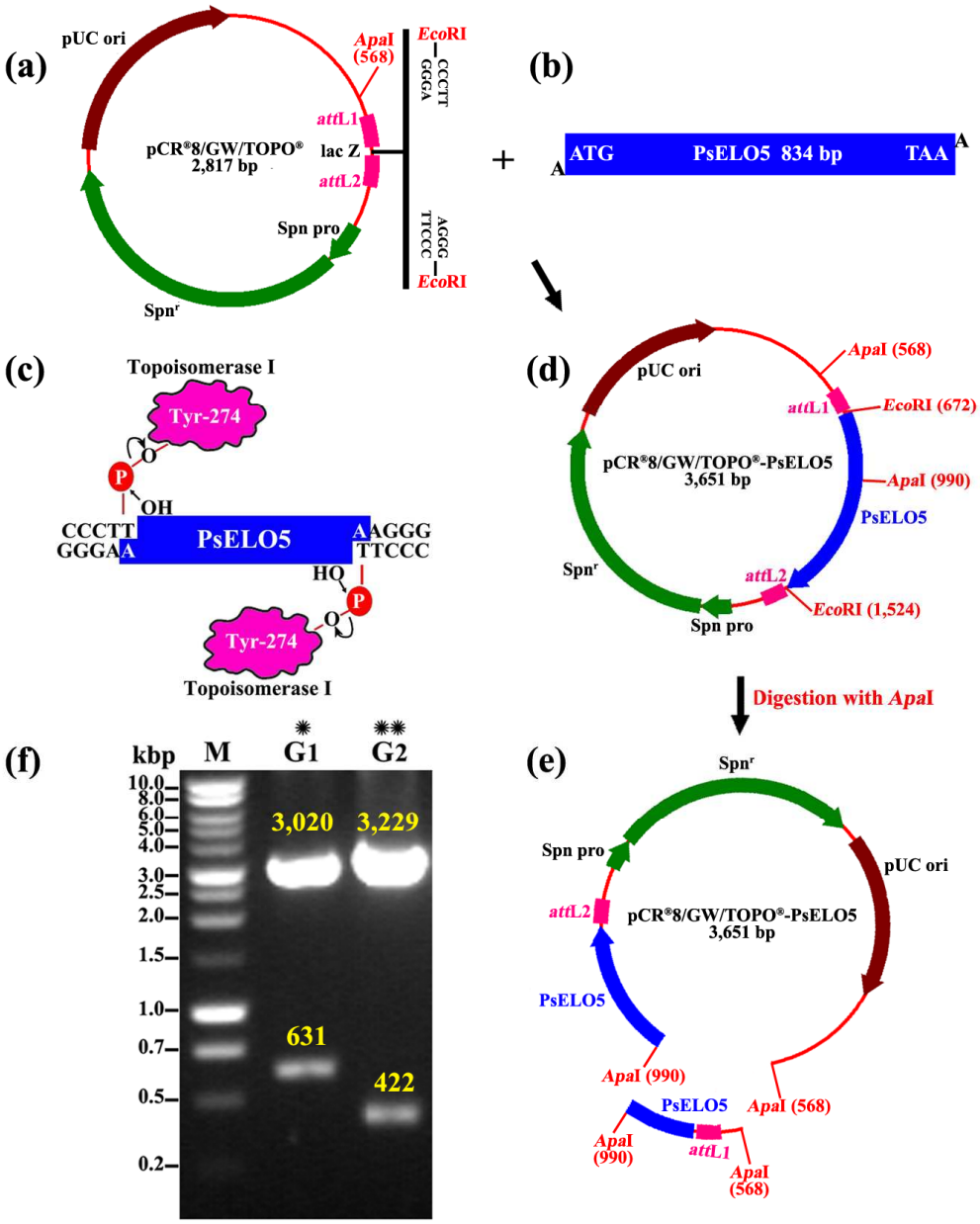

Figure 4.5 Construction of the plasmid pCR®8/GW/TOPO®-PsELO5. (a) pCR®8/GW/TOPO® vector (Invitrogen). (b) PCR products. (c) Topoisomerase reaction. (d) Recombinant plasmid pCR®8/GW/TOPO®-PsELO5. (e and f) Plasmid DNA isolated from *E. coli* cultures and digested with *Apa*I. The DNA sizes in kbp are indicated on the right.

M : 1 kbp DNA Ladder (Promega)

G1-2 : Plasmid DNA from clone No. 1 and 2

G1 : Approximately 3,020 and 631 bp sized DNA

G2 : Approximately 3,229 and 422 bp sized DNA

* : The reverse orientation of PsELO5 in pCR®8/GW/TOPO® vector

** : The forward orientation of PsELO5 in pCR®8/GW/TOPO® vector

between the DNA and enzyme can subsequently be attacked by the 5′ hydroxyl of the original cleaved strand, reversing the reaction and releasing topoisomerase (Figure 4.5c) (Shuman, 1994), resulting in plasmid named pCR®8/GW/TOPO®-PsELO5 (approximately 3,651 bp) (Figure 4.5d). To prevent the reverse orientation of PsELO5 in pCR®8/GW/TOPO® vector in the subsequent step, restriction enzyme was used for verification: *Apa*I digested single site at 318 and 568 bp-positions of PsELO5 cDNA and pCR®8/GW/TOPO® vector, respectively (Figure 4.5e). The forward orientation of PsELO5 cDNA in pCR®8/GW/TOPO® vector was demonstrated in the plasmid clone G2 since it showed the approximately 3,229 and 422 bp sized DNA, whereas the plasmid from G1 contained the reverse orientation of PsELO5 cDNA in pCR®8/GW/TOPO® vector because it provided two distinguish DNA bands at approximately 3,020 and 631 bp (Figure 4.5f). Therefore clone G2 was selected for sequencing with GW1 and GW2 primers, yielding the plasmid *att*L1-PsELO5-*att*L2.

4.2.2 Construction of *P. patens* expression vector

Gateway-compatible plant destination vector was used for protein over-expression of PsELO5 in *P. patens*. The resulting recombinant plasmid G2 has PsELO5 gene flanked by *att*L recombination sequence and it then was consequently recombined with *att*R sites of a desired destination vectors, pMDC32 (Figure 4.6a) and pMDC43 (Figure 4.7a), yielding the recombinant plasmids pMDC32-PsELO5 (approximately 10,932 bp) (Figure 4.6b) and pMDC43-PsELO5 (approximately 11,666 bp) (Figure 4.7b). Both resulting plasmids were verified by digestion with *Eco*RI (Figure 4.6c and 4.7c). After screening the two plasmids pMDC32-PsELO5 (K1-2) (Figure 4.6d), both were released the approximately 852 bp sized gene of interest (B) from the approximately 9,736 and 344 bp sized of vector (A1 and A2) (Figure 4.6d). Similarly, the seven plasmids pMDC43-PsELO5 (R1-R7) were released the approximately 852 bp sized gene of interest (B) from the approximately 10,470 and 344 bp sized of vector (A1 and A2) (Figure 4.7d). Therefore clone K1 and R5 were selected for large scale plasmid DNA purification since clone K1 indicated that the expression construct contained a *Pavlova* sp. Δ^5-elongase driven by a tandemly duplicated CaMV 35S promoter (K1), while clone R5 contained a *Pavlova* sp. Δ^5-elongase driven by a tandemly duplicated CaMV35S promoter together with GFP and

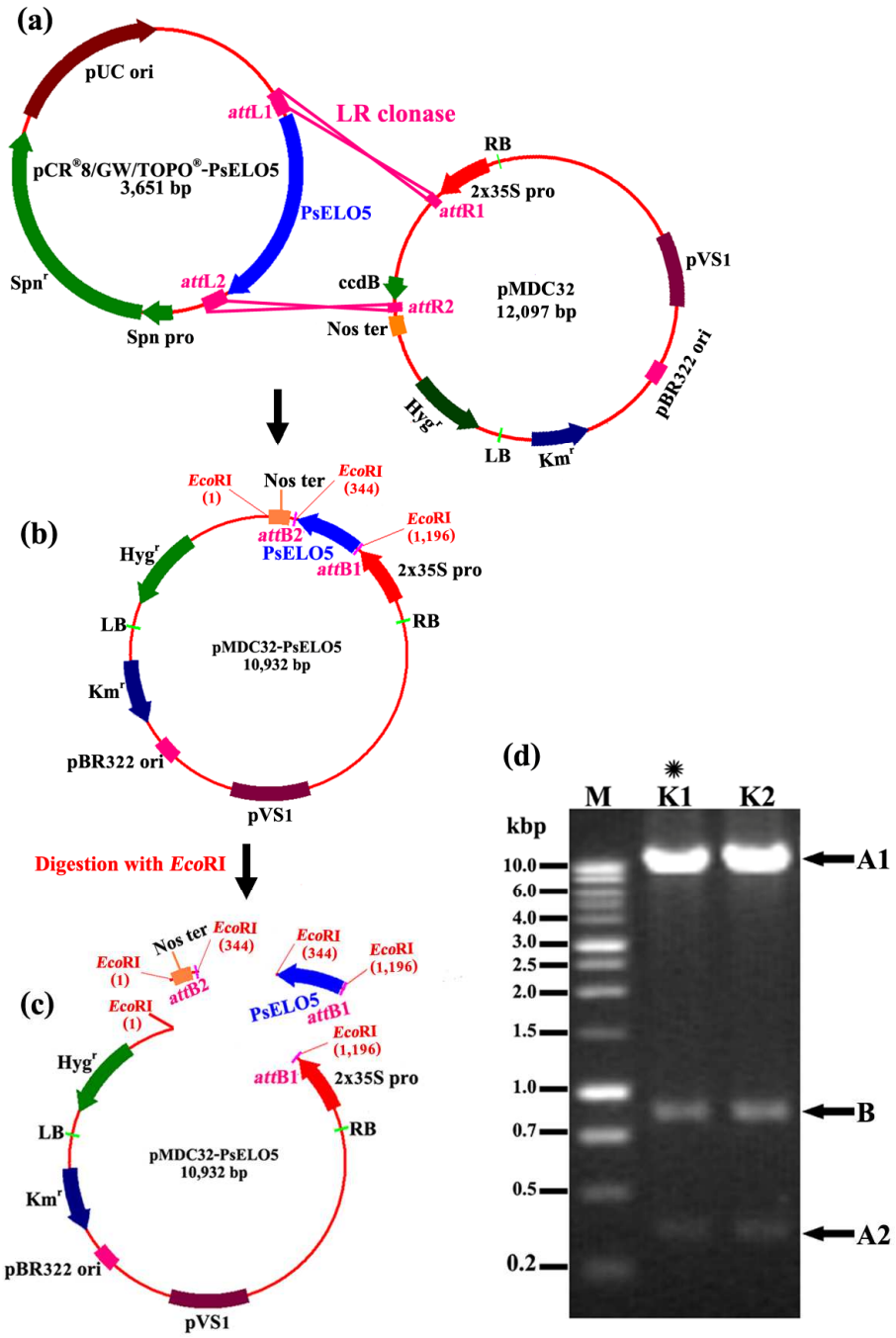

Figure 4.6 Construction of *P. patens* over-expression vector, pMDC32-PsELO5. (a) Recombination reaction. (b) Recombination plasmid pMDC32-PsELO5. (c and d) The plasmid DNA isolated from *E. coli* cultures and digested with *Eco*RI. The DNA sizes in kbp are indicated on the left.

M	: 1 kbp DNA Ladder (Promega)
K1-2	: Plasmid DNA from clone No. 1 and 2
A1 and A2	: Approximately 9,736 and 344 bp sized pMDC32 vector
B	: Approximately 852 bp sized gene of *Pavlova* sp. Δ^5-elongase
*	: Selected plasmid DNA for large scale plasmid DNA purification

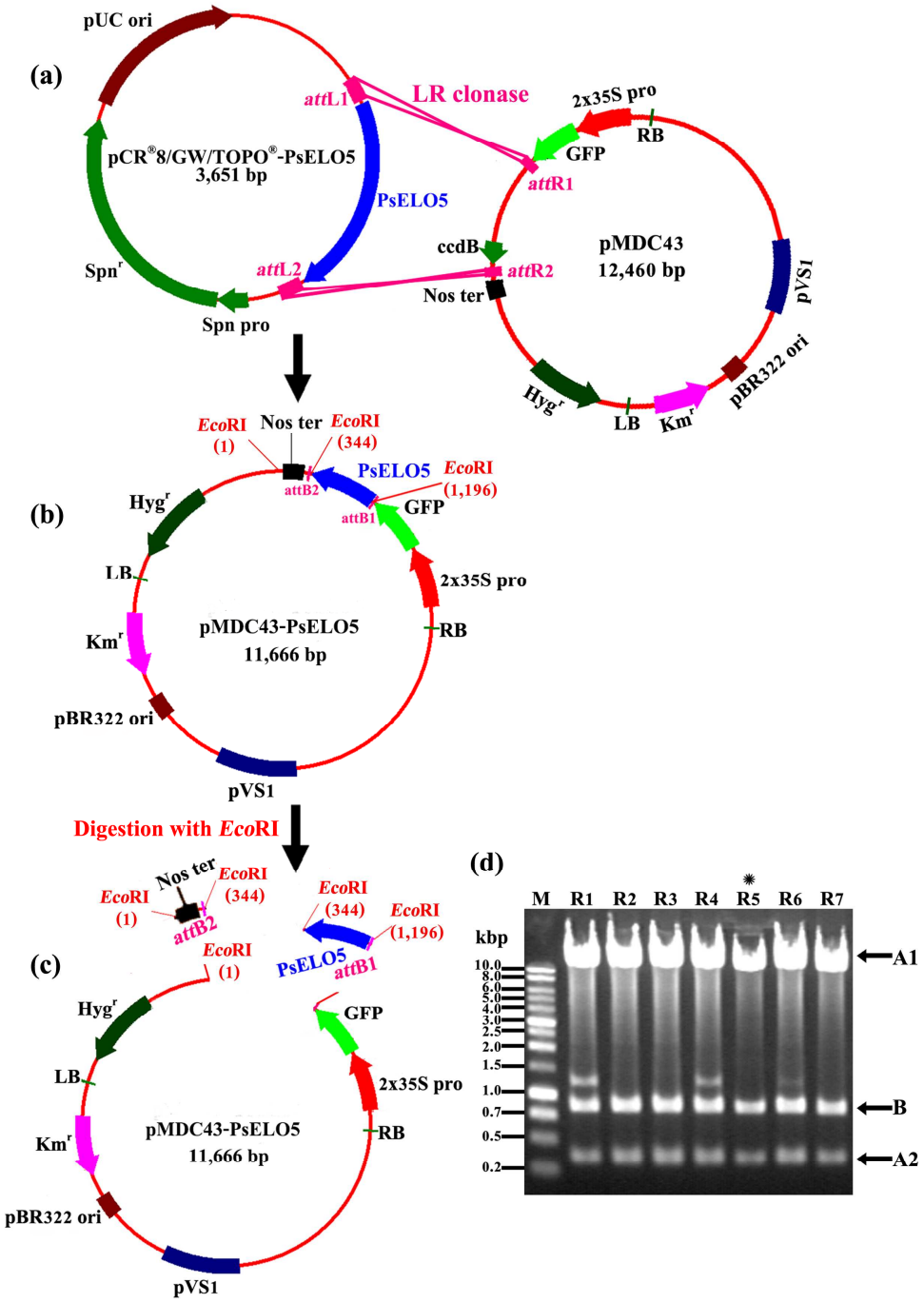

Figure 4.7 Construction of *P. patens* over-expression vector, pMDC43-PsELO5. (a) Recombination reaction. (b) Recombination plasmid pMDC43-PsELO5. (c and d) The plasmid DNA isolated from *E. coli* cultures and digested with *Eco*RI. The DNA sizes in kbp are indicated on the left.

M	: 1 kbp DNA Ladder (Promega)
R1-7	: Plasmid DNA from clone No. 1, 2, 3, 4, 5, 6 and 7
A1 and A2	: Approximately 10,470 and 344 bp sized pMDC43 vector
B	: Approximately 852 bp sized gene of *Pavlova* sp. Δ^5-elongase
*	: Selected plasmid DNA for large scale plasmid DNA purification

nos terminator with hygromycin resistance selection cassette which used to transform into the moss protoplasts (Figure 4.6d and 4.7d).

4.2.3 Protoplast transformation and regeneration

After protoplast transformation with pMDC32-PsELO5 or pMDC43-PsELO5, transformed plants that still survived on the BCD medium containing hygromycin B were defined as stable transformants, while wild type cannot grow on selection medium (Figure 4.8 and 4.9). Protoplasts transformed with linear plasmids, pMDC32-PsELO5 and pMDC43-PsELO5 gave 36 and 47% stable transformants from 250 and 180 picked regenerants, respectively, on the selective medium. All transformants were morphologically indistinguishable from the wild type plant. They gave rise to normal filamentous growth and gametophore formation (Figure 4.8c and 4.9c).

4.2.4 Fatty acid analysis of *P. patens* by GC and GC-MS

To produce ADA and ω-3 DPA in *P. patens*, it is necessary to express the Δ^5-elongase gene (Figure 4.10). Generally, various promoters are used to facilitate gene expression in plants. The CaMV 35S promoter is highly active in most of the transgenic plants. However, a tandemly duplicated CaMV 35S promoter showed a six fold higher expression level of activity in *P. patens* than the normal CaMV 35S promoter (Horstmann *et al*., 2004). In this study, *P. patens* was transformed with the two recombinant plasmids, pMDC32-PsELO5 that contains PsELO5 cDNA (Pereira *et al*., 2004b) or pMDC43-PsELO5 carrying a gene PsELO5 fused to C-terminus of GFP6, driven by a tandemly duplicated CaMV 35S promoter and nos terminator, and contained the Hyg^r gene as a selection marker. One hundred and seventy-seven stable hygromycin-resistant transgenic lines (92 and 85 lines for *P. patens* transformed with pMDC32-PsELO5 and pMDC43-PsELO5, respectively) were screened by co-migration and spiking with known fatty acid standards and by the mass spectrometry (MS) fragmentation patterns. GC analysis of FAMEs of all transgenic lines showed that they contained only one additional fatty acid peak (retention time, RT = 14.7 min) compared to the wild type (Figure 4.11 and 4.12). This was identical to that of the methyl ester of authentic ADA and this compound, when investigated by

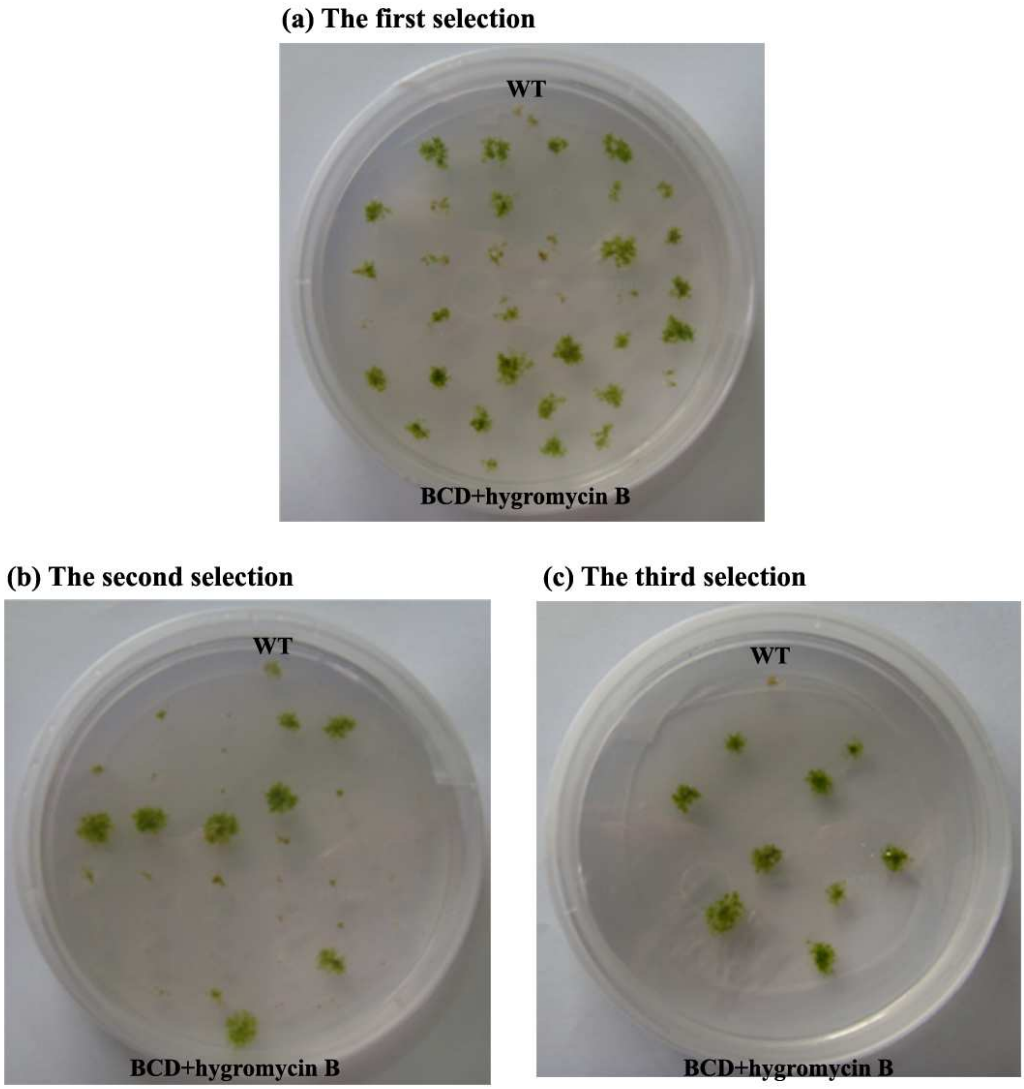

Figure 4.8 Regeneration of transgenic *P. patens* transformed by pMDC32-PsELO5 on the selective BCD medium containing hygromycin B (25 μg/ml).

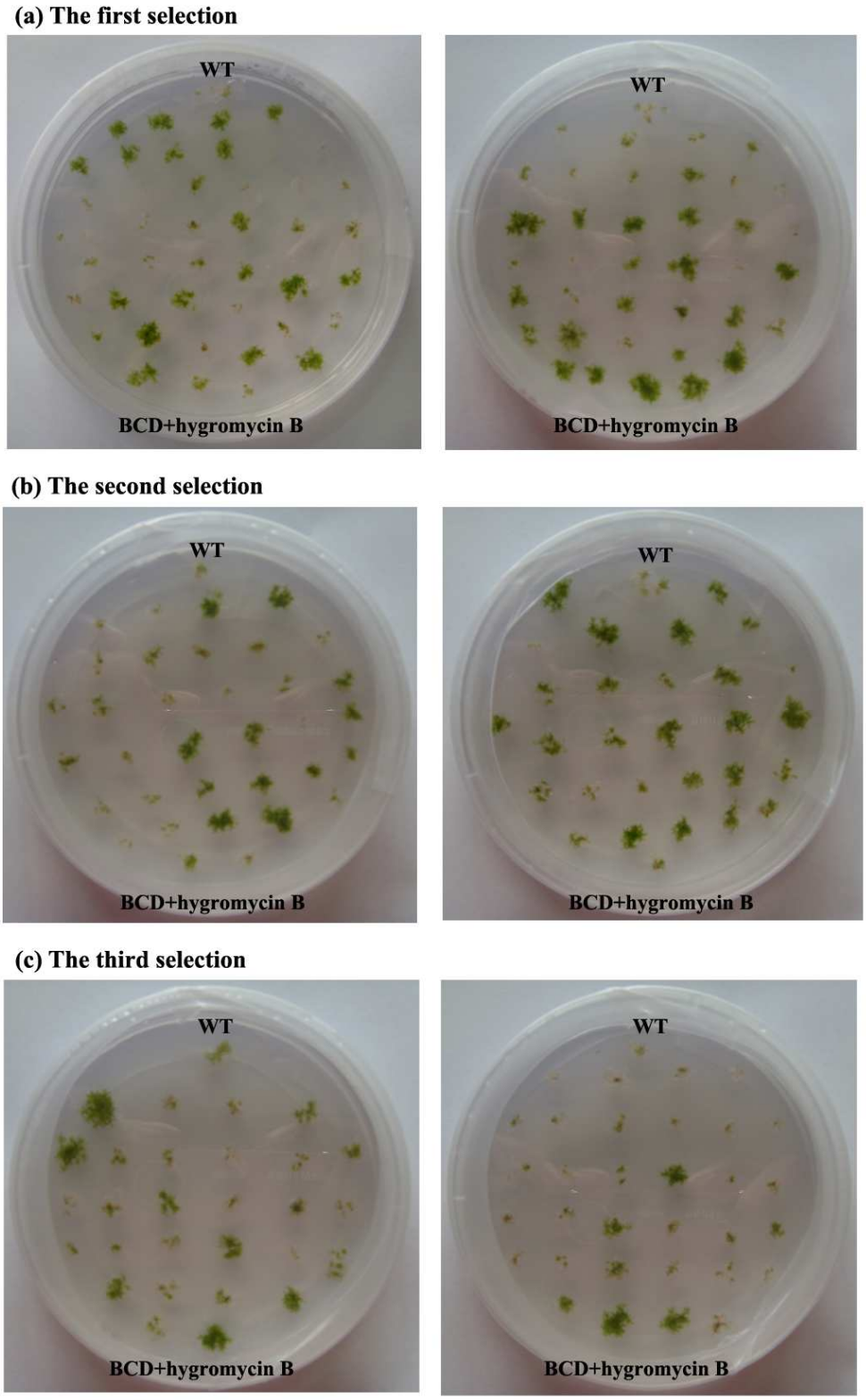

Figure 4.9 Regeneration of transgenic *P. patens* transformed by pMDC43-PsELO5 on the selective BCD medium containing hygromycin B (25 μg/ml).

GC-MS, displayed a molecular ion of 346 m/z, which is the expected molecular ion for methyl ester of ADA as well as the fragmentation patterns identical to that of the authentic ADA methyl ester (Figure 4.13). It was therefore considered to be ADA, an ω-6 elongation product of the PsELO5. Further estimation of ADA quantity from the calibration ADA standard revealed that the four pMDC43-PsELO5 transgenics with the highest ADA production lines (N15, N64, N70 and N77) obviously produced 22.6-46.4 times higher levels of ADA compared to the six transgenic line (C1, C2, C3, C4, C5 and C6) containing the pMDC32-PsELO5 construct (Table 4.1), while no ADA was detected in the control wild type (Figure 4.11 and 4.12; Table 4.1).

However, an ω-3 DPA was not observed from any transgenic lines cultivated in BCD media (Figure 4.11 and 4.12; Table 4.1). This might due to vary low amount of substrate EPA naturally present in *P. patens*. However, it has been reported that lower temperature could activate EPA production. This evidenced may cause by the more availability of dissolved oxygen at lower temperatures (Harris and James, 1969) which lead to enhance fatty acid synthesis by aerobic desaturase and elongase enzymes (Higashiyama *et al*., 1999). Jang *et al*. (2005) reported that EPA production of *Mortierella alpina* ATCC 32222 was the highest at 12^{o}C (Jang *et al*., 2005). Similarly, the EPA yield of *M. alpina* cultures was enhanced at low culture temperature (12-15^{o}C) (Jang *et al*., 2000). Moreover, the improvement of EPA production in microalgae by temperature shifting has been reported (Jiang and Gao, 2004). Jiang and Gao (2004) showed that EPA yield in the *Phaeodactylum tricornutum* increased up to 6.6 mg/l after application of a two-stage culture with temperature shifting from 25^{o}C for 6 days to 15^{o}C for 12 h, being raised by 120% compared with the control. In addition, *P. patens* contains high proportions of ARA (Grimsley *et al*., 1981; Kaewsuwan *et al*., 2006). ARA plays an important role as a precursor for EPA production, which involve the enzyme Δ^{17}-desaturase. Previously a novel gene from an EPA-rich fungus (*Saprolegnia diclina*), namely sdd17, had been identified (Pereira *et al*., 2004a). This gene encodes an ω-3 desaturase that is mainly involved in EPA production from its ω-6 C_{20} PUFA substrate (ARA), specifically by heterologous expression in *Saccharomyces cerevisiae*, somatic soya bean embryos (Pereira *et al*., 2004a) and mammalian cells (Chen *et al*., 2010). So that genetic engineering could be applied to obtain stable transgenic *P. patens* producing a high

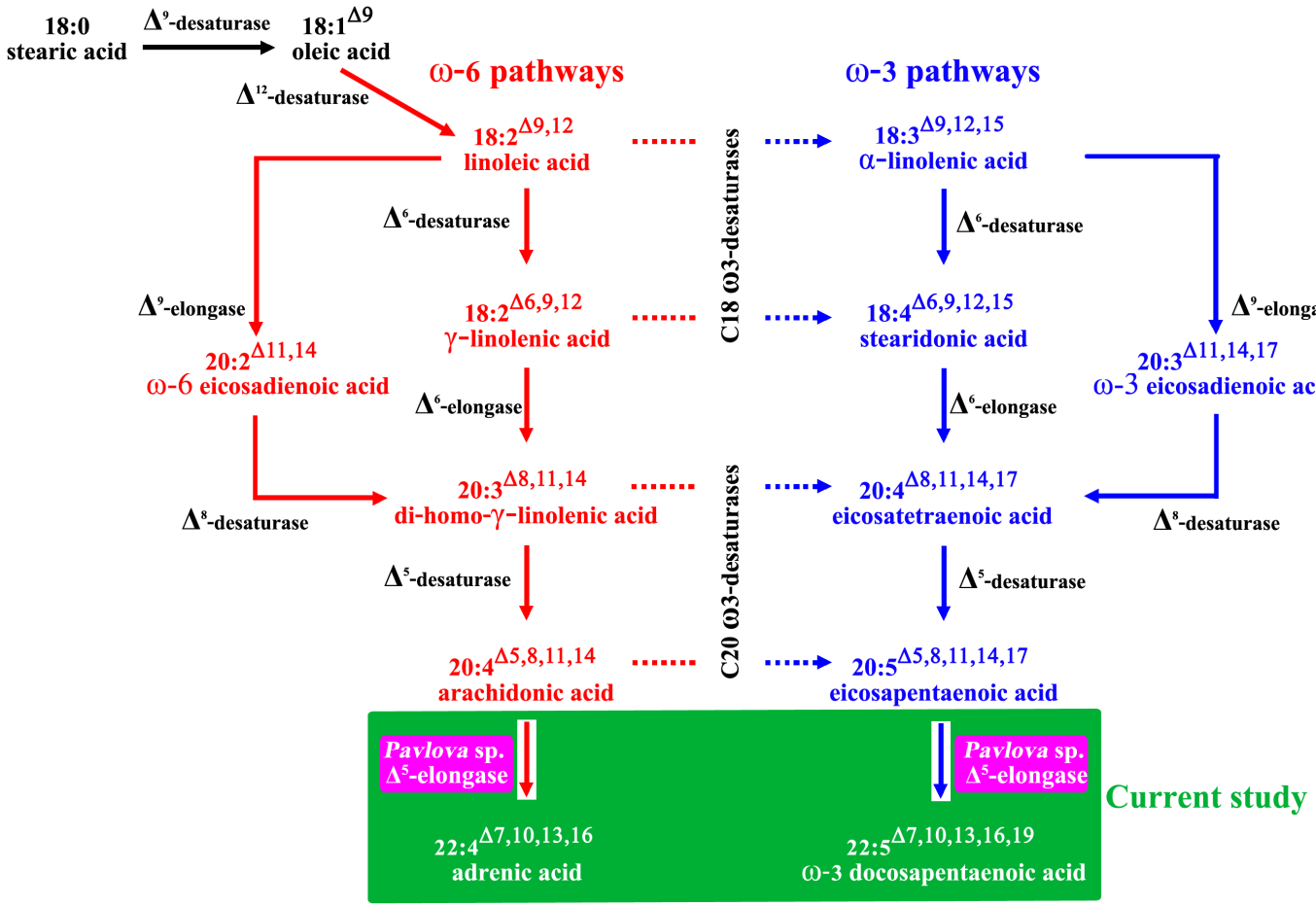

Figure 4.10 A simplified scheme of polyunsaturated fatty acid (PUFA) biosynthesis pathway in lower eukaryotes (modified from Pereira *et al*., 2003).

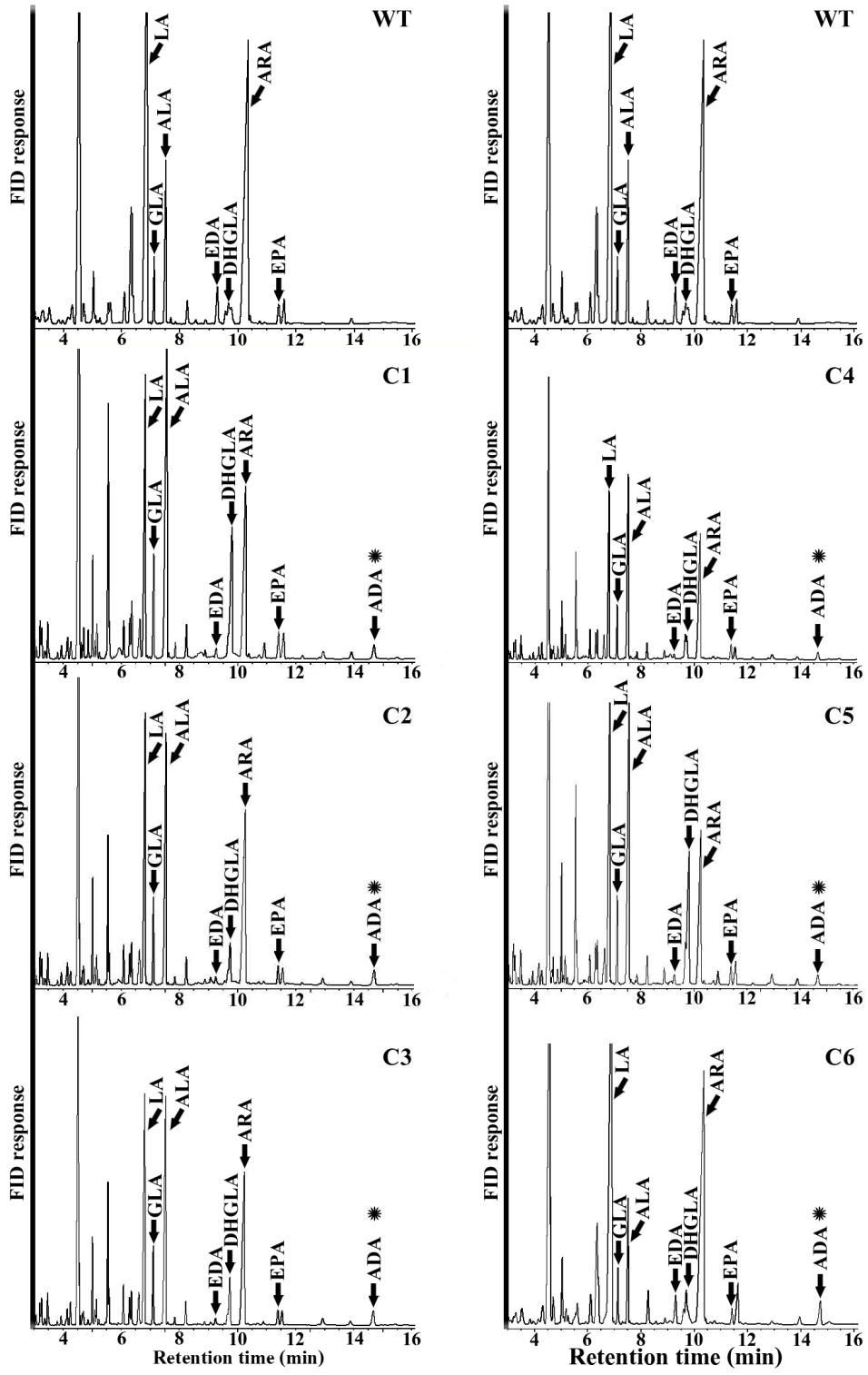

Figure 4.11 Fatty acid profiles of *P. patens* wild type (WT) and the transgenic lines (C1-6). The FAMEs of the total lipids were analyzed by GC. The chromatograms WT and C1-6 show the FAMEs of the protonemata grown in liquid BCD medium for 14 days. The additional peak which corresponds to the retention time of ADA is indicated by asterisk.

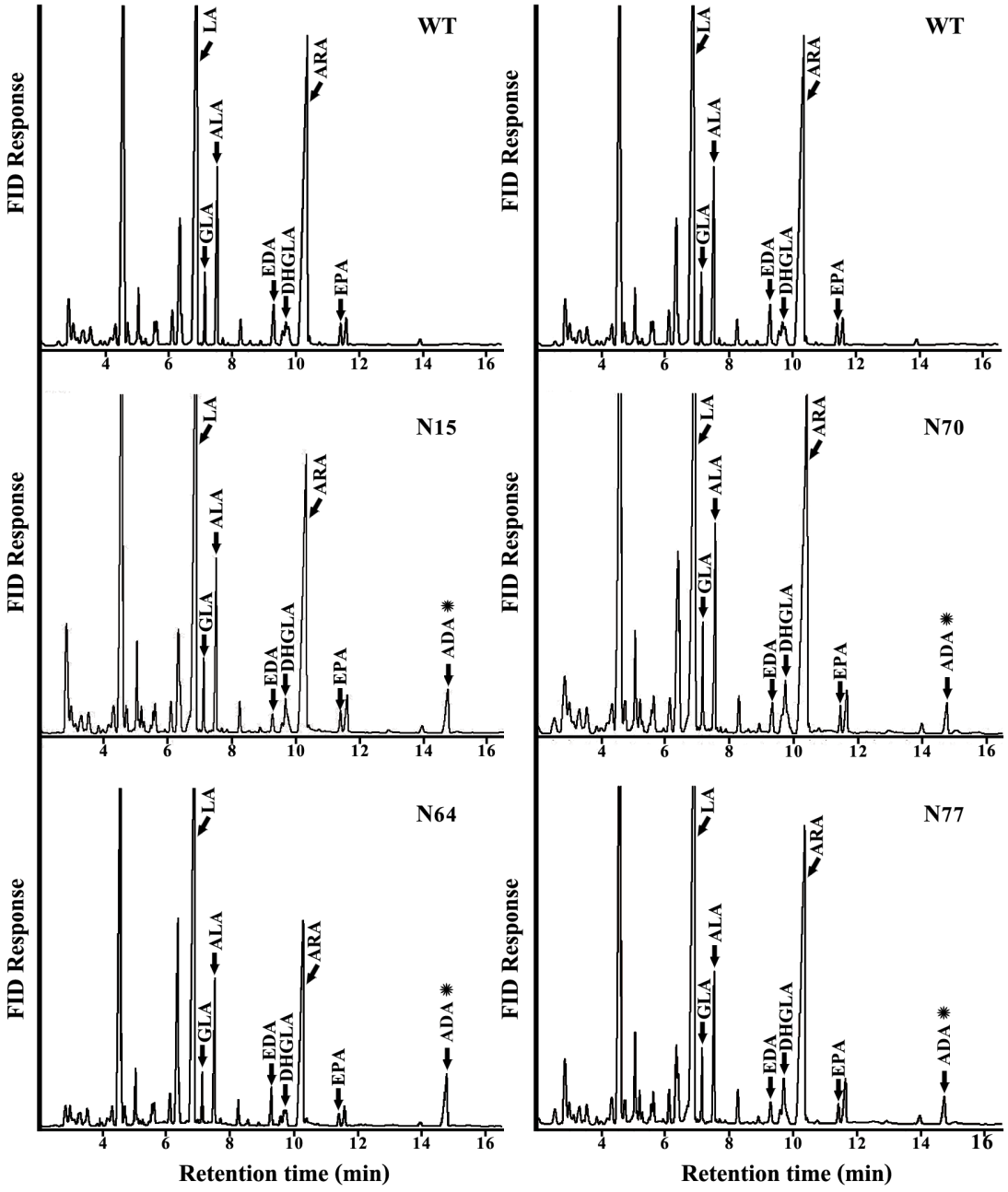

Figure 4.12 Fatty acid profiles of *P. patens* wild type (WT) and the transgenic lines (N15, N64, N70 and N77). The FAMEs of the total lipids were analyzed by GC. The chromatograms WT, N15, N64, N70 and N77 show the FAMEs of the protonemata grown in liquid BCD medium for 14 days. The additional peak which corresponds to the retention time of ADA is indicated by asterisk.

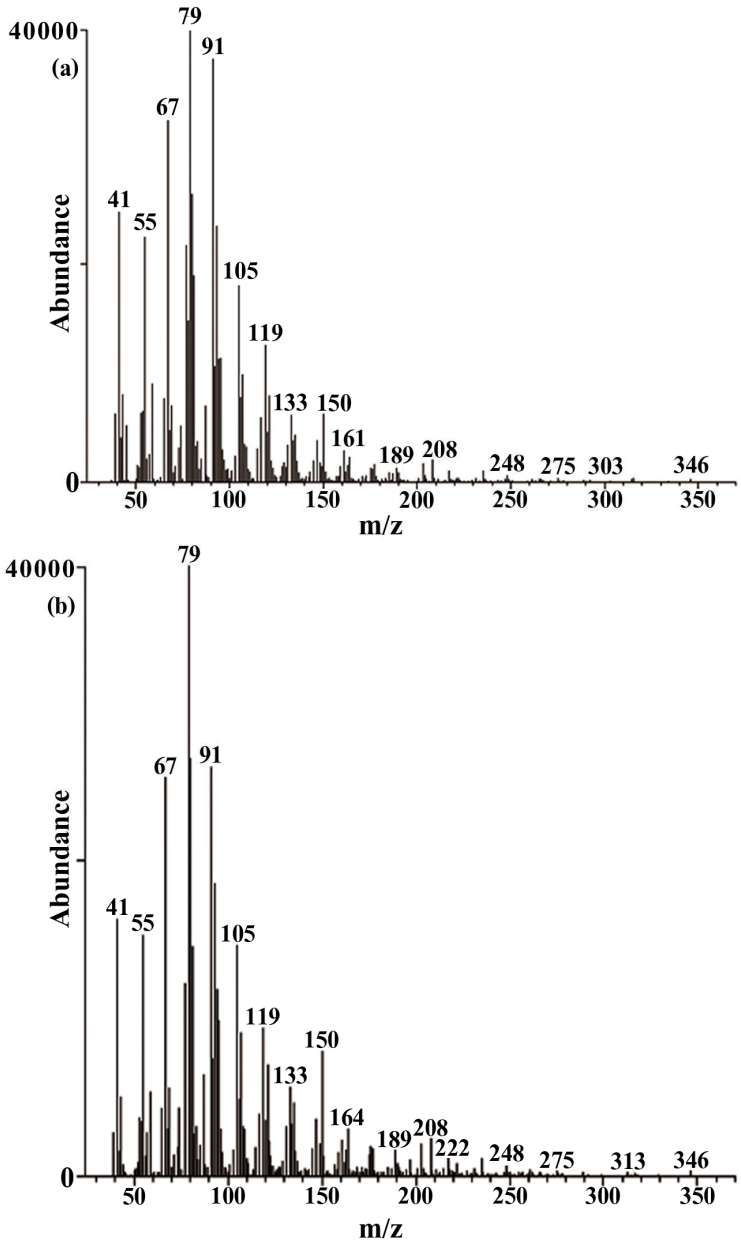

Figure 4.13 GC-MS analysis of FAMEs of the novel peak identified in *P. patens* carrying pMDC32-PsELO5 or pMDC43-PsELO5. A comparison is shown of the mass spectra of the novel peak (a) and an authentic ADA standard (b).

Table 4.1 Biomass and polyunsaturated fatty acid (PUFA) production from the wild type (WT) and transgenic *P. patens* grown in liquid BCD medium for14 days.

Transgenic lines no.	**Biomass (g/l)**	**ω-6 PUFA production (mg/l)**						**ω-3 PUFA production (mg/l)**		
		LA	**GLA**	**EDA**	**DHGLA**	**ARA**	**ADA**	**ALA**	**EPA**	**ω-3 DPA**
WT	5.53±0.95	45.58±8.94	2.96±0.54	2.50±0.75	1.27±0.37	42.89±5.85	nd	9.71±1.75	1.29±0.22	nd
C1	4.07±0.75	27.14±7.73	3.81±0.44	0.41±0.04	5.45±0.44	16.52±2.06	0.17±0.05	16.21±2.34	0.47±0.05	nd
C2	3.83±0.24	24.67±6.98	2.88±0.73	0.45±0.03	1.61±0.27	17.32±3.21	0.15±0.09	12.12±1.95	0.48±0.09	nd
C3	3.77±0.37	21.17±8.53	2.98±0.34	0.41±0.02	1.61±0.52	12.63±2.22	0.15±0.04	10.88±3.09	0.58±0.08	nd
C4	5.17±0.66	22.76±5.45	3.45±0.41	0.53±0.07	2.13±0.33	20.28±2.63	0.22±0.06	15.57±1.88	0.96±0.03	nd
C5	4.40±0.51	33.65±4.44	3.95±0.74	0.66±0.02	7.02±0.27	18.20±2.85	0.20±0.08	18.56±2.34	0.61±0.07	nd
C6	4.83±0.45	41.33±8.48	2.88±0.33	2.05±0.66	1.45±0.22	37.25±5.33	0.42±0.08	8.67±1.22	1.22±0.35	nd
N15	5.43±0.45	63.24±6.77	4.68±0.48	5.80±0.70	1.90±0.34	46.08±6.52	4.47±0.89	13.53±2.04	1.60±0.18	nd
N64	6.00±0.38	64.36±5.04	3.85±0.37	2.52±0.54	4.35±0.54	64.17±7.07	6.97±0.74	13.35±1.85	2.07±0.25	nd
N70	4.97±0.66	69.49±7.84	5.67±0.28	3.10±0.61	4.25±0.61	50.53±5.85	3.57±0.68	14.05±2.65	1.84±0.11	nd
N77	5.03±0.61	53.22±5.83	3.62±0.32	2.52±0.44	4.78±0.53	55.00±6.22	3.40±0.55	9.55±1.38	1.69±0.20	nd

nd, not detected.

level of EPA for further ω-3 DPA production. Successful application of such techniques should help the increasing amount of EPA substrate in *P. patens*.

Expression of the fusion construct in *P. patens* in this study confirmed that ADA, an ω-6 C_{22}-PUFA, was produced from the native ARA substrate, whereas ω-3 DPA production was not generated from the endogenous EPA substrate. The Δ^5-elongation conversion efficiency in *P. patens* for ω-6 PUFAs was higher than for ω-3 PUFAs, probably due to lesser amount of EPA substrate in *P. patens*. Recently, the cotton Δ^{12}-desaturase (FAD2-4)- and marine microalgae *Pavlova viridis* C_{20}-elongase-GFP fusion polypeptides appeared to be functionally expressed in transgenic *Arabidopsis plants* and *E. coli*, respectively, and were shown to localized in the cytoplasmic membrane (Niu *et al*., 2009; Zhang *et al*., 2009). These results also showed that when PsELO5 was attached to the C-terminal of GFP6, PsELO5 function was stronger than with a non-fusion protein. This evidence suggests that the chimeric elongase produced has higher activity, better membrane integration, or greater stability. Similarly, the functional expression of the human KDEL receptor in *Lactococus lastis* has been improved more than ten times by using GFP fusion to the C-terminus (Drew *et al*., 2001). Whereas a fusion gene between GFP and COP1 (Constitutively Photomorphogenic 1) exhibited biological activities identical to the native protein, as shown by genetic complementation of a lethal cop1 allele in transgenic *Arabidopsis* (Von Arnim *et al*., 1998). Nevertheless, these provide the evidences that GFP does not degrade the function of fusion protein. Furthermore, GFP as a reporter gene under regulatory control of 35S promoter, was proved to reduce or avoid the gene silencing in transgenic soybean (El-Shemy *et al*., 2008). Thus the GFP gene in a vector system may play a useful role for transgenic evaluation and avoid gene silencing in transformed plants. These results indicated that expression of the transgene PsELO5 and PsELO5 fused to C-terminus of GFP6, under the control of a tandemly duplicated CaMV35S promoter, were therefore successful. The highest production of ADA (6.97±0.74 mg/l) from the available endogenous ARA substrate was with the transgenic line N64. Although a low level of expression was obtained, other stronger promoters might be applied for higher level gene expression in *P. patens*, including complete rice actin (Act1) (Horstmann *et al*., 2004), wheat early-

methionine labeled (EM) (Knight *et al*., 1995), and maize ubiquitin promoters (Bezanilla *et al*., 2003).

4.2.5 Molecular analysis by PCR and Southern blotting

The specific integration of the transformed DNA into *P.patens* was analyzed by PCR using genomic DNA from the ten transgenic lines (C1, C2, C3, C4, C5, C6, N15, N64, N70 and N77) and the wild type (WT). PCR with the primer pair PsELO5-For/PsELO5-Rev amplified a fragment of 0.8 kbp pairs (kbp), which corresponded to PsELO5 cDNA (Figures 4.14a and b; Figure 4.14d and e) and with the primer pair Hyg^r-For/Hyg^r-Rev, a fragment of 1.0 kbp corresponded to hygromycin resistance coding region from each of the ten transgenic lines (C1, C2, C3, C4, C5, C6, N15, N64, N70 and N77) (Figure 4.14a and c; Figure 4.14d and f), where as the wild type (WT) gave negative results as presented in Figure 4.14b, c, e and f. The length of bands suggested the successful DNA integration, and indicated that PsELO5 and hygromycin resistance genes were transferred into the *P. patens* genome. However, a low number of copies of a transgene in a plant chromosome have a much lower incidence of instability (Jones, 2005). In addition, stably transformed transgenic *P. patens* usually have multiple numbers of integrated transgenes in the genome (Kamisugi *et al*., 2006).

To analyze the integration patterns of transgenes, 14 day-old protonemata of transgenic lines (C6, N15 and N64) and wild type were assessed by Southern blot analysis using probes for the PsELO5 and Hyg^r genes. Transgenic line C6 and lines N15 and N64 were identified as having higher ADA when *P. patens* transformed with pMDC32-PsELO5 and pMDC43-PsELO5, respectively, and were therefore chosen for molecular analysis of the transgene. The results showed that hybridization of genomic DNA from the transgenic lines C6 and N15 digested with *Eco*RV and probed with the PsELO5 probe detected strong signals of 2.3 and 3.0 (a) kbp, respectively (Figure 4.15a2; Figure 4.16a2) and the same size of 2.6 (b) kbp were probed with the Hyg^r probe (Figure Figure 4.15a2; Figure 4.16a2), consistent with the predicted sizes of the relevant fragments resulting from *Eco*RV digestion of pMDC32-PsELO5 (Figure 4.15a1) and pMDC43-PsELO5 (Figure 4.16a1), whereas weak signals of similar sized DNA of line N15 were obtained from transgenic line

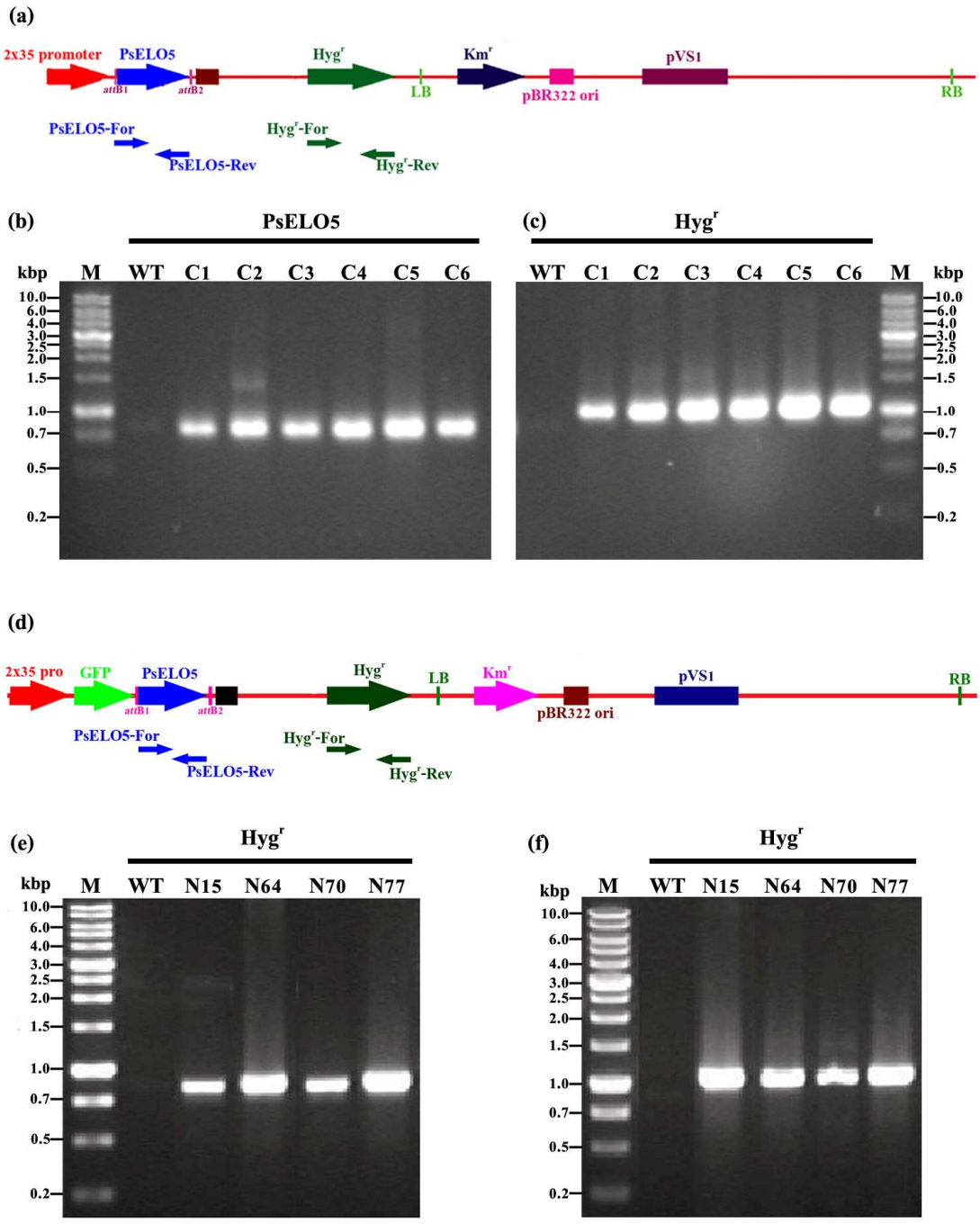

Figure 4.14 Structure of the linear fragments pMDC32-PsELO5 (a) and pMDC43-PsELO5 (d) used for *P. patens* transformation was digested with *Hind*III and verification of PsELO5 and Hyg^r by PCR amplification of *P. pa*tens wild type (WT) compared to transgenic lines C1-6 (b and c), N15, N64, N70 and N77 (e and f). The lettered arrows indicate the binding sites of primers used for PCR analysis. The DNA sizes in kbp are indicated on the left and right.

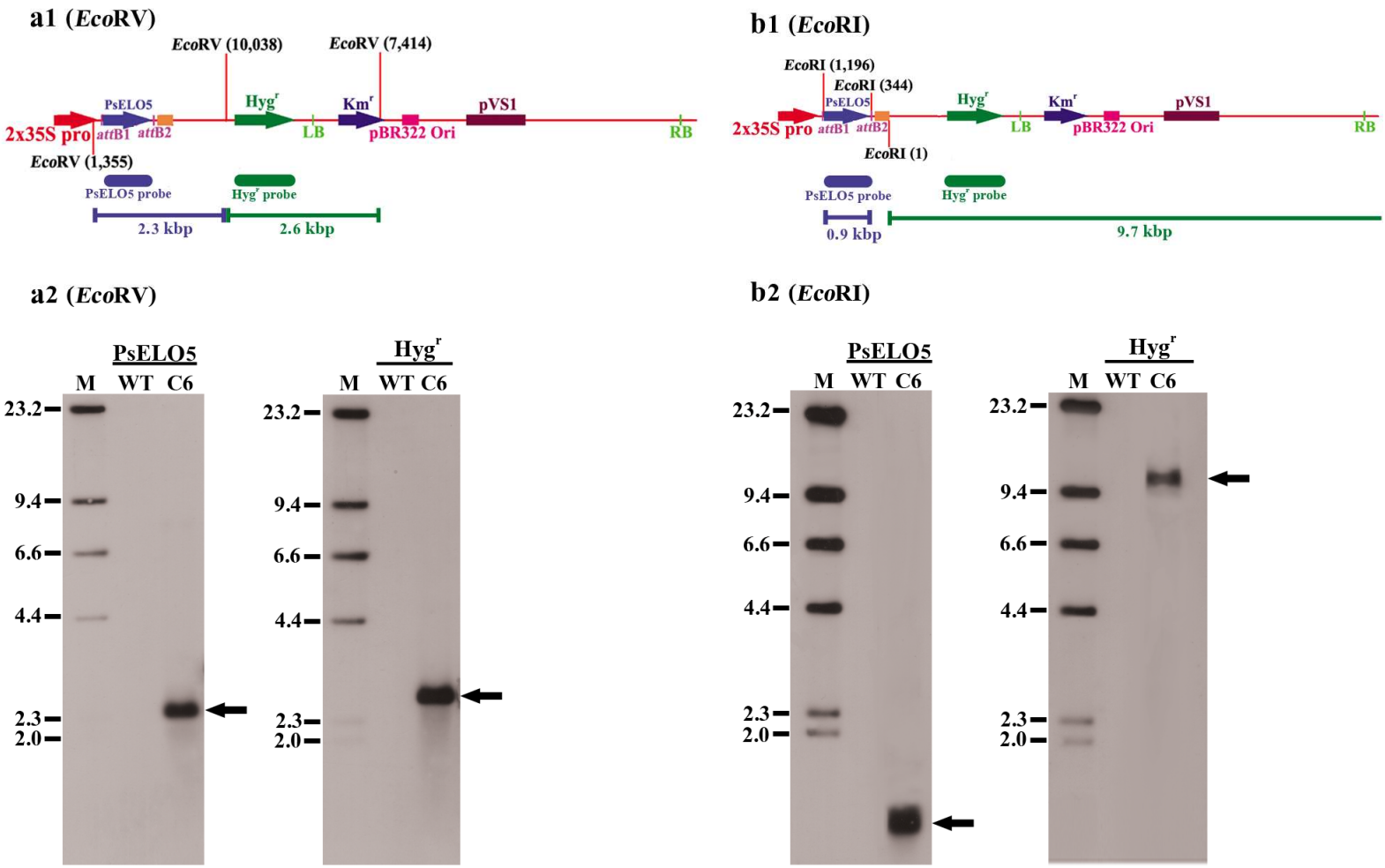

Figure 4.15 Restriction sites of *Eco*RV and *Eco*RI in pMDC32-PsELO5 construct (a1 and b1) and Southern blotting of *P. patens* wild type (WT) compared with transgenic line (C6) (a2 and b2). DNA sizes in kbp are indicated on the left.

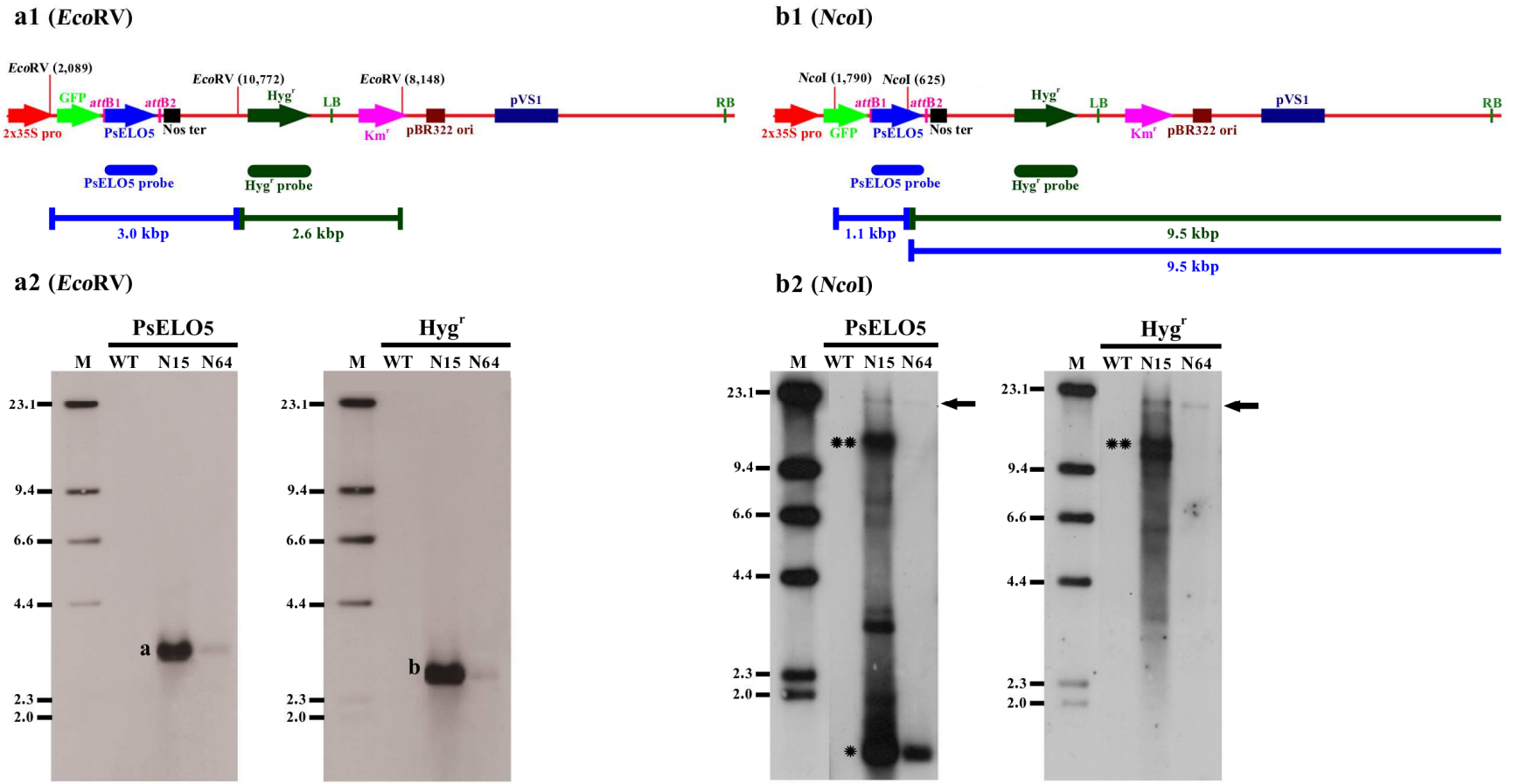

Figure 4.16 Restriction sites of *Eco*RV and *Nco*I in pMDC43-PsELO5 construct (a1 and b1) and Southern blotting of *P. patens* wild type (WT) compared with transgenic line (N15 and N64) (a2 and b2). DNA sizes in kbp are indicated on the left.

N64 (Figure 4.16a2). Similarly, digestion with *Eco*RI generated a single strongly hybridizing fragment of 0.9 and 9.7 kbp (Figure 4.15b2) in transgenic line C6 when hybridized with PsELO5 and Hyg^r probes, respectively, which are the sizes of transgene fragments (Figure 4.15b1). This indicates that line N64 has fewer copies of the transgene than lines C6 and N15.

Digestion with *Nco*I which cuts at 625 bp site within PsELO5 cDNA, produced a high intensity band of 1.1 kbp (*) in transgenic line N15 when hybridized with PsELO5 probe, while a lower intensity band was detected in line N64 (Figure 4.16b2). An additional fragment of 10.5 kbp (**) which is the predicted size of fragments generated by *Nco*I from multiple tandemly repeated copies of pMDC43-PsELO5, hybridized with either PsELO5 or Hyg^r probes (Figure 4.16b1 and b2). However, hybridization with these probes from transgenic line N15 produced the several additional DNA fragments, whereas only one of the flanking sequences was detected in line N64 (arrowed).

These results suggest that line N64 contains only a single copy of the expression construct, whereas there are either multiple copies with rearrangements or several insertion sites of the construct in line C6 and N15. Therefore both single copy and multiple copies of plasmid DNA containing the full length of PsELO5 gene were not only integrated into the transgenic *P. patens* genome and stably inherited to its culture, but also led to successful functional expression. The effects of transgenic copy number on the level of gene expression are known to be complex. Though it was anticipated that the increase of transgene copy number would increase expression level (Dai *et al*., 2001; El-Shemy *et al*., 2007), it is now known that gene co-suppression phenomena frequently occur in transgenic plants with repeated transgene or an unusual structure such as inverted repeats (Vaucheret *et al*., 1998). Moreover, an increased copy number of transgene can correlate with an increased risk of silencing (Lessard *et al*., 2002). Transgenic line N64 with single copy number improved C_{22}-PUFA production rather more than the line with multiple copies of transgene (C6 and N15), suggesting that lower copy number may permit potentially greater gene expression since multiple copy number integration could inhibit transgene expression and even lead to transgene silencing in transgenic plants (Stam *et al*., 1997).

However, the chromosomal insertion site was not controlled in this experiment and so the differences may result from position effects.

4.3 Optimization of culture medium for biomass and C_{22} PUFA production using RSM

Although a tandemly duplicated CaMV35S promoter has been used for transformation, it might not be strong enough for gene expression (Zeidler *et al*., 1996; Horstmann *et al*., 2004). Apart from using stronger promoters, optimization of culture medium is a useful alternative tool for product enhancement. In this study, the highest production line (C6) was further optimized by the RSM experiments (Rao *et al*., 2000). The observed responses (biomass or ADA production) of transgenic *P. patens* (C6) for studying the effects of sucrose (A), KNO_3 (B) and glutamate (C) are summarized in Table 4.2.

Table 4.3 shows the regression coefficient of each variable in terms of linear, quadratic and interaction along with *p*-value for biomass and ADA production. Coefficients with lower *p*-values ($p<0.05$) are more significant. The coefficient estimates and the corresponding *p*-values suggest that among test variables used in the study, sucrose (A), sucrose^2 (A^2), $KNO_3{}^2$ (B^2), glutamate^2 (C^2) were significant for both biomass and ADA production, whereas KNO_3 (B) was significant only for biomass production. In addition, interactions between sucrose (A) and KNO_3 (B); and KNO_3 (B) and glutamate (C) were also significant for biomass production while interaction between sucrose (A) and glutamate (C) was significant for ADA production. Other interactions were found to be insignificant.

The corresponding second-order regression equation provided levels of biomass and ADA production can be predicted by Eqs. (2) and (3), respectively.

$$Y_{\text{biomass (g/l)}} = 16.87 - 0.43A + 0.93B - 0.17C - 0.74A^2 - 0.43B^2 - 0.46C^2 + 0.56AB - 0.22AC + 0.62BC \quad (2)$$

$$Y_{\text{ADA (mg/l)}} = 3.05 - 0.54A + 0.04B + 0.14C - 0.29A^2 - 0.26B^2 - 0.27C^2 + 0.02AB - 0.61AB + 0.13BC \quad (3)$$

Table 4.2 Effect of sucrose (A), potassium nitrate (B) and glutamate (C) concentrations on biomass and ADA production by the transgenic line (C6) using the central composite design technique.

Runs	Sucrose (A) (g/l)	Potassium nitrate (B) (g/l)	Glutamate (C) (g/l)	Biomass production[a] (g/l)		ADA production[a] (mg/l)	
				Actual	Predicted	Actual	Predicted
1	40 (-1)	0.6 (-1)	1.0 (-1)	15.50	15.88	1.88	2.10
2	80 (1)	0.6 (-1)	1.0 (-1)	14.73	14.33	2.02	2.27
3	40 (-1)	1.0 (1)	1.0 (-1)	15.63	15.38	2.04	1.95
4	80 (1)	1.0 (1)	1.0 (-1)	16.10	16.07	1.78	2.05
5	40 (-1)	0.6 (-1)	2.0 (1)	15.30	14.74	3.62	3.32
6	80 (1)	0.6 (-1)	2.0 (1)	12.67	12.32	1.01	1.07
7	40 (-1)	1.0 (1)	2.0 (1)	16.90	16.71	3.98	3.70
8	80 (1)	1.0 (1)	2.0 (1)	17.50	16.53	1.61	1.37
9	20 (-2)	0.8 (0)	1.5 (0)	14.77	14.78	2.77	2.98
10	100 (2)	0.8 (0)	1.5 (0)	12.47	13.05	1.01	0.83
11	60 (0)	0.4 (-2)	1.5 (0)	13.11	13.28	2.06	1.93
12	60 (0)	1.2 (2)	1.5 (0)	16.57	16.99	1.93	2.09
13	60 (0)	0.8 (0)	0.5 (-2)	15.53	15.39	2.03	1.69
14	60 (0)	0.8 (0)	2.5 (2)	13.97	14.71	1.86	2.23
15	60 (0)	0.8 (0)	1.5 (0)	16.80	16.87	3.05	3.05
16	60 (0)	0.8 (0)	1.5 (0)	16.93	16.87	3.00	3.05
17	60 (0)	0.8 (0)	1.5 (0)	16.63	16.87	3.00	3.05
18	60 (0)	0.8 (0)	1.5 (0)	16.60	16.87	3.09	3.05
19	60 (0)	0.8 (0)	1.5 (0)	16.80	16.87	3.08	3.05
20	60 (0)	0.8 (0)	1.5 (0)	16.87	16.87	3.04	3.05

ADA, adrenic acid.

[a]The values given in the table are the means of three dependent experiments.

Table 4.3 Analysis of variance (ANOVA) for response surface quadratic model of biomass and ADA production of the transgenic line (C6).

Factor	**Biomass production**							**ADA production**						
	C.E.[a]	**S.E.**[b]	**SS**[c]	**Df**[d]	**MS**[e]	***F*-value**	**Probe > *P*** ***P*-value**	**C.E.**[a]	**S.E.**[b]	**SS**[c]	**Df**[d]	**MS**[e]	***F*-value**	**Probe > *P*** ***P*-value**
Model	16.87	0.22	40.58	9	4.51	14.74	**0.0001**[*]	3.05	0.11	12.00	9	1.33	16.52	**< 0.0001**[*]
A	-0.43	0.14	3.00	1	3.00	9.82	**0.0106**[*]	-0.54	0.071	4.64	1	4.64	57.47	**<0.0001**[*]
B	0.93	0.14	13.78	1	13.78	45.04	**< 0.0001**[*]	0.039	0.071	0.025	1	0.025	0.31	0.5905
C	-0.17	0.14	0.47	1	0.47	1.53	0.2449	0.14	0.071	0.29	1	0.29	3.64	0.0853
AB	0.56	0.20	2.49	1	2.49	8.15	**0.0171**[*]	-0.019	0.10	0.002767	1	0.002767	0.034	0.8568
AC	-0.22	0.20	0.38	1	0.38	1.23	0.2938	-0.61	0.10	2.97	1	2.97	36.77	**0.0001**[*]
BC	0.62	0.20	3.04	1	3.04	9.94	**0.0103**[*]	0.13	0.10	0.14	1	0.14	1.69	0.2221
A^2	-0.74	0.11	13.74	1	13.74	44.90	**< 0.0001**[*]	-0.29	0.057	2.06	1	2.06	25.49	**0.0005**[*]
B^2	-0.43	0.11	4.73	1	4.73	15.46	**0.0028**[*]	-0.26	0.057	1.69	1	1.69	21.00	**0.0010**[*]
C^2	-0.46	0.11	5.22	1	5.22	17.08	**0.0020**[*]	-0.27	0.057	1.86	1	1.86	23.09	**0.0007**[*]

The bold values indicate the significance at or above the 95.0% confidence level.

[*]Significant at $p < 0.05$; [a]Coefficient estimate; [b]Standard error; [c]Sum of squares; [d]Degree of freedom; [e]Mean squares.

A, sucrose; B, potassium nitrate; C, glutamate. ADA, adrenic acid.

The fit of the model for biomass and ADA production expressed by the coefficients of regression R^2 which were found to be 0.9299 and 0.9370, respectively, indicating that the second-order polynomial model Eqs. (2) and (3) could explain 92.99% and 93.70% of the total variation, respectively.

Three-dimensional and 2-D contour plots are the graphical representations of the regression equation and help in the identification of the type of interactions between test variables. The maximum predicted value is indicated by the surface confined in the smallest ellipse in the contour diagram (Tanyildizi *et al*., 2005). The circular contour plots indicate that the interaction between the corresponding variables is negligible. An elliptical or saddle nature of the contour plots indicates significance of the interactions between the corresponding variables. Figure 4.17 and 4.18 depicts the significant interaction between two variables by keeping the other variables at their middle levels for biomass and ADA production.

The interaction effects of sucrose (A)-potassium nitrate (B) and potassium nitrate (B)-glutamate (C) on biomass production are presented in Figure 4.17. At middle sucrose concentration (60 g/l), an increase in biomass production was obviously observed with the high level of potassium nitrate (1.00-1.20 g/l) (Figure 4.17a1 and a2) and glutamate (2.00 g/l) (Figure 4.17b1 and b2) used. The evidence from this study suggested that the cell growth was induced by relatively middle concentration of sucrose. Recently, it was reported that sucrose plays a central role in plant growth and development as a primary transport form of carbon and energy in plant cell cultures and also as a regulation of gene expression and signal transduction (Smeekens, 2000). However, the optimal sucrose concentration may vary with different plant species. e.g., Gertlowski and Petersen (1993) studied the influence of sucrose concentration on biomass production in culture of *Coleus blumei* and found that a high initial sucrose concentration of 60 g/l led to a high biomass accumulation without an obvious lag phase. Zhong *et al*. (1994) found that the production of biomass increased with an increase of sucrose concentration from 30 to 45 g/l in culture medium of *Perilla frutescens*, while Zhong and Yoshida (1995) and Shinde *et al*. (2009) found that the growth rate increased with an increase of sucrose concentration up to 60 and 70 g/l in the culture medium of *P. frutescens* and *Psoralea corylifolia*, respectively. Moreover, an even higher sucrose concentration of 70-100

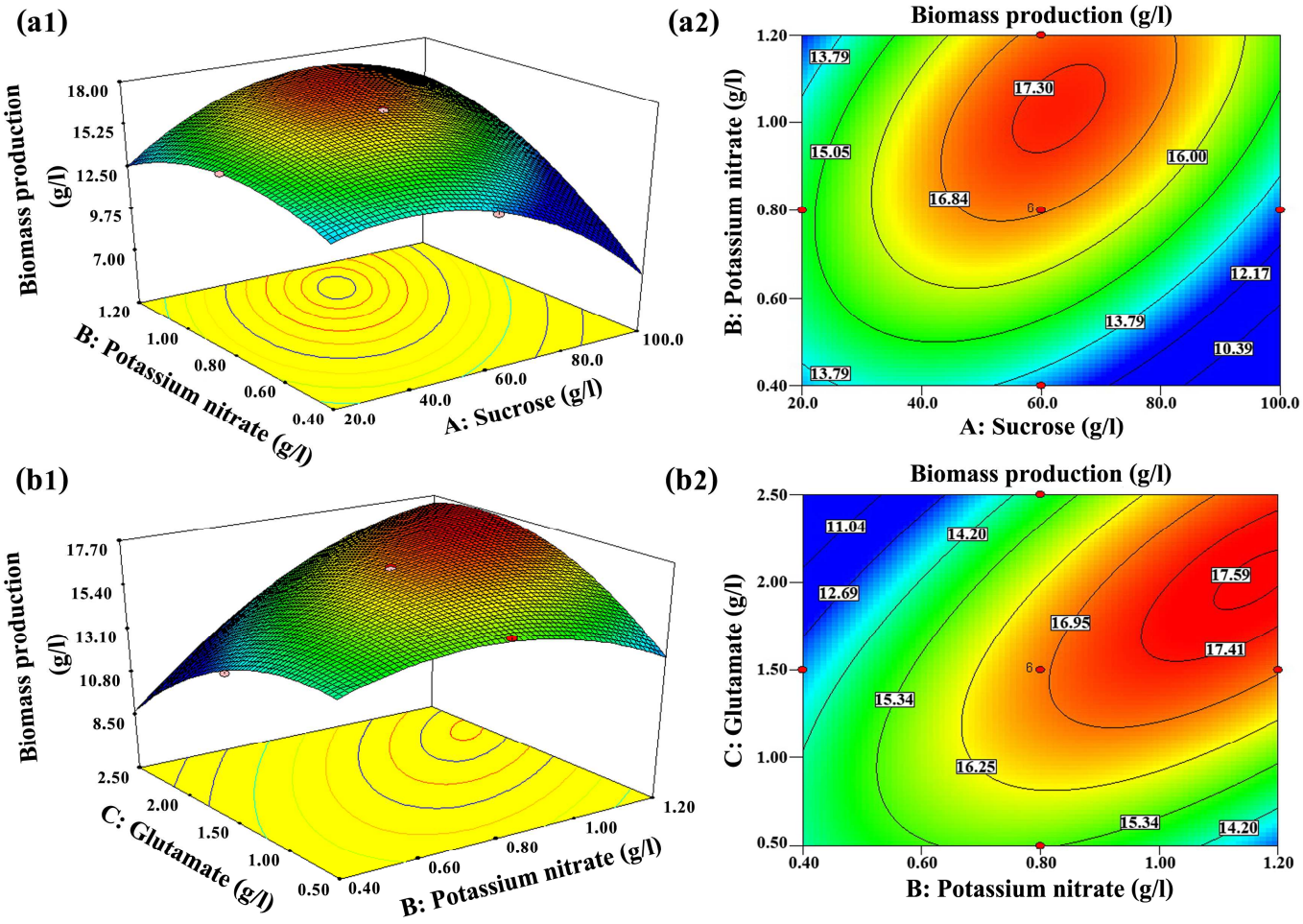

Figure 4.17 Response surface and corresponding contour plots showing the effects of sucrose and potassium nitrate (a1 and a2), potassium nitrate and glutamate (b1 and b2) on biomass production of the transgenic line C6.

g/l seemed to repress the cell growth. The result suggested that the cell growth was repressed by relatively higher concentration of sucrose, which led to a relatively higher osmotic pressure (Kimball *et al*., 1975).

It has been well known that nitrogen is an important nutrient affecting the growth of many organisms such as bacteria, algae, diatom and plant. Nitrate-N is widely used as the sole nitrogen source for microalgae culture because there is less likelihood of pH shift in the medium compared to ammonium-N (Yongmanitchai and Ward, 1991). However, the influence of nitrogen source might be species specific. Yongmanitchai and Ward (1991) found that the production of biomass increased with an increase of nitrate concentration from 0.25 to 1.00 g/l, but decreased at concentration of nitrate of 1.5 g/l in the culture of *P. tricornutum*. Wen and Chen (2001b) indicated that potassium nitrate was the most favorable nitrogen source nitrogen source for biomass production by the diatom *Nitzschia laevis* and found that the production of biomass increased with an increasing nitrate concentration from 0.065 to 0.620 g/l.

Glutamate is involved in nitrogen metabolism and is required as an essential precursor of protein and nucleotide synthesis as well as a substrate for energy metabolism in the organism (Wice *et al*., 1981). In addition, glutamate can stimulate aerobic glycolysis (Pellerin and Magistretti, 1994). Therefore, glutamate could potentially have a substantial influence on cell growth. Cliquet and Jackson (1999) and Yu *et al*. (2003) reported that glutamate supported biomass accumulations of *Paecilomyces fumosoroseus* and *M. alpina*, respectively.

Figure 4.18 shows the significant interaction between sucrose (A) and glutamate (C) on ADA production. Maximum ADA production was obtained at relatively low concentration (20 g/l) of sucrose and high glutamate concentration (2.00-2.50 g/l). In plant cell cultures, sucrose was hydrolyzed to glucose and fructose by extracellular and/or cell wall bound invertase (Martinez and Park, 1993). These sugars could be converted directly to acetyl-CoA used for fatty acids synthesis and provided additional reducing power, NADPH, for the various desaturation enzymes needed to produce ARA (Jin *et al*., 2008; Jin *et al*., 2009), which is precursor of ADA biosynthesis. Glutamate was demonstrated to have a role in activating acetyl-CoA carboxylase (ACC; EC 6.4.1.2). ACC catalyzes the formation of malonyl-CoA, an

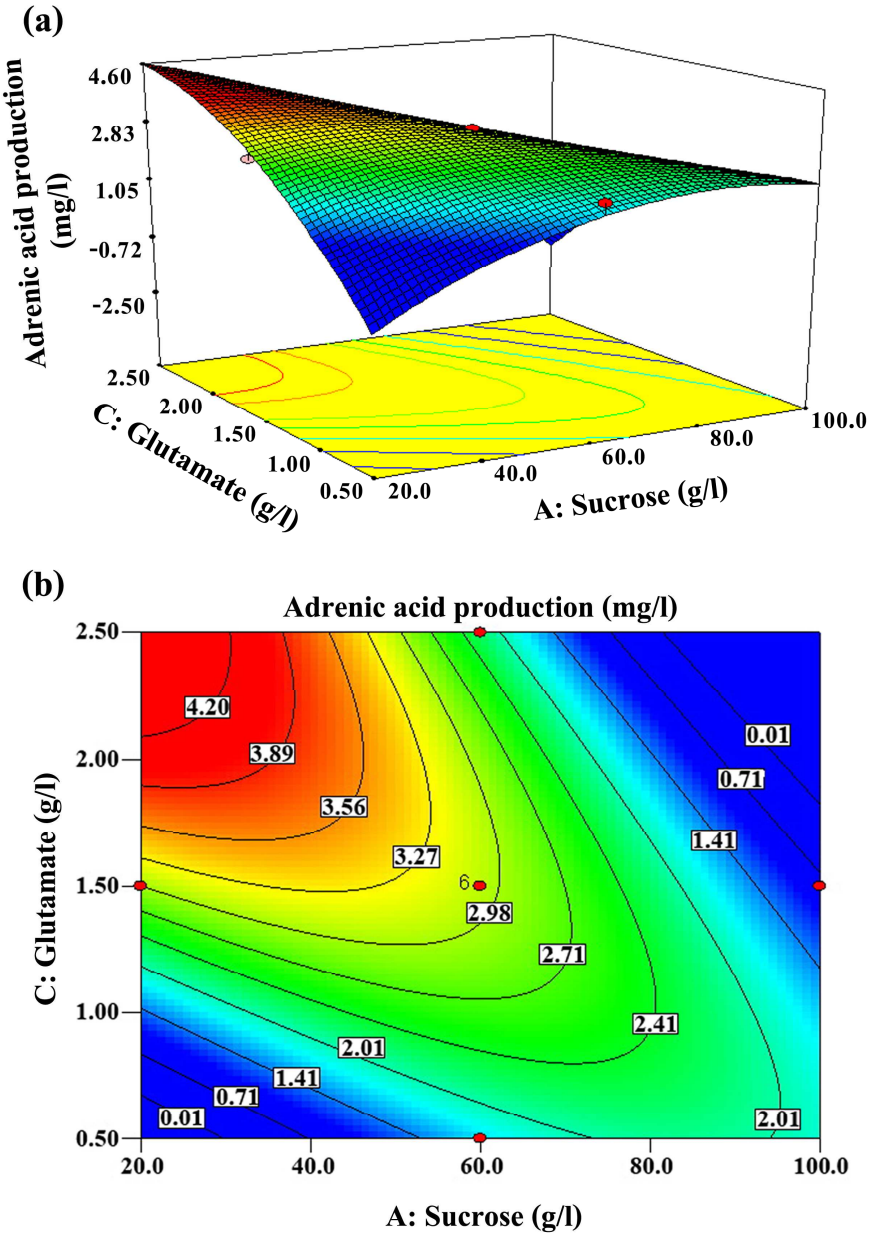

Figure 4.18 Response surface (a) and corresponding contour plots (b) showing the effects of sucrose and glutamate on ADA production of the transgenic line (C6).

essential substrate for fatty-acid synthase and for fatty acyl chain elongation systems (Kowluru *et al*., 2001). Furthermore, glutamate can be utilized for fatty acid synthesis, either directly through the generation of keto acids or acetyl-CoA (Albers *et al*., 1996). Yu *et al*. (2003) studied the influence of glutamate concentration on total lipids and ARA production and found that supplementation of less than 0.8 g/l glutamate could increase total lipids and ARA production. However, supplementation of greater than 0.8 g/l glutamate led to a decrease in the total lipids in biomass as well as ARA production. Singh and Ward (1998) found that glutamate was the best nitrogen sources for DPA production by *Pythium acanthicum*. Certik *et al*. (1999) reported that glutamate was one of the potentially available nitrogen sources for increasing G6PDH activities and enhancing PUFA biosynthesis. However, when glutamate concentration is too high (greater than 0.8 g/l), glutamate will be converted to proline accompanied by NADPH consumption (Andarwulan and Shetty, 1999), which is necessary for ARA biosynthesis.

4.4 Experimental validation of the optimized conditions

The information from the equation models (Eqs. 2 and 3) and the plots (Figure 4.17 and 4.18), relating to the optimal levels of sucrose (A), potassium nitrate (B) and glutamate (C) for maximum biomass (Experiment A) and ADA (Experiment B) production are summarized in Table 4.4. The predicted and actual experimental responses (biomass and ADA production) for each set of variables are also presented. Maximum production rates of 17.15 g/l DCW and 1.77 mg/l ADA, and 13.05 g/l DCW and 4.48 mg/l ADA, were obtained from experiments A and B, respectively.

This represents 90-97 and 81-99% validity of the prediction models, respectively. This study therefore suggests that the final optimal culture conditions would be sucrose 61.79 and 22.06 g/l; potassium nitrate 1.18 and 1.00 g/l; glutamate 2.05 and 2.35 g/l; These conditions would lead to maximum production of biomass of 17.15 g/l and ADA of 4.48 mg/l, respectively, which is 3.55-fold and 10.66-fold higher, respectively, than production rates in the non-optimization study (4.83 g/l biomass and 0.42 mg/l ADA).

Table 4.4 Predicted and actual biomass and ADA production by *P. patens* suspension cultures using various culture conditions.

Experiments[a]	**Sucrose (A) (g/l)**	**Potassium nitrate (B) (g/l)**	**Glutamate (C) (g/l)**	**Biomass production**[b] **(g/l)**			**ADA production**[b] **(mg/l)**		
				Actual	**Predicted**	**%validity**	**Actual**	**Predicted**	**%validity**
A	61.79	1.18	2.05	17.15	17.65	90	1.77	2.16	81
B	22.06	1.00	2.35	13.05	14.38	97	4.48	4.51	99

The cells were cultured in 250-ml shake-flasks containing the total volume of 100 ml final production liquid medium with 4 g inoculums and incubated for 14 days.

[a]A and B, experiments based on maximum growth and ADA production conditions, respectively.

[b]Represents mean of the responses (biomass and ADA production) based on three separate experiments.

ADA, adrenic acid.

4.5 Effects of EPA and oil supplementation on biomass, ADA and ω-3 DPA in transgenic *P. patens*

Although only ADA, an ω-6 C_{22}-PUFA was initially produced in the transgenic lines, the further experiments were carried out to manipulate ω-3 DPA, an ω-3 C_{22}-PUFA production in *P. patens* by EPA and vegetable oil supplementation. In general, EPA is a directly precursor for ω-3 DPA and vegetable oils contain various fatty acids that serve as precursors of long chain fatty acid (LC-FA) biosynthesis. In addition, it has been reported that supplementation with 1% oil improve biomass and PUFA production in *M. alpina* (Jang *et al*., 2005). Therefore the five highest ADA producing lines (C6, N15, N64, N70 and N77) were grown in the previously optimized medium (liquid BCD medium containing 22.06 g/l of sucrose, 1.00 g/l of potassium nitrate and 2.35 g/l glutamate, supplemented with 0.1 mM of EPA (Figure 4.19) or 1.0% vegetable oil mixture comprising linseed oil, soybean oil, sunflower oil, corn oil, and palm oil (0.2% of each oil) (Figure 4.20). An additional peak (RT = 15.7 min) was detected which was identical to the retention time of authentic ω-3 DPA from both experiments (Figure 4.19 and 4.20). This compound also showed a molecular ion of 344 m/z, which is the expected molecular ion of methyl ester of ω-3 DPA as well as a fragmentation pattern identical to that of the authentic ω-3 DPA methyl ester (Figure 4.21). This event can be concluded that ω-3 DPA was successfully activated in *P. patens* by exogenous substrate supplementation.

This study also confirmed that PsELO5 is specific only for ARA and EPA which are C_{20} PUFA, without any activity toward C_{16} and C_{18} fatty acids, which is in agreement with the previous report (Pereira *et al*., 2004b). Based on the specificity to substrate fatty acids, ELO-like enzymes can be classified broadly into three groups: one is specific to saturated and monounsaturated fatty acid (SFA and MUFA), another to PUFA of fixed chain-length (“single-step”), and the other is to PUFA with variable chain-lengths (“multi-step”) (Meyer *et al*., 2004). PsELO5 showed specificity only to C_{20} PUFA (Pereira *et al*., 2004b); this specificity also seen with algal Δ^5-elongases from *Ostreococcus tauri, Thalassiosira pseudonana* (Meyer *et al*., 2004), and liverwort *Marchantia polymorpha* (Kajikawa *et al*., 2006), and thus PsELO5 belongs to the second group (“PUFA single-step”).

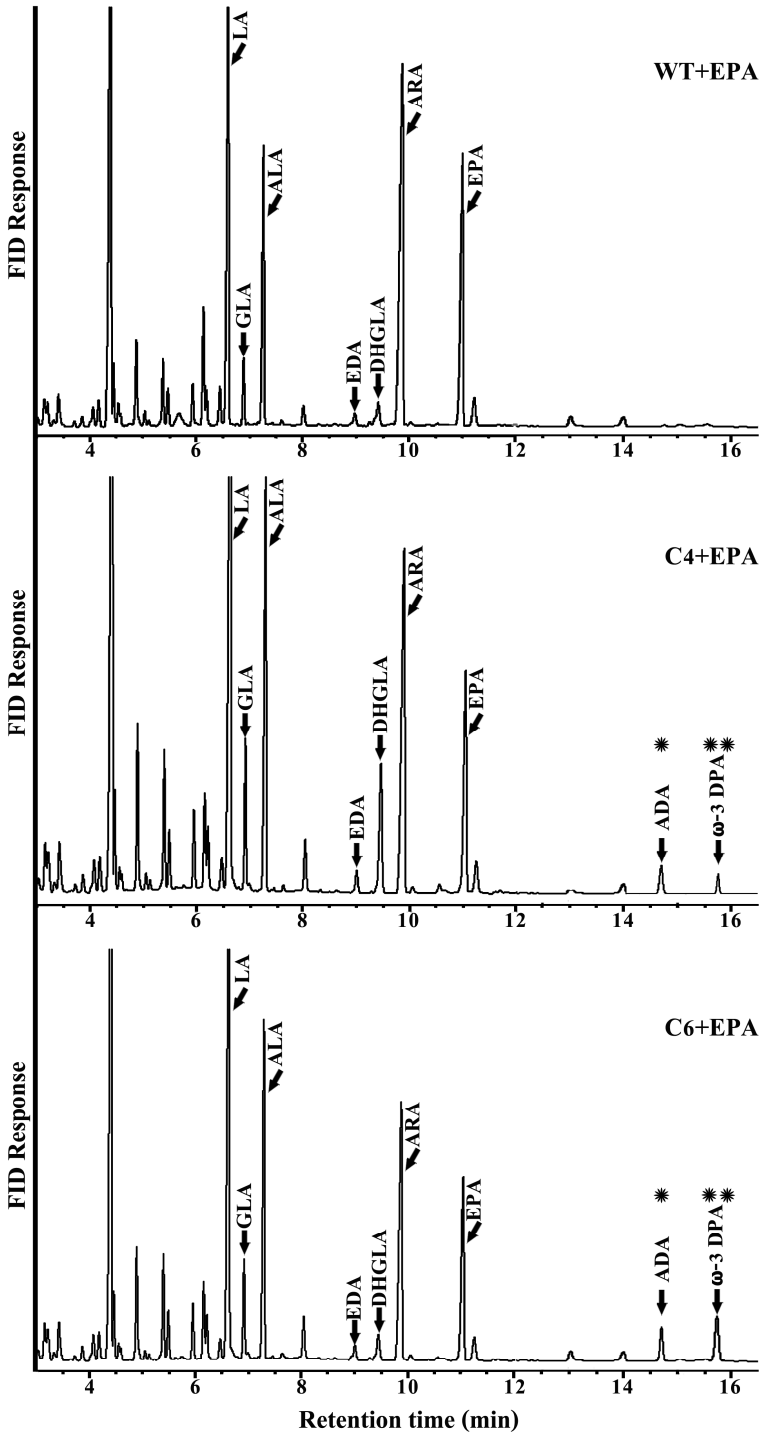

Figure 4.19 Gas chromatographic analysis of fatty acid methyl esters (FAMEs) from 14 day-old protonemata *P. patens* wild type (WT) and transgenic lines (C4 and C6). The protonemata is grown in optimized liquid BCD medium containing 22.06 g/l of sucrose, 1.00 g/l of potassium nitrate and 2.35 g/l glutamate and supplemented with 0.1 mM EPA. The additional peaks which correspond to the retention time of ADA and ω-3 DPA are indicated by single asterisk and double asterisks, respectively.

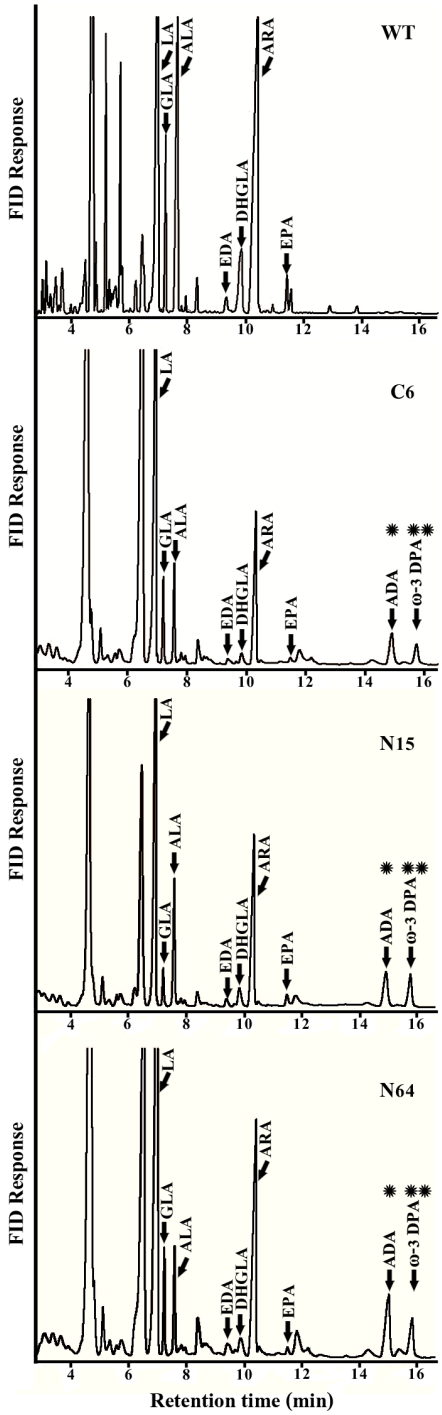

Figure 4.20 Gas chromatographic analysis of fatty acid methyl esters (FAMEs) from 14 day-old protonemata *P. patens* wild type (WT) and transgenic lines (C6, N15, and N64). The protonemata is grown in previously optimized liquid BCD medium containing 22.06 g/l of sucrose, 1.00 g/l of potassium nitrate and 2.35 g/l glutamate and supplemented with a total of 1.0% vegetable oils including linseed oil, soybean oil, sunflower oil, corn oil, and palm oil (0.2% of each oil). The additional peaks which correspond to the retention time of ADA and ω-3 DPA are indicated by single asterisk and double asterisks, respectively.

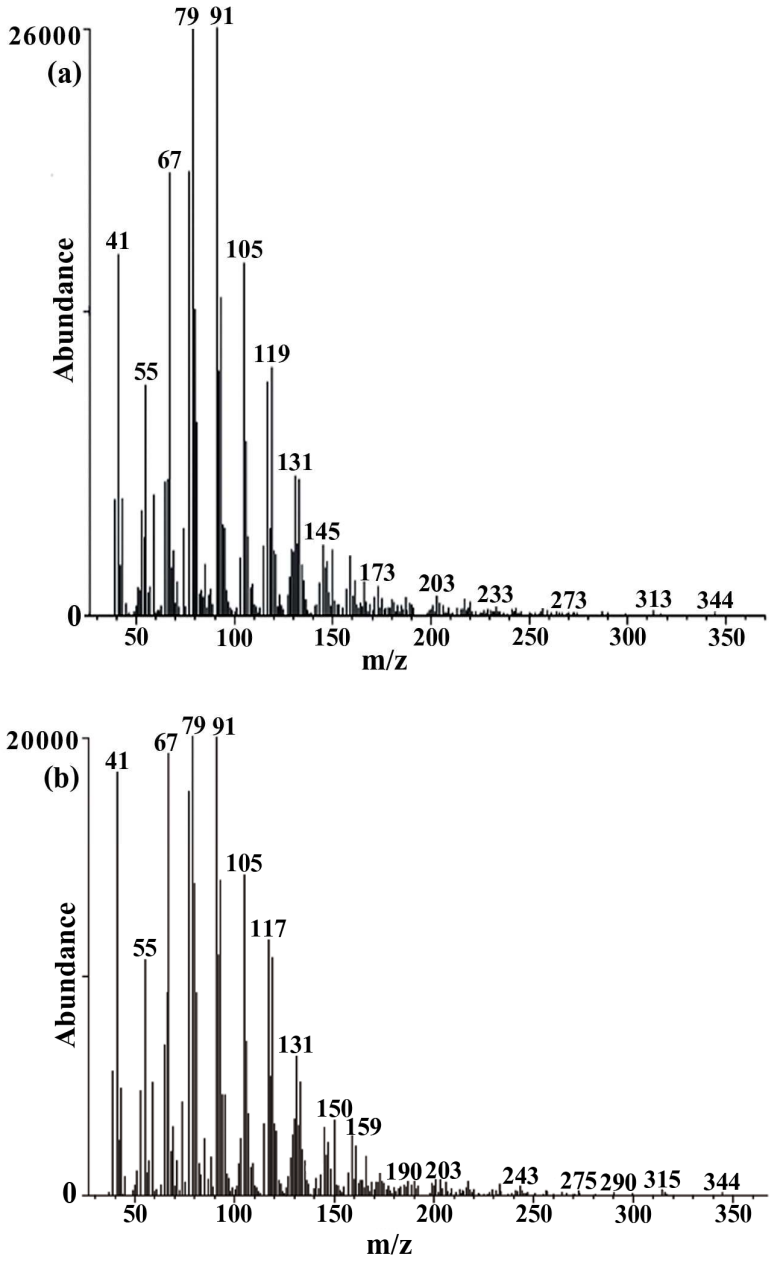

Figure 4.21 GC-MS analysis of FAMEs of the novel peak identified in *P. patens* carrying pMDC32-PsELO5 or pMDC43-PsELO5. A comparison is shown of the mass spectra of the novel peak (a) and an authentic ω-3 DPA standard (b).

The effect of the vegetable oil supplement on the biomass and PUFA production of transgenic *P. patens* plants compared with the wild type is illustrated in Table 4.5. Supplementation with a total of 1.0% vegetable oils increased biomass 2.24-fold and PUFAs 4.04-9.03-fold, compared to the amounts detected in the wild type in the previously optimized liquid BCD medium without oil supplement. In the same way, the addition of oils enhanced biomass and PUFAs in transgenic *P. patens* (C6, N15, N64, N70 and N77) especially C_{22}-PUFAs, ADA and ω-3 DPA (Figure 4.22a and b; Table 4.5), whereas EDA decreased in those transgenic lines. Vegetable oils generally contain high levels of C_{18}-fatty acid, precursors for LC-FA biosynthesis. For example, LA is the major fatty acid in soybean oil, corn oil and sunflower oil (56-85%), ALA is the major fatty acid in linseed oil (58%) (Jang *et al*., 2005), and oleic acid (OA) is rich in palm oil (30-45%) (Mhanhmad *et al*., 2011). Therefore the addition of oils allowed moss to convert C_{18}-fatty acid substrates to LC-PUFAs. Shinmen *et al*. (1989) showed that olive oil and soybean oil addition increased the accumulation of ARA in *Mortierella* fungi and supplementation of oils stimulates cell growth, EPA, DHA and total PUFA production in *M. alpina* (Jang *et al*., 2005). The decrease in EDA levels observed in the transgenic *P. patens* was probably due to the presence of PsELO5-encoded elongase.

Therefore, metabolic engineering with PsELO5 and PsELO5-GFP6 fusion together with oil supplementation successfully activated both ω-6 and ω-3 C_{22}-elongation products, ADA and ω-3 DPA, in transgenic lines from 11.2 to 24.3 and 6.3 to 11.7 mg/l, respectively. These results indicate the maximum accumulation of ADA (2.3% of total fatty acids) and ω-3 DPA (1.1% of total fatty acids) in transgenic line N64 (Table 4.6), 2-11 times higher than other similar studies performed by heterologous expression of multiple PUFA synthesizing genes in higher plants (0.1-1.2% of total fatty acids) (Tables 4.6 and 4.7). This is the first report on producing an ω-3 DPA, DHA precursor, in non-seed lower plant.

Table 4.5 Biomass and polyunsaturated fatty acid (PUFA) production from the wild type (WT) and transgenic *P. patens* expressing PsELO5 grown for 14 days.

Line	Biomass[a]	Biomass[b]	ω-3 PUFA production (mg/l)					
	(g/l)	(g/l)	ALA[a]	ALA[b]	EPA[a]	EPA[b]	ω-3 DPA[a]	ω-3 DPA[b]
WT	5.53±0.95	12.43±0.85	9.71±1.75	39.60±3.75	1.29±0.22	7.71±0.41	nd	nd
C6	4.83±0.45	9.60±0.63	8.67±1.22	13.94±1.84	1.22±0.35	0.96±0.15	nd	6.35±0.43
N15	5.43±0.45	9.37±0.52	13.53±2.04	20.48±0.94	1.60±0.18	1.83±0.08	nd	10.27±0.32
N64	6.00±0.38	9.03±0.98	13.35±1.85	15.36±0.87	2.07±0.25	1.45±0.07	nd	11.75±0.41
N70	4.97±0.66	9.33±0.73	14.05±2.65	16.20±2.73	1.84±0.11	1.04±0.05	nd	7.60±0.21
N77	5.03±0.61	9.70±0.57	9.55±1.38	16.03±3.08	1.69±0.20	0.92±0.12	nd	8.56±0.18

Line	ω-6 PUFA production (mg/l)											
	LA[a]	LA[b]	GLA[a]	GLA[b]	EDA[a]	EDA[b]	DHGLA[a]	DHGLA[b]	ARA[a]	ARA[b]	ADA[a]	ADA[b]
WT	45.58±8.94	210.68±20.75	2.96±0.54	11.96±0.87	2.50±0.74	10.74±1.28	1.27±0.37	11.85±0.87	42.89±5.85	196.88±13.96	nd	nd
C6	41.33±8.48	88.68±8.39	2.88±0.33	9.09±1.55	2.05±0.66	0.90±0.14	1.45±0.22	2.64±0.32	37.25±5.33	46.85±4.85	0.42±0.08	11.18±0.75
N15	63.24±6.77	70.35±12.95	4.68±0.48	5.06±0.74	5.80±0.70	2.17±0.37	1.90±0.34	5.86±0.54	46.08±6.52	53.56±3.86	4.47±0.89	13.31±0.84
N64	64.36±5.04	144.90±19.76	3.85±0.37	10.86±1.56	2.52±0.54	0.73±0.12	4.35±0.54	5.21±0.24	64.17±7.07	73.41±4.73	6.97±0.74	24.31±0.43
N70	69.49±7.84	86.98±16.85	5.67±0.28	13.36±1.37	3.10±0.61	0.61±0.08	4.25±0.61	5.27±0.11	50.53±5.85	60.27±2.79	3.57±0.68	12.59±0.63
N77	53.22±5.83	111.51±15.96	3.62±0.32	14.29±1.83	2.52±0.44	0.28±0.04	4.78±0.53	4.83±0.77	55.00±6.22	59.83±6.40	3.40±0.55	16.23±0.73

[a]PUFA production from *P. patens* grown for 14 days in liquid BCD medium.

[b]PUFA production from *P. patens* grown for 14 days in optimized liquid BCD medium supplemented with a total of 1.0% vegetable oils including linseed oil, soybean oil, sunflower oil, corn oil, and palm oil (0.2% of each oil).

nd, not detected.

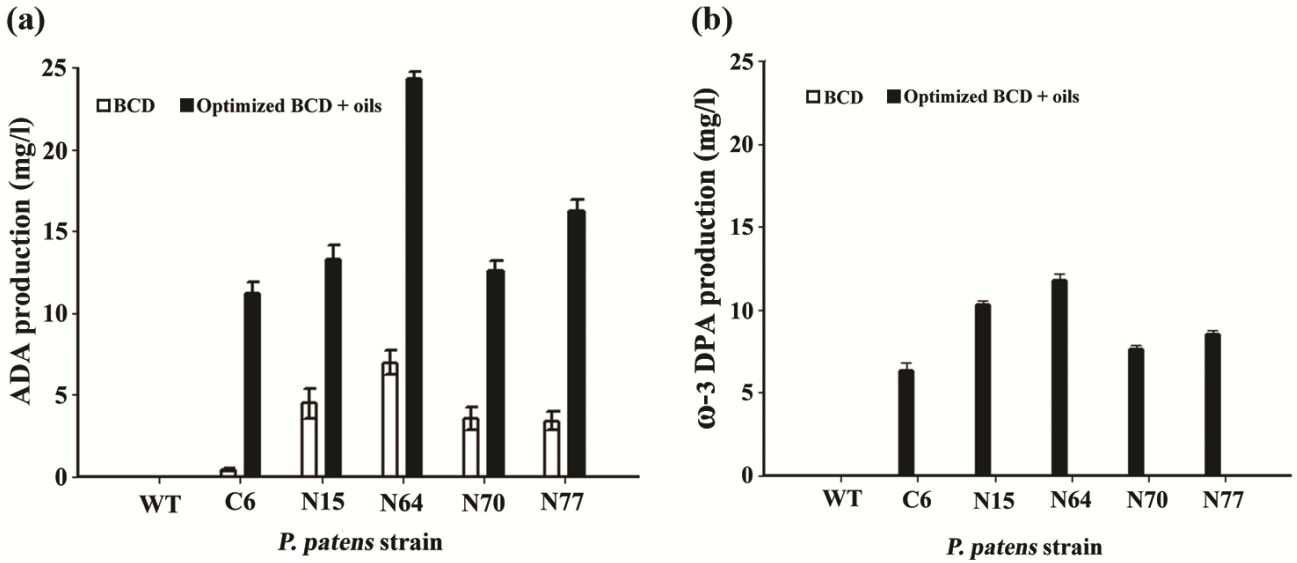

Figure 4.22 Comparisons of ADA (a) and ω-3 DPA (b) production from 14 day-old protonemata *P. patens* wild type (WT) and transgenic lines (C6, N15, N64, N70 and N64) grown in basal liquid BCD medium, and in previously optimized liquid BCD medium containing 22.06 g/l of sucrose, 1.00 g/l of potassium nitrate and 2.35 g/l of glutamate and supplemented with a total of 1.0% vegetable oils including linseed oil, soybean oil, sunflower oil, corn oil, and palm oil (0.2% of each oil).

Table 4.6 Total fatty acid and new C22 PUFA production from the wild type (WT) and transgenic *P. patens* expressing PsELO5 grown for 14 days.

Line	SA and MUFA (mg/l)							
	16:0[a]	**16:0[b]**	**16:1[a]**	**16.1[b]**	**18:0[a]**	**18:0[b]**	**18:1[a]**	**18:1[b]**
WT	85.20±11.75	361.79±15.95	1.72±0.17	33.71±4.85	1.25±0.07	24.48±2.23	14.08±1.81	101.37±9.83
C6	79.82±13.85	329.25±22.72	2.17±0.12	34.97±5.06	2.40±0.50	20.57±1.95	7.62±1.47	206.42±16.93
N15	82.14±11.54	572.76±18.05	1.63±0.31	27.21±3.94	1.09±0.13	17.92±5.33	11.94±1.78	157.64±7.94
N64	86.98±11.00	433.38±20.32	1.37±0.16	42.20±3.61	1.17±0.13	32.05±3.31	15.78±2.06	242.23±35.64
N70	89.56±10.57	297.33±9.98	2.78±0.39	26.09±2.30	2.48±0.49	25.34±1.45	6.98±1.67	227.81±16.48
N77	79.30±19.01	507.18±12.02	1.15±0.06	33.51±4.37	0.92±0.16	37.31±2.99	10.18±2.31	255.72±20.62

Line	Fatty acid production (mg/l)						Total fatty acid production (mg/l)		C_{22} PUFA (% total fatty acids)			
	SFA[a]	**SFA[b]**	**MUFA[a]**	**MUFA[b]**	**PUFA[a]**	**PUFA[b]**	**Total[a]**	**Total[b]**	**ADA[a]**	**ADA[b]**	**DPA[a]**	**DPA[b]**
WT	86.45±11.71	386.27±13.73	15.80±1.93	135.08±5.34	106.13±26.62	489.69±36.13	208.38±37.93	1011.04±39.11	nd	nd	nd	nd
C6	82.22±14.08	349.83±22.39	9.79±1.52	241.39±20.03	94.96±19.55	180.83±33.47	186.97±15.96	772.05±33.04	0.22±0.03	1.46±0.33	nd	0.82±0.16
N15	83.22±11.60	590.67±12.81	13.57±1.54	184.85±4.48	141.51±30.52	183.17±38.83	238.30±17.45	958.70±22.87	1.87±0.30	1.39±0.23	nd	1.07±0.17
N64	88.16±10.90	465.43±22.99	17.14±2.21	284.43±39.24	161.71±13.73	288.06±56.86	267.01±0.88	1037.91±60.88	2.61±0.31	2.33±0.32	nd	1.13±0.22
N70	92.04±10.31	322.67±10.43	9.76±1.80	253.90±16.90	152.57±28.92	204.27±50.38	254.37±20.34	780.84±52.98	1.39±0.16	1.62±0.29	nd	0.97±0.15
N77	80.22±19.17	544.48±15.01	11.33±2.37	289.24±16.26	133.78±4.25	232.73±22.52	225.34±16.50	1066.45±15.95	1.51±0.07	1.52±0.26	nd	0.80±0.10

[a]PUFA production from *P. patens* grown for 14 days in liquid BCD medium.

[b]PUFA production from *P. patens* grown for 14 days in optimized liquid BCD medium supplemented with a total of 1.0% vegetable oils including linseed oil, soybean oil, sunflower oil, corn oil, and palm oil (0.2% of each oil).

nd, not detected.

Table 4.7 Examples of polyunsaturated fatty acid (PUFA) production in transgenic plants.

Plant host	**Target gene**	**New fatty acid production (% of total fatty acid)**	**Reference**
Arabidopsis thaliana	*Danio rerio* Δ^5/Δ^6-desaturase, *Caenorhabditis elegans* Δ^6-elongase, *Pavlova salina* Δ^5-elongase and *P. salina* Δ^4-desaturase	GLA (0.4%), SDA (1.5%), DHGLA (1.5%), ETA (0.8%), ARA (1.0%), EPA (2.4%), ω-3 DPA (0.1%), DHA (0.5%)	Robert *et al*., (2005)
Brassica juncea	*Pythium irregulare* Δ^6-desaturase, *Thraustochytrium* sp. Δ^5-desaturase, *P. patens* Δ^6-elongase, *Calendula officinalis* Δ^{12}-desaturase, *Thraustochytrium* sp. Δ^6-elongase, *P. irregulare* ω3-desaturase, *Thraustochytrium* sp. Δ^4 desaturase, *Thraustochytrium* sp. lysophosphatidyl acyltransferase, *Oncorhynchus mykiss* elongase	GLA (27.3%), SDA (2.2%), DHGLA (1.9%), ETA (1.1%), ARA (4.0%), EPA (8.1%), ω-3 DPA (0.1%), DHA (0.2%)	Wu *et al*., (2005a)
Nicotiana benthamiana	*Micromonas pusilla* Δ^6-desaturase, *Pyramimonas cordata* Δ^6-elongasea[a] and *P. salina* Δ^5-desaturase	GLA (2.1%), ARA (0.6%), SDA (1.5%), ETA (0.6%), EPA (10.7%), ω-3 DPA (0.3%)	Petrie *et al*., (2010c)
N. benthamiana	*Echium plantagineum* Δ^6-desaturase, *P. cordata* Δ^6-elongasea[a] and *P. salina* Δ^5-desaturase	GLA (4.4%), ARA (1.3%), SDA (2.4%), ETA (0.1%), EPA (3.4%), ω-3 DPA (0.2%)	Petrie *et al*., (2010c)
N. benthamiana	*Ostreococcus tauri* Δ^6-desaturase, *P. cordata* Δ^6-elongasea[a] and *P. salina* Δ^5-desaturase	GLA (5.8%), ARA (1.2%), SDA (1.1%), ETA (0.4%), EPA (9.6%), ω-3 DPA (0.2%)	Petrie *et al*., (2010c)
N. benthamiana	*P. salina* Δ^9-elongase, Δ^8-desaturase, Δ^5-desaturase, Δ^5-elongase and Δ^4-desaturase	EDA (1.7%), DHGLA (0.5%), ARA (2.4%), ADA (1.2%), ETrA (1.5%), ETA (0.2%), EPA (1.2%), ω-3 DPA (0.6%), DHA (0.7%)	Petrie *et al*., (2010b)
Physcomitrella patens	*Pavlova* sp. Δ^5-elongase	ADA (2.3%), ω-3 DPA (1.1%)	Current study

[a] *P. cordata* Δ^6-elongase displays some Δ^5-elongase activity.

CHAPTER 5

CONCLUSIONS

The Δ^5-elongase gene has been cloned from marine algae *Pavlova* sp. The open reading frame (ORF) of the cloned PsELO5 cDNA is 834 bp from an ATG start to a TAA stop codons and codes for 277 amino acids. This amino acid polypeptides contained four conserved motifs KxxExxDT (Box 1), QxxFLHxYHH (Box 2) the extended histidine-rich box, NxxxHxxMYxYY (Box 3), and a tyrosine-rich box, TxxQxxQ (Box 4) and the secondary structure analysis of PsELO5 gene showed that the encoded polypeptides contained six putative transmembrane domains.

Heterologous expression of PsELO5 and PsELO5-GFP6 fusion in *P. patens* resulted in the production of C_{22}-PUFA, ADA (0.15±0.04-6.97±0.74 mg/l) without any exogenous ARA substrate addition. The four pMDC43-PsELO5 transgenics with the highest ADA production lines (N15, N64, N70 and N77) obviously produced 22.6-46.4 times higher levels of ADA compared to the six transgenic line (C1-C6) containing the pMDC32-PsELO5 construct, while no ADA was detected in the control wild type. However, an ω-3 DPA was not detected from any transgenic lines cultivated in BCD media. The highest production of ADA (6.97±0.74 mg/l) from the available endogenous ARA substrate was with the transgenic line N64.

Molecular analysis (PCR and Southern Blotting) confirmed that *Pavlova* sp. Δ^5-elongase was transferred into *P. patens* genome. Both single copy and multiple copies of the expression construct were observed in transgenic *P. patens* genome.

Optimization of biomass and ADA production in transgenic *P. patens* by statistically based experimental design, RSM indicated that sucrose, KNO_3 and glutamate significantly influenced on biomass production, whereas sucrose and glutamate considerably affected to ADA production. The optimal culture conditions studied by CCD would be 61.79 g/l sucrose, 1.18 g/l KNO_3 and 2.05 g/l glutamate for biomass production and 22.06 g/l sucrose, 1.00 g/l KNO_3 and 2.35 g/l glutamate for ADA production. This optimized conditions led to the maximum biomass and ADA

production of 17.15 g/l and 4.48 mg/l, respectively, which were 3.55-fold and 10.66-fold higher, respectively, than production rates in the non-optimization study (4.83 g/l DCW and 0.42 mg/l ADA).

In addition, metabolic engineering with PsELO5 and PsELO5-GFP6 fusion together with oil supplementation successfully activated both ω-6 and ω-3 C_{22}-elongation products, ADA and ω-3 DPA, in transgenic lines from 11.18±0.75 to 24.31±0.43 and 6.35±0.43 to 11.75±0.41 mg/l, respectively. The maximum accumulation of ADA (2.3% of total fatty acids) and ω-3 DPA (1.1% of total fatty acids) was achieved in transgenic line N64.

The efficient biosynthesis of C_{22} LC-PUFAs in transgenic *P. patens* plants has now been conclusively demonstrated in this study, using reverse-engineering and nutritional supplementation approaches. This heterologous expression system has not only realized the possibility of producing the important nutritional compounds in transgenic plants, but also provided a new experimental tool with which to better investigate plant lipid metabolism. Finally, *P. patens* is therefore served as an alternative source of further ω-6 DPA and DHA production.

REFERENCES

Aasen, I. M., Moreto, T., Katla, T., Axelesson, L. and Storro, I. 2000. Influence of complex nutrients, temperature and pH on bacteriocin production by *Lactobacillus sakei* CCUG 42687. Appl. Microbiol. Biotechnol. 53: 159-66.

Abbadi, A., Domergue, F., Bauer, J., Napier, J. A., Welti, R., Zahringer, U., Cirpus, P. and Heinz, E. 2004. Biosynthesis of very-long-chain polyunsaturated fatty acids in transgenic oilseeds: constraints on their accumulation. Plant Cell 16: 2734-2748.

Agaba, M. K., Tocher, D. R., Dickson, R., Dick, J. R. and Teale, A. J. 2004. Zebrafish cDNA encoding multifunctional fatty acid elongase involved in production of eicosapentaenoic (20:5n-3) and docosahexaenoic (22:6n-3) acids. Mar. Biotechnol. 6: 251-261.

Agaba, M. K., Tocher, D. R., Zheng, X., Dickson, C. A., Dick, J. R. and Teale, A. J. 2006. Cloning and functional characterisation of marine and freshwater teleost fish. Comp. Biochem. Phys. B 142: 342-352.

Akhtar, H. H., Mirza, A. Q., Nawazish, M. N. and Chughuta, M. I. D. 1983. Effect of triglycerides on the production of lipids and lipases by *Mucor hiemalis*. Can. J. Microbiol. 29: 664-669.

Aki, T., Matumoto, Y., Morinaga, T., Kawamoto, S., Shigeta, S., Ono, K. and Suzuki, O. 1998. Lipid composition of a newly isolated polyunsaturated fatty acid-producing fungus, *Achlya* sp. ma-2801. J. Ferment. Bioeng. 86: 504-507.

Albers, E., Larsson, C., Liden, G., Niklasson, C. and Gustafsson, L. 1996. Influence of the nitrogen source on *Saccharomyces cerevisiae* anaerobic growth and product formation. Appl. Environ. Microb. 62: 3187-3195.

Alonso, D. L. and Maroto, F. G. 2000. Plants as 'chemical factories' for the production of polyunsaturated fatty acids. Biotechnol. Adv. 18: 481-497.

Andarwulan, N. and Shetty, K. 1999. Improvement of pea (*Pisum sativum*) seed vigour response by fish protein hydrolysates in combination with acetyl salicylic acid. Process Biochem. 35: 159-165.

Ansari, K. A. and Shoeman, D. W. 1990. Arachidonic and docosahexaenoic acid content of bovine brain myelin: implications for the pathogenesis of multiple sclerosis. Neuro. Chem. Res. 15: 7-11.

Ashton, N. W. and Cove, D. J. 1977. The isolation and preliminary characterization of auxotrophic and analogue resistance mutants in the moss *Physcomitrella patens*. Mol. Gen. Genet. 154: 87-95.

Ashton, N. W., Grimsley, N. H. and Cove, D. J. 1979. Analysis of gametophytic development in the moss, *Physcomitrella patens*, using auxin and cytokinin resistant mutants. Planta 144: 427-435.

Babcock, T., Helton, W. S. and Espat, N. J. 2000. Eicosapentaenoic acid (EPA): an antiinflammatory ω-3 fat with potential clinical applications. Nutrition 16: 1116-1118.

Bajpai, P. K., Bajpai, P. and Ward, O. P. 1991a. Arachidonic acid production by fungi. Appl. Environ. Microb. 57: 1255-1258.

Bajpai, P. K., Bajpai, P. and Ward, O. P. 1991b. Optimization of production of docosahexaenoic acid (DHA) by *Thraustochytrium aureum* ATCC34304. J. Am. Oil Chem. Soc. 68: 509-514.

Barclay, W. R., Meager, K. M., Abril, J. R. 1994. Heterotrophic production of long-chain omega-3 fatty acids utilizing algae and algae-like microorganisms. J. Appl. Phycol. 6: 123-129.

Bates, P. D., Durrett, T. P., Ohlrogge, J. B. and Pollard, M. 2009. Analysis of acyl fluxes through multiple pathways of triacylglycerol synthesis in developing soybean embryos. Plant Physiol. 150: 55-72.

Bazan, N. G. and Scott, B. L. 1990. Dietary omega-3 fatty acids and accumulation of docosahexaenoic acid in rod photoreceptor cells of the retina and at synapses. Ups. J. Med. Sci. Suppl. 49: 97-107.

Beaudoin, F., Michaelson, L. V., Hey, S. J., Lewis, M. J., Shewry, P. R., Sayanova, O. and Napier, J. A. 2000. Heterologous reconstitution in yeast of the polyunsaturated fatty acid biosynthetic pathway. Proc. Natl. Acad. Sci. USA 97: 6421-6426.

Benolken, R. M., Anderson, R. E. and Wheeler, T. G. 1973. Membrane fatty acids associated with the electrical response in visual excitation. Science 182: 1253-1254.

Bezanilla, M., Pan, A. and Quatrano, R. S. 2003. RNA interference in the moss *Physcomitrella patens*. Plant Physiol. 133: 470-474.

Bierfreund, N. M., Tintelnot, S., Reski, R. and Decker, E. L. 2004. Loss of GH3 function does not affect phytochrome-mediated development in a moss, *Physcomitrella patens*. J. Plant Physiol. 161: 823-836.

Birch, D. G., Birch, E. E., Hoffman, D. R. and Uauy, R. D. 1992a. Retinal development in very-low-birth-weight in fants fed diets differing in omega-3 fatty acids. Invest. Ophthalmol. Visual Sci. 33: 2365-2376.

Birch, E. E., Birch, D. G., Hoffman, D. R. and Uauy, R. 1992b. Dietary essential fatty acid supply and visual acuity development. Invest. Ophthalmol. Visual Sci. 33: 3242-3253.

Bonaa, K. H., Bjerve, K. S. and Nordoy, A. 1992. Habitual fish consumption, plasma phospholipid fatty acids, and serum lipid: the Tromso study. Am. J. Clin. Nutr. 55: 1126-1134.

Bougle, D., Denise, P., Uimard, F., Nouvelet, A., Penniello, M. J. and Guillois, B. 1999. Early neurological and neurophysiological development of the preterm infant and polyunsaturated fatty acids supply. Clin. Neuro. Physiol. 110: 1363-1370.

Brick, E. E., Garfield, S., Hoffman, D. R., Uauy, R. and Birch, D. G. 2000. A randomized controlled trial of early dietary supply of long chain polyunsaturated fatty acids and mental development in term infants. Dev. Med. Child. Neurol. 42: 174-181.

Browse, J. and Somerville, C. 1991. Glycerolipid synthesis-biochemistry and regulation. Annu. Rev. Plant Physiol. Plant Mol. Biol. 42: 467-506.

Burja, A. M., Radianingtyas, H., Windust, A. and Barrow, C. J. 2006. Isolation and characterization of polyunsaturated fatty acid producing *Thraustochytrium* species: screening of strains and optimization of omega-3 production. Appl. Microbiol. Biotechnol. 72: 1161-1169.

Calder, P. C. 1997. N-3 polyunsaturated fatty acids and cytokine production in health and diseases. Ann. Nutr. Metab. 41: 203-234.

Campbell, W. B., Falck, J. R., Okita, J. R., Johnson, A. R. and Callahan, K. S. 1985. Synthesis of dihomoprostaglandins from adrenic acid (7,10,13,16-

docosatetraenoicacid) by human endothelial cells. Biochim. Biophys. Acta 837: 67-76.

Carlson, S. E., Werkman, S. H., Peeples, J. M., Cooke, R. J. and Tolley, E. A. 1993. Arachidonic acid status correlates with first year growth in preterm infants. Proc. Natl. Acad. Sci. USA 90: 1073-1077.

Certik, M., Megova, J. and Horenitzky, R. 1999. Effect of nitrogen sources on the activities of lipogenic enzymes in oleaginous fungus *Cunninghamella echinulata*. J. Gen. Appl. Microbiol. 45: 289-293.

Chen, F. 1996. High cell density culture of microalgae in heterotrophic growth. Trend Biotechnol. 14: 421-426.

Cheng, B., Wu, G., Vrinten, P., Falk, K., Bauer, J. and Qiu, X. 2010. Towards the production of high levels of eicosapentaenoic acid in transgenic plants: the effects of different host species, genes and promoters. Transgenic Res. 19: 221-229.

Cheng, M. H., Walker, T. H., Hulbert, G. J. and Raman, D. R. 1999. Fungal production of eicosapentaenoic and arachidonic acids from industrial waste streams and crude soybean oils. Bioresour. Technol. 67: 101-110.

Chen, R., Matsui, K., Ogawa, M., Oe, M., Ochiai, M, Kawashima, H., Sakuradani, E., Shimizu, S., Ishimoto, M., Hayashi, M., Murooka, Y. and Tanaka, Y. 2006. Expression of Δ6, Δ5 desaturase and GLELO elongase genes from *Mortierella alpina* for production of arachidonic acid in soybean [*Glycinemax* (L.) Merrill] seeds. Plant Sci. 170: 339-406.

Chen, Y., Zhang, M. and Gou, K. 2010. SDD17 desaturase can convert arachidonic acid to eicosapentaenoic acid in mammalian cells. Biochem. Biophys. Res. Commun. 394: 158-162.

Chiou, S. Y., Su, W. W. and Su, Y. C. 2001. Optimizing production of polyunsaturated fatty acids in *Marchantia polymorpha* cell suspension culture. J. Biotechnol. 85: 247-257.

Chi, Z., Pyle, D., Wen, Z., Frear, C. and Chen, S. 2007. A laboratory study of producing docosahexaenoic acid from biodiesel-waste glycerol by microalgal fermentation. Process Biochem. 42: 1537-1545.

Chodok, P., Kanjana-Opas, A. and Kaewsuwan, S. 2010. The Plackett–Burman design for evaluating the production of polyunsaturated fatty acids by *Physcomitrella patens*. J. Am. Oil Chem. Soc. 87: 521-529.

Cho, S. H., Quatrano, R. S. and Shin, J. S. 2007. Transgenesis of *Physcomitrella patens*. Transgenic Plant J. 1: 99-103.

Choudhari, S. and Singhal, R. 2008. Media optimization for the production of β-carotene by *Blakeslea trispora*: Astatistical approach. Bioresour. Technol. 99: 722-730.

Cinti, D. L., Cook, L., Nagi, M. N. and Suneja, S. K. 1992. The fatty acid elongation system of mammalian endplasmic reticulum. Prog. Lipid Res. 31: 1-51.

Cliquet, S. and Jackson, M.A. 1999. Influence of culture conditions on production and freeze-drying tolerance of *Paecilomyces fumosoroseus* blastospores. J. Ind. Microbiol. Biotechnol. 23: 97-102.

Corrigan, F. M., Horrobin, D. F., Skinner, E. R., Besson, J. A. and Cooper, M.B. 1998. Abnormal content of *n*-6 and *n*-3 long-chain unsaturated fatty acids in the phosphoglycerides and cholesterol esters of parahippocampal cortex from Alzheimer's disease patients and its relationship to acetyl CoA content. Int. J. Biochem. Cell Biol. 30: 197-207.

Cove, D. J. 1992. Regulation of development in the moss, Physcomitrella patens. In: Brody, S. Cove, D. J., Ottolenghi, S., Russo, V. E. A. (ed). Developmental biology. A molecular genetic approach. Heidelberg: Springer Verlag, pp 179-193.

Cove, D. J. 2000. The moss, *Physcomitrella patens*. J. plant growth regul. 19: 275-283.

Cove, D. J. 2005. The moss *Physcomitrella patens*. Annu. Rev. Genet. 39: 339-358.

Cove, D. J., Knight, C. D. and Lamparter, T. L. 1997. Mosses as model systems. Trends in Plant Sci. 2: 99-105.

Cromwick, A. M., Birrer, G. A. and Gross, R. A. 1996. Effects of pH and aeration on γ-poly (Glutamic Acid) formation by *Bacillus licheniformis* in controlled batch fermenter cultures. Biotechnol. Bioeng. 50: 222-227.

Cunnane, S. C., Plourde, M., Pifferi, F., Bégin, M., Féart, C. and Barberger-Gateau, P. 2009. Fish, docosahexaenoic acid and Alzheimer's disease. Prog. Lipid Res. 48: 238-256.

Curtis, M. D. and Grossniklaus, U. 2003. A gateway cloning vector set for high-throughput functional analysis of genes in Planta. Plant Physiol. 133: 462-469.

Dai, S., Zheng, P., Marmey, P., Zhang, S., Tian, W., Chen, S., Bechy, R. N. and Fauquet, C. 2001. Comparative analysis of transgenic rice plants obtained by *Agrobacterium*-mediated transformation and particle bombardment. Mol. Breed 7: 25-33.

Damude, H. G., Zhang, H., Farrall, L., Ripp, K. G., Tomb, J. F., Hollerbach, D. and Yadav, N. S. 2006. Identification of bifunctional Δ12/ω3 fatty acid desaturases

for improving the ratio of ω3 to ω6 fatty acids in microbes and plants. Proc. Natl. Acad. Sci. USA 103: 9446-9451.

Decker, E. L., Frank, W., Sarnighausen, E. and Reski, R. 2006. Moss systems biology en route: phytohormones in *Physcomitrella* development. Plant Biol. 8: 397-406.

Dittrich, F., Zajonc, D., Hühne, K., Hoja, U., Ekici, A., Greiner, E., Klein, H., Hofmann, J., Bessoule, J. J., Sperling, P. and Schweizer, E. 1998. Fatty acid elongation in yeast-biochemical characteristics of the enzyme system and isolation of elongation-defective mutants. Eur. J. Biochem. 252: 477-485.

Domergue, F., Lerchl, J., Zahringer, U. and Heinz, E. 2002. Cloning and functional characterization of *Phaeodactylum tricornutum* front-end desaturases involved in eicosapentaenoic acid biosynthesis. Eur. J. Biochem. 269: 4105-4113.

Domergue, F., Spiekermann, P., Lerchl, J., Beckmann, C., Kilian, O., Kroth, P. G., Boland, W., Zahringer, U. and Heinz, E. 2003. New insight into *Phaeodactylum tricornutum* fatty acid metabolism. Cloning and functional characterization of Plastidial and microsomal Δ12-fatty acid desaturases. Plant Physiol. 131: 1648-1660.

Drew, D. E., vin Heijne, G., Nordlund, P., de Gier, J. W. 2001. Green fluorescent protein as an indicator to monitor membrane protein overexpression in *Escherichia coli*. FEBS Lett. 507: 220-224.

Earley, K. W., Haag, J. R., Pontes, O., Opper, K., Juehne, T., Song, K. and Pikaard, C. S. 2006. Gateway-compatible vectors for plant functional genomics and proteomics. Plant J. 45: 616-629.

El-Shemy, H. A., Khalafalla, M. M. and Ishimoto, M. 2008. The role of green fluorescent protein (GFP) in transgenic plants to reduce gene silencing phenomena. Curr. Issues Mol. Biol. 11 (Suppl. 1): i21-i28.

Engel, P. P. 1968. Induction of biochemical and morphological mutants in moss *Physcomitrella patens*. Am. J. Bot. 55: 438.

Esfhani, M., Kucirka, E. M., Timons, F. X., Tyagi, S., Lord, A. E. and Henry, S. A. 1981. Effect of exogenous fatty acids on growth, membrane fluidity, and phospholipids fatty acid composition in yeasts. J. Supramol. Struct. Cell. Biochem. 15: 119-128.

Fan, K. W., Chen, F., Jones, E. B. G. and Vrijmoed, L. L. P. 2001. Eicosapentaenoic and docosahexaenoic acids production by and okara-utilizing potential.of thraustochytrids. J. Ind. Microbiol. Biotechnol. 27: 199-202.

Fliesler, S. J. and Anderson, R. E. 1983. Chemistry and metabolism of lipids in the vertebrate retina. Prog. Lipid Res. 22: 79-131.

Frank, W., Decker, E. L. and Reski, R. 2005. Molecular tool to study *Physcomitrella patens*. Plant Biol. 7: 220-227.

Freeman, M. P., Hibbeln, J. R., Wisner, K. L., Davis, J. M., Mischoulon, D., Peet, M., Keck, P. E., Marangell, L. B., Richardson, A. J., Lake, J. and Stoll, A. L. 2006. Omega-3 fatty acids: evidence basis for treatment and future research in psychiatry. J. Clin. Psychiatry 67: 1954-1967.

Frohman, M.A., Dush, M.K. and Martin, G.R. 1988. Rapid production of full-length cDNAs from rare transcripts: Amplification using a single gene-specific oligonucleotide primer. Proc. Nati. Acad. Sci. USA 85: 8998-9002.

Gandhi, S. R. and Weet, J. D. 1991. Production of the polyunsaturated fatty acids arachidonic acid and eicosapentaenoic acid by the fungus *Pythium ultimum*. J. Gen. Microbiol. 137: 1825-1830.

German, O. L., Insua, M. F., Gentili, C., Rotstein, N. P. and Politi, L. E. 2006a. Docosahexaenoic acid prevents apoptosis of retina photoreceptors by activating the ERK/MAPK pathway. J. Neurochem. 98: 1507-1520.

German, O. L., Miranda, G. E., Abrahan, C. E., Rotstein, N. P. 2006b. Ceramide is a mediator of apoptosis in retina photoreceptors. Invest. Ophthalmol. Visual Sci. 47: 1658-1668.

Gertlowski, C. and Petersen, M. 1993. Influence of the carbon source on growth and rosmarinic acid production in suspension cultures of *Coleus blumei*. Plant Cell Tissue Org. Cult. 34: 183-190.

Gibbs, A. and Seviour, R. 1996. Does the agitation rate and/or oxygen saturation influence exopolysaccharide production by *Aureobasidium pullulans* in batch culture. Appl. Microbiol. Biotechnol. 46: 503-510.

Gill, I. and Valivety, R. 1997. Polyunsaturated fatty acids, part l: occurrence, biological activities and application. Tibtech. 15: 401-409.

Girke, T., Schmidt, H., Zahringer, U., Reski, R. and Heinz, E. 1998. Identification of a novel Δ6-acyl-group desaturase by targeted gene disruption in *Physcomitrella patens*. Plant J. 15: 39-48.

Gremillon, L., Kiessling, J., Hause, B., Decker, E. L., Reski, R. and Sarnighausen, E. 2007. Filamentous temperature-sensitive Z (FtsZ) isoforms specifically interact in the chloroplasts and in the cytosol of *Physcomitrella patens*. New Phytol. 176: 299-310.

Grimsley, N. H., Ashton, N. W. and Cove, D. J. 1977. The production of somatic hybrids by protoplast fusion in the moss *Physcomitrella patens*. Mol. Gen. Genet. 154: 97-100.

Grimsley, N. H., Grimsley, J. M. and Hartmann, E. 1981. Fatty acid composition of mutants of the moss *Physcomitrella patens*. Phytochemistry 20: 1519-1524.

Guallar, E., Sanz-Gallardo, M. I., Van't Veer, P., Aro, A., Gomez-Aracena, J., Kark, J. D., Riemersma, R. A., Martin-Moreno, J. M. and Kok, F. J. 2002. Mercury, fish oils, and the risk of myocardial infarction. New Engl. J. Med. 347: 1747-1754.

Guchhait, R. H., Polakis, S. E., Dimroth, P., Stoll, E., Moss, J. and Lane, M. D. 1974. Acetyl-CoA carboxylase system of E. coli: purification and properties of the biotin protein carboxylase, carboxytransferase and carboxyl carrier protein components. J. Biol. Chem. 249: 6633-6645.

Harris, P. and James, A. T. 1969. Effect of low temperatures on fatty acid biosynthesis in seed. Biochem. Biophys. Acta 187: 13-18.

Hartley, J. L., Temple, G. F. and Brasch, M. A. 2000. DNA cloning using in vitrosite-specific recombination. Genome Res. 10: 1788-1795.

Hastings, N., Agaba, M. K., Tocher, D. R., Zheng, X., Dickson, C. A., Dick, J. R. and Teale, A. J. 2005. Molecular cloning and functional characterization of fatty acyl desaturase and elongase cDNAs involved in the production of eicosapentaenoic and docosahexaenoic acids from α-linolenic acid in Atlantic salmon (*Salmo salar*). Mar. Biotechnol. 6: 463-474.

Hernandez, M. L., Mancha, M. and Martinez-Rivas, J. M. 2005. Molecular cloning and characterization of genes encoding two microsomal oleate desaturases (*FAD2*) from olive. Phytochemistry 66: 1417-1426.

Higashiyama, K., Murakami, K., Tsujimura, H., Matsumoto, N. and Fujikawa, S. 1999. Effects of dissolved oxygen on the morphology of an arachidonic acid production by *Mortierella alpina* 1S-4. Biotechnol. Bioeng. 63: 442-448.

Higashiyama, K., Yaguchi, T., Akimoto, K. and Fukikawa, S. 1998. Effects of mineral addition on the growth morphology of and arachidonic acid production by *Mortierella alpina* 1S-4. J. Am. Oil Chem. Soc. 75: 1815-1819.

Hohe, A. and Reski, R. 2002. Optimisation of a bioreactor culture of the moss *Physcomitrella patens* for mass production of protoplasts. Plant Sci. 163: 69-74.

Hohe, A., Decker, E. L., Gorr, G., Schween, G. and Reski, R. 2002a. Tight control of growth and cell differentiation in photoautotrophically growing moss (*Physcomitrella patens*) bioreactor cultures. Plant Cell Rep. 20: 1135-1140.

Hohe, A., Rensing, S. A., Mildner, M., Lang, D. and Reski, R. 2002b. Day length and temperature strongly influence sexual reproduction and expression of a novel MADS-box gene in the moss *Physcomitrella patens*. Plant Biol. 4: 595-602.

Hohe, A., Schween, G. and Reski, R. 2001. Establishment of a semicontinuous bioreactor culture of *Physcomitrella patens* for mass production of protoplasts. Acta Hort. 560: 425-428.

Horstmann, V., Huether, C. M., Jost, W., Reski, R. and Decker, E. L. 2004. Quantitative promoter analysis in *Physcomitrella patens*: a set of plant vectors activating gene expression within three orders of magnitude. BMC Biotechnol. 4: 1-13.

Hostmark, A. T., Bjerkedal, T., Kierulf, P., Flaten, H. and Ulshagen, K. 1988. Fish oil and plasma fibrinogen. Br. Med. J. 297: 180-181.

Hou, C. T. 2008. Production of arachidonic acid and dihomo-gamma-linolenic acid from glycerol by oil-producing filamentous fungi, *Mortierella* in the ARS culture collection. J. Ind. Microbiol. Biotechnol. 35: 501-6.

Hsiao, T. Y., Holmes, B. and Blanch, H. W. 2007. Identification and functional analysis of a delta-6 desaturase from the marine microalga *Glossomastix chrysoplasta*. Mar. Biotechnol. 9: 154-165.

Hur, B. K., Cho, D.W., Kim, H.J., Park, C.I. and Suh, H. J. 2002. Effect of culture conditions on growth and production of docosahexaenoic acid (DHA) using *Thraustochytrium aureum* ATCC 34304. Biotechnol. Bioprocess Eng. 7: 10-15.

Inagaki, K., Aki, T., Fukuda, Y., Kawamoto, S., Shigeta, S., Ono, K. and Suzuki, O. 2000. Identification and expression of a rat fatty acid elongase involved in the biosynthesis of C18 fatty acids. Biosci. Biotechnol. Biochem. 66: 613-621.

Iskandarov, U., Khozin-Goldberg, I. and Cohen, Z. 2010. Identification and Characterization of Δ12, Δ6, and Δ5 desaturases from the green microalga *Parietochloris incisa*. Lipids 45: 519-530.

Iskandarov, U., Khozin-Goldberg, I., Ofir, R. and Cohen, Z. 2009. Cloning and characterization of the Δ6 polyunsaturated fatty acid elongase from the green microalga *Parietochloris incisa*. Lipids 44: 545-554.

Jackson, M. R., Nilsson, T. and Peterson, P. A. 1990. Identification of a consensus motif for retention of transmembrane proteins in the endoplasmic reticulum. EMBO J. 9: 3153-3162.

Jakobsson, A., Westerberg, R. and Jacobsson, A. 2006. Fatty acid elongases in mammals: Their regulation and roles in metabolism. Prog. Lipid Res. 45: 237-249.

Jang, H. D., Lin, Y. Y. and Yang, S. S. 2000. Polyunsaturated fatty acid production with *Mortierella alpina* by solid substrate fermentation. Bot. Bull. Acad. Sin. 41: 41-48.

Jang, H. D., Lin, Y. Y. and Yang, S. S. 2005. Effect of culture media and conditions on polyunsaturated fatty acids production by *Mortierella alpina*. Bioresour. Technol. 96: 1633-1644.

Jareokitmongkol, S., Shimizu, S. and Yamada, H. 1993. Production of an eicosapentaenoic acid-containing oil by a Δ12 desaturase-defective mutant of *Mortierella alpina* IS-4. J. Am. Oil Chem. Soc. 70: 119-123.

Jensen, R. G. 1996. The lipids in human milk. Prog. Lipid Res. 35: 53-92.

Jiang, C., Schommer, C. K., Kim, S. Y. and Suh, D. Y. 2006. Cloning and characterization of chalcone synthase from the moss, *Physcomitrella patens*. Phytochemistry 67: 2531-2540.

Jiang, H. and Gao, K. 2004. Effects of lowering temperature during culture on the production of polyunsaturated fatty acids in the marine diatom *Phaeodactylum tricornutum* (Bacillariophyceae). J. Phycol. 40: 651-654.

Jiang, Y. and Chen, F. 2000a. Effects of temperature and temperature shift on docosahexaenoic acid production by the marine microalga *Crypthecodinium cohnii*. J. Am. Oil Chem. Soc. 77: 613-617.

Jiang, Y. and Chen, F. 2000b. Effects of medium glucose concentration and pH on docosahexaenoic acid content of heterotrophic *Crypthecodinium cohnii*. Process Biochem. 35: 1205-1209.

Jin, M. J., Huang, H., Xiao, A. H., Gao, Z., Liu, X. and Peng, C. 2009. Enhancing arachidonic acid production by *Mortierella alpina* ME-1 using improved mycelium aging technology. Bioprocess Biosyst. Eng. 32: 117-122.

Jin, M. J., Huang, H., Xiao, A. H., Zhang, K., Liu, X., Li, S. and Peng, C. 2008. A novel two-step fermentation process for improved arachidonic acid production by *Mortierella alpina*. Biotechnol. Lett. 30: 1087-1091.

Jones, H. D. 2005. Wheat transformation: current technology and applications to grain development and composition. J. Cereal Sci. 41: 137-147.

Kaewsuwan, S., Cahoon, E. B., Perroud, P. F., Wiwat, C., Panvisavas, N., Quatrano, R. S., Cove, D. J. and Bunyapraphatsara, N. 2006. Identification and functional characterization of the moss *Physcomitrella patens* Δ^5-desaturase gene involved in arachidonic and eicosapentaenoic acid biosynthesis. J. Biol. Chem. 281: 21988-21997.

Kajikawa, M., Yamato, K. T., Kohzu, Y., Nojiri, M., Sakuradani, E., Shimizu, S., Sakai, Y., Fukuzawa, H. and Ohyama, K. 2004. Isolation and characterization of Δ^6-desaturase, an ELO-like enzyme and Δ^5-desaturase from the liverwort *Marchantia polymorpha* and production of arachidonic and eicosapentaenoic acids in the methylotrophic yeast *Pichia pastoris*. Plant Mol. Biol. 54: 335-352.

Kajikawa, M., Yamato, K. T., Sakai, Y., Fukuzawa, H., Ohyama, K. and Kohchi, T. 2006. Isolation and functional characterization of fatty acid Δ5-elongase gene from the liverwort *Marchantia polymorpha* L. FEBS Lett. 580: 149-154.

Kalil, S. J., Maugeri, F. and Rodrigues, M. I. 2000. Response surface analysis and simulation as a tool for bioprocess design and optimization. Process Biochem. 35: 539-550.

Kamisugi, Y., Schlink, K., Rensing, S. A., Schween, G., von Stackelberg, M., Cuming, A. C., Reski, R. and Cove, D. J. 2006. The mechanism of gene targeting in *Physcomitrella patens*: homologous recombination, concatenation and multiple integration. Nucleic Acids Res. 34: 6205-6214.

Kang, D. H., Anbu, P., Kim, W. H. and Kur, B. 2008. Co-expression of Elo-like enzyme and Δ5, Δ4-desaturases derived from *Thraustochytrium aureum* ATCC 34304 and the production of DHA and DPA in *Pichia pastoris*. Biotechnol. Bioprocess Eng. 13: 483-490.

Kang, J., Snapp, A. R. and Lu, C. 2011. Identication of three genes encoding microsomal oleate desaturases (FAD2) from the oil seed crop *Camelina sativa*. Plant Physiol. Biochem. 49: 223-229.

Kelley, D. S., Siegel, D., Vemuri, M. and Mackey, B. E. 2007. Docosahexaenoic acid supplementation improves fasting and postprandial lipid profiles in hypertriglyceridemic men. Am. J. Clin. Nutr. 86: 324-333.

Kendrick, A. and Ratledge, C. 1992. Lipids of selected molds grown for production of n-3 and n-6 polyunsaturated fatty acids. Lipids 27: 15-20.

Kennedy, E. P. 1961. Biosynthesis of complex lipids. Fed. Proc. Transl. Suppl. 20: 934-940.

Kimball, S. L., Deversdraf, W. D. and Bingham, E. T. 1975. Influence of osmotic potential on the growth development of soybean tissue culture. Crop Sci. 15: 750-752.

Kitano, M., Matsukawa, R. and Karube, I. 1997. Changes in eicosapentaenoic acid content of *Naviculasaprophilla*, *Rhodomonassalina* and *Nitzschia* sp. under mixotrophic conditions. J. Appl. Phycol. 9: 559-563.

Knight, C. D., Cove, D. J., Cuming, A. C. and Quatrano, R. S. 2002. Moss gene technology. In PM Gilmartin, C Bowter, eds, Molecular Plant Biology, Vol 2. Oxford University Press, New York, pp. 285-301.

Knight, C. D., Sehgak, A., Atwal, K., Wallave, J. C., Cove, D. J., Coates, D., Quatrano, R. S., Bahadur, S., Stockley, P. G. and Cuming, A. C. 1995. Molecular responses to abscisic acid and stress are conserved between moss and cereals. Plant Cell 7: 499-506.

Koduri, P. K. H., Gordon, G. S., Barker, E. I., Colpitts, C. C., Ashton, N. W. and Suh, D. Y. 2010. Genome-wide analysis of the chalcone synthase superfamily genes of *Physcomitrella patens*. Plant Mol. Biol. 72: 247-263.

Koprivova, A., Altmann, F., Gorr, G., Kopiva, S., Reski, R. and Decker, E. L. 2003. *N*-glycosylation in the moss *Physcomitrella patens* is organized similarly to that in higher plants. Plant Biol. 5: 582-591.

Koprivova, A., Meyer, A. J., Schween, G., Herschbach, C., Reski, R. and Kopriva, S. 2002. Functional knock out of the adenosine 5'-phosphosulfate reductase gene in *Physcomitrella patens* revives an old route of sulfate assimilation. J. Biol. Chem. 277: 32195-32201.

Kowluru, A., Chen, H. Q., Modrick, L. M. and Stefanelli, C. 2001. Activation of acetyl-CoA carboxylase by a glutamate- and magnesium-sensitive protein phosphatase in the Islet β-cell. Diabetes 50: 1580-1587.

Lan, W. Z., Qin, W. M. and Yu, L. J. 2002. Effect of glutamate on arachidonic acid production from *Mortierella alpina*. Lett. Appl. Microbiol. 35: 357-360.

Laoteng, K., Ruenwai, R., Tanticharoen, M. and Cheevadhanarak, S. 2005. Genetic modification of essential fatty acids biosynthesis in *Hansenula polymorpha*. FEMS Microbiol. Lett. 245: 169-178.

Lee, J. C., Anbu, P., Kim, W. H., Noh, M. J., Lee, S. J., Seo, J. W. and Hu, B. K. 2008. Identification of Δ9-elongation activity from *Thraustochytrium aureum* by heterologous expression in *Pichia pastoris*. Biotechnol. Bioprocess Eng. 13: 524-532.

Leonard, A. E., Bobik, E. G., Dorado, J., Kroeger, P. E., Chuang, L. T., Thurmond, J. M., Parker-Bames, J. M., Das, T., Huang, Y. S. and Murkerji, P. 2000. Cloning of a human cDNA encoding a novel enzyme involved in the elongation of long chain polyunsaturated fatty acids. Biochem J. 350: 765-770.

Lessard, P. A., Kulaveerasingam, H., Rork, G. M., Strong, A. and Sinskey, A. J. 2002. Manipulating gene expression for the metabolic engineering of plants. Metab. Eng. 4: 67-79.

Li, L., Wang, X., Gai, J. and Yu, D. 2007. Molecular cloning and characterization of a novel microsomal oleate desaturase gene from soybean. J. Plant Physiol. 164: 1516-1526.

Li, M., Ou, X., Yang, X., Guo, D., Qian, X., Xing, L. and Li, M. 2011. Isolation of a novel C18-Δ9 polyunsaturated fatty acid specific elongase gene from DHA-producing *Isochrysis galbana* H29 and its use for the reconstitution of the alternative Δ8 pathway in *Saccharomyces cerevisiae*. Biotechnol. Lett. 33: 1823-1830.

Li, Z. Y. and Ward, O. P. 1994. Production of docosahexaenoic acid by *Thraustochytrium roseum*. J. Ind. Microbiol. 13: 238-241.

Ludwig-Muller, J., Julke, S., Bierfreund, N. M., Decker, E. L. and Reski, R. 2009. Moss (*Physcomitrella patens*) GH3 proteins act in auxin homeostasis. New Phytol. 181: 323-338.

Lu, H., Li, J. N., Chai, Y. R. and Zhang, X. K. 2009. Identification and characterization of a novel Δ6-fatty acid desaturase gene from *Rhizopus nigricans*. Mol. Biol. Rep. 36: 2291-2297.

Martin, A., Lang, D., Hanke, S. T., Mueller S. J. X., Sarnighausen, E. and Reski, R. 2009a. Targeted gene knockouts reveal overlapping functions of the five *Physcomitrella patens* FtsZ isoforms in chloroplast division, chloroplast shaping, cell patterning, plant development, and gravity sensing. Mol. Plant 2: 1359-1372.

Martin, A., Lang, D., Heckmann, J., Zimmer, A. D., Vervliet-Scheebaum, M. and Reski, R. 2009b. A uniquely high number of ftsZ genes in the moss *Physcomitrella patens*. Plant Biol. 11: 744-750.

Martinez, B. C. and Park, C. H. 1993. Characteristics of batch suspension cultures of preconditioned *Coleus blumei* cells: sucrose effect. Biotechnol. Prog. 9: 97-100.

Martinez, M. 1992. Tissue levels of polyunsaturated fatty acids during early human development. J. Pedriatr. 120: S129-S138.

Martinez, M. and Mougan, I. 1998. Fatty acid composition of human brain phospholipids during normal development. J. Neurochem. 71: 2528-2533.

McDaniel, S. F., von Stackelberg, M., Richardt, S., Quatrano, R. S., Reski, R. and Rensing, S. A. 2010. The speciation history of the Physcomitrium-Physcomitrella species complex. Evolution 64: 217-231.

Medina, A. R., Grima, E. M., Gimenez, A. G. and Gonzalez, M. J. I. 1998. Downstream processing of algal polyunsaturated fatty acids. Biotechnol. Adv. 16: 517-580.

Meireles, L. A., Guedes, A. C. and Malcata, F. X. 2003. Lipid class composition of the microalga *Pavlova lutheri*: eicosapentaenoic and docosahexaenoic acids. J. Agric. Food Chem. 51: 2237-2241.

Meyer, A., Kirsch, H., Domergue, F., Abbadi, A., Sperling, P., Bauer, J., Cirpus, P., Zank, T. K., Moreau, H., Roscoe, T. J., Zahringer, U. and Heinz, E. 2004. Novel fatty acid elongases and their use for the reconstitution of docosahexaenoic acid biosynthesis. J. Lipid Res. 45: 1899-1909.

Mhanhmad, S., Leewanich, P., Punsuvon, V., Chanprame, S. and Srinvies, P. 2011. Seasonal effects on buck components and fatty acid composition in Dura oil pal, (*Elaeis guineensis*). Afri. J. Agric. Res. 6: 1835-1843.

Molina, G. E., Sanchez, P. J. A., Garcia, S. J. L., Garcia, C. F. and Lopez, A. D. 1992. EPA from *Isochrysis galbana*, growth conditions and productivity. Process Biochem. 27: 299-305.

Morais, S., Monroig, O., Zheng, X., Leaver, M. J. and Tocher, D. R. 2009. Highly unsaturated fatty acid synthesis in atlantic salmon: characterization of ELOVL5- and ELOVL2-like elongases. Mar. Biotechnol. 11: 627-639.

Muhid, F., Nawi, W. N. N. W., Kader, A. J. A., Yusoff, W. M. W. and Hamid, A. A. 2008. Effect of metal ion concentration on lipid and gamma linolenic acid production by *Cunninghamella* sp. 2A1. J. Biol. Sci. 8: 62-67.

Nakagawa, T., Ishiguro, S. and Kimura, T. 2009. Gateway vectors for plant transformation. Plant Biotechnol. 26: 275-284.

Na-Ranong, S., Laoteng, K., Kittakoop, P., Tanticharoen, M. and Cheevadhanarak, S. 2005. Substrate specificity and preference of Δ6-desaturase of *Mucor rouxii*. FEBS Lett. 579: 2744-2748.

Neuringer, M., Connor, W. E., Lin, D. S., Barstad, L. and Luck, S. 1986. Biochemical and functional effects of prenatal and postnatal omega 3 fatty acid deficiency on retina and brain in rhesus monkeys. Proc. Natl. Acad. Sci. USA 83: 4021-4025.

Neuringer, M., Connor, W. E., VanPetten, C. and Barstad, L. 1984. Dietary omega-3 fatty acid deficiency and visual loss in infant rhesus monkeys. J. Clin. Invest. 73: 272-276.

Nichols, D. S., Brown, J. L., Nichols, P. D. and McMeekin, T. A. 1997. Production of eicosapentaenoic and arachidonic acids by an Antarctic bacterium: response to growth temperature. FEMS Microbiol. Lett. 152: 349-354.

Nilsson, A., Olsson, T., Ulfstedt, M., Thelander, M. and Ronne, H. 2011. Two novel types of hexokinases in the moss *Physcomitrella patens*. BMC Plant Biol. 11: 32-47.

Nisha, A., Rastogi, N. K. and Venkateswaran, G. 2011. Optimization of media components for enhanced arachidonic acid production by *Mortierella alpina* under submerged cultivation. Biotechnol. Bioprocess Eng. 16: 229-237.

Nisha, A. and Venkateswaran, G. 2011. Effect of culture variables on mycelial arachidonic acid production by *Mortierella alpina*. Food Bioprocess Technol. 4: 232-240.

Niu, Y., Kong, J., Fu, L., Yang, J. and Xu, Y. 2009. Identification of a novel C20-elongase gene from the marine microalgae *Pavlova viridis* and its expression in *Escherichia coli*. Mar. Biotechnol. 11: 17-23.

Nordoy, A. 1991. Is there a rational use for *n*-3 fatty acids (fish oils) in clinical medicine? Drugs 42: 331-342.

Nuutila, A. M., Aura, A. M., Kiesvaara, M. and Kauppinen, V. 1997. The effects of salinity nitrate concentration, pH and temperature on eicosapentaenoic acid (EPA) production by the red unicellular *Porphyridium cruentum*. J. Biotechnol. 55: 55-63.

O'Brien, J. S. and Sampson, E. L. 1965. Fatty acid and fatty aldehyde composition of the major brain lipids in normal human gray matter, white matter, and myelin. J. Lipid Res. 6: 545-551.

Oh, C. S., Toke, D. A., Mandala, S. and Martin, C. E. 1997. ELO2 and ELO3, homologues of the *Saccharomyces cerevisiae* ELO1 gene, function in fatty acid elongation and are required for sphingolipid formation. J. Biol. Chem. 272: 17376-17384.

Parker-Barnes, J. M., Das, T., Bobik, E., Leonard, A. E., Thurmond, J. M., Chaung, L. T., Huang, Y. S. and Mukerji, P. 2000. Identication and characterization of an enzyme involved in the elongation of *n*-6 and *n*-3 polyunsaturated fatty acids. Proc. Natl. Acad. Sci. USA 97: 8284-8289.

Passorn, S., Laoteng, K., Rachadawong, S., Tanticharoen, M. and Cheevadhanarak, S. 1999. Heterologous expression of *Mucor rouxii* Δ^{12}-desaturase gene in *Saccharomyces cerevisiae*. Biochem. Biophys. Res. Commun. 263: 47-51.

Pellerin, L. and Magistretti, P.J. 1994. Glutamate uptake into astrocytes stimulates aerobic glycolysis: a mechanism coupling neuronal activity to glucose utilization. Proc. Natl. Acad. Sci. USA 91: 10625-10629.

Pereira, S. L., Leonard, A. E. and Mukerji, P. 2003. Recent advances in the study of fatty acid desaturases from animals and lower eukaryotes. Prostaglandins Leukot. Essent. Fatty Acids 68: 97-106.

Pereira, S. L., Huang, Y. S., Bobik, E. G., Kinney, A. J., Stecca, K. L., Packer, J. C. and Mukerji, P. 2004a. A novel omega3-fatty acid desaturase involved in the biosynthesis of eicosapentaenoic acid. Biochem. J. 378: 665-671.

Pereira, S. L., Leonard, A. E., Huang, Y. S., Chuang, L. T. and Mukerji, P. 2004b. Identification of two novel microalgal enzymes involved in the conversion of the ω3-fatty acid, eicosapentaenoic acid, into docosahexaenoic acid. Biochem J. 384: 357-366.

Petrie, J. R., Liu, Q., Mackenzie, A. M., Shrestha, P., Mansour, M. P., Robert, S. S., Frampton, D. F., Blackburn, S. I., Nichols, P. D. and Singh, S. P. 2010a. Isolation and characterisation of a high-efficiency desaturase and elongases from microalgae for transgenic LC-PUFA production. Mar. Biotechnol. 12: 430-438.

Petrie, J. R., Mackenzie, A. M., Shrestha, P. and Liu, Q. 2010b. Isolation of three novel long-chain polyunsaturated fatty acid Δ^9-elongase and the transgenic assembly of the entire *Pavlova salina* docosahexaenoic acid pathway in *Nicotiana benthamiana*. J. Phycol. 46: 917-925.

Petrie, J. R., Shrestha, P., Mansour, M. P., Nichols, P. D., Liu, Q. and Singh, S. P. 2010c. Metabolic engineering of omega-3 long chain polyunsaturated fatty acids in plants using an acyl-CoA Δ^6-desaturase with ω3-preference from the marine microalga *Micromonas pusilla*. Metab. Eng. 12: 233-240.

Petrie, J. R. and Singh, S. P. 2011. Expanding the docosahexaenoic acid food web for sustainable production: engineering lower plant pathways into higher plants. AoB PLANTS doi:10.1093/aobpla/plr011.

Peyou-Ndi, M. M., Watts, J. L. and Browse, J. 2000. Identification and characterization of an animal Δ^{12} fatty acid desaturase gene by heterologous

expression in *Saccharomyces cerevisiae*. Arch. Biochem. Biophys. 376: 399-408.

Pirtle, I. L., Kongcharoensuntorn, W., Nampaisansuk, M., Chapman, K. D. and Pirtle, R. M. 2001. Molecular cloning and functional expression of the gene for a cotton Δ-12 fatty acid desaturase (FAD2). Biochim. Biophys. Acta 1522: 122-129.

Prigge, M. J. and Bezanilla, M. 2010. Evolutionary crossroads in developmental biology: *Physcomitrella patens*. Development 137: 3535-3543.

Qiang, H., Zhengyu, H., Cohen, Z. and Richmond, A. 1997. Enhancement of eicosapentaenoic acid (EPA) and γ-linolenic acid (GLA) production by manipulating algal density of outdoor cultures of *Monodus subterraneus* (Eustigmatophyta) and *Spirulina platensis* (Cyanobacteria). Eur. J. Phycol. 32: 81-86.

Qi, B., Beaudoin, F., Fraser, T., Stobart, A. K., Napier, J. A. and Lazarus, C. M. 2002. Identification of a cDNA encoding a novel C18-Δ^9 polyunsaturated fatty acid-specific elongating activity from the docosahexaenoic acid (DHA)-producing microalga, *Isochrysis galbana*. FEBS Lett. 510: 159-165.

Qi, B., Fraser, T., Mugford, S., Dobson, G., Sayanova, O., Butler, J., Napier, J. A., Stobart, A. K. and Lazarus, C. M. 2004. Production of very long chain polyunsaturated omega-3 and omega-6 fatty acids in plants. Nat. Biotechnol. 22: 739-745.

Rao, J. K., Kim, C. and Rhee, S. 2000. Statistical optimization of medium for the production of recombinant hirudin from *Saccharomyces cerevisiae* using response surface methodology. Process Biochem. 35: 639-647.

Renaud, S. M., Thinh, L. V. and Parry, D. L. 1999. The gross chemical composition and fatty acid composition of tropical Australia microalgae for possible use in mariculture. Aquaculture 170: 147-59.

Rensing, S. A., Lang, D., Zimmer, A. D., Terry, A., Salamov, A., Shapiro, H., Nishiyama, T., Perroud, P. F., Lindquist, E. A., Kamisugi, Y. et al. 2008. The *Physcomitrella* genome reveals evolutionary insights into the conquest of land by plants. Science 319: 64-69.

Reski, R. 2005. Do we need another model plant? Plant Biol. 7: 219.

Reski, R. and Abel, W. O. 1985. Induction of budding on chloronemata and caulonemata of the moss, *Physcomitrella patens*, using isopentenyladenine. Planta 165: 354-358.

Reski, R., Faust, M., Wang, X. H., Wehe, M. and Abel, W. O. 1994. Genome analysis of the moss *Physcomitrella patens* (Hedw.) B.S.G. Mol. Gen. Genet. 244: 352-359.

Reutter, K. and Reski, R. 1996. Production of a heterologous protein in bioreactor cultures of fully differentiated moss plants. Plant Tissue Cult. Biotechnol. 2: 142-147.

Roberts, A. W. and Bushoven, J. T. 2007. The cellulose synthase (CesA) gene superfamily of the moss *Physcomitrella patens*. Plant Mol. Biol. 63: 207-219.

Robert, S. S., Petrie, J. R., Zhou, X. R., Mansour, M. P., Blackburn, S. I., Green, A. G., Singh, S. P. and Nichols, P. D. 2009. Isolation and characterisation of a Δ5-fatty acid elongase from the marine microalga *Pavlova salina*. Mar. Biotechnol. 11: 410-418.

Robert, S. S., Singh, S. P., Zhou, X. R., Petrie, J. R., Blackburn, S. I., Mansour, P. M., Nichols, P. D., Liu, Q. and Green, A. G. 2005. Metabolic engineering of *Arabidopsis* to produce nutritionally important DHA in seed oil. Funct. Plant Biol. 32: 473-479.

Rotstein, N. P., Aveldano, M. I., Barrantes, F. J. and Politi, L. E. 1996. Docosahexaenoic acid is required for the survival of rat retinal photoreceptors in vitro. J. Neurochem. 66: 1851-1859.

Rotstein, N. P., Aveldano, M. I., Barrantes, F. J., Roccamo, A. M. and Politi, L. E. 1997. Apoptosis of retinal photoreceptors during development in vitro: protective effect of docosahexaenoic acid. J. Neurochem. 69: 504-513.

Rotstein, N. P., Politi, L. E., German, O. L. and Girotti, R. 2003. Protective effect of docosahexaenoic acid on oxidative stress-induced apoptosis of retina photoreceptors. Invest. Ophthalmol. Visual Sci. 44: 2252-2259.

Saelao, S., Kanjana-Opas, A. and Kaewsuwan, S. 2011. Optimization of biomass and arachidonic acid production by *Aureispira maritima* using response surface methodology. J. Am. Oil Chem. Soc. 88: 619-629.

Sajbidor, J., Kozelouhova, D. and Certik, M. 1992. Influence of some metal ions on the lipid content and arachidonic acid production by *Mortierella* sp. Folia Microbiol. 37: 404-406.

Sakuradani, E., Ando, A., Ogawa, J. and Shimizu, S. 2009. Improved production of various polyunsaturated fatty acids through filamentous fungus *Mortierella alpina* breeding. Appl. Microbiol. Biotechnol. 84: 1-10.

Sakuradani, E., Murata, S., Kanamaru, H. and Shimizu, S. 2008. Functional analysis of a fatty acid elongase from arachidonic acid-producing *Mortierella alpina* 1S-4. Appl. Microbiol. Biotechnol. 81: 497-503.

Sargent, J. R. and Tacon, A. G. J. 1999. Development of farmed fish: a nutritionally necessary alternative to meat. Proc. Nutr. Sci. 58: 377-383.

Sayanova, O., Haslam, R. P., Calern, M. V., Lpez, N. R., Worthy, C., Rooks, P., Allen, M. J. and Napier, J. A. 2011. Identication and functional characterisation of genes encoding the omega-3 polyunsaturated fatty acid biosynthetic pathway from the coccolithophore *Emiliania huxleyi*. Phytochemistry 72: 594-600.

Sayanova, O., Haslam, R. P., Guschina, I., Lloyd, D., Christie, W. W., Harwood, J. L. and Napier, J. A. 2006a. A bifunctional Δ12,Δ15-desaturase from *Acanthamoeba castellanii* directs the synthesis of highly unusual *n*-1 series unsaturated fatty acids. J. Biol. Chem. 281: 36533-36541.

Sayanova, O., Haslam, R. P., Qi, B., Lazarus, C. M. and Napier, J. A. 2006b. The alternative pathway C_{20} Δ8-desaturase from the non-photosynthetic organism *Acanthamoeba castellanii* is an atypical cytochrome b_5-fusion desaturase. FEBS Lett. 580: 1946-1952.

Schaefer, D. G. 2001. Gene targeting in *Physcomitrella patens*. Cur. Opin. Plant Biol. 4: 143-150.

Schaefer, D. G. and Zryd, J. P. 1997. Efficient gene targeting in the moss *Physcomitrella patens*. Plant J. 11: 1195-1206.

Schaefer, D., Zryd, J. P., Knight, C. D. and Cove, D. J. 1991. Stable transformation of the moss *Physcomitrella patens*. Mol. Gen. Genet. 226: 418-424.

Schaefer, E. F., Bongard, V., Beiser, A. S., Lamon-Fava, S., Robins, S. J., Au, R., Tucker, K. L., Kyle, D. J., Wilson, P. W. F. and Wolf, P. A. 2006. Plasma phosphatidylcholine docosahexaenoic acid content and risk of dementia and Alzheimer disease: the Framingham Heart Study. Arch. Neurol. 63: 1545-1550.

Schneiter, R., Tatzer, V., Gogg, G., Leitner, E. and Kohlwein, S. D. 2000. Elo1p-Dependent Carboxy-Terminal Elongation of C14:1Δ^9 to C16:1Δ^{11} Fatty Acids in *Saccharomyces cerevisiae*. J. Bacteriol. 182: 3655-3660.

Schulte, J. and Reski, R. 2004. High throughput cryopreservation of 140000 *Physcomitrella patens* mutants. Plant Biol. 6: 119-127.

Schween, G., Gorr, G., Hohe, A. and Reski, R. 2003. Unique tissue-specific cell cycle in *Physcomitrella patens*. Plant Biol. 5: 1-9.

Shinde, A. N., Malpathak, N. and Fulzele, D. P. 2009. Optimized production of isoflavones in cell cultures of *Psoralea corylifolia* L. Using elicitation and precursor feeding. Biotechnol. Bioprocess Eng. 14: 162-168.

Shinmen, Y., Katoh, K., Shimizu, S., Jareonkitmongkol, S. and Yamada, H. 1991. Production of arachidonic acid and eicosapentaenoic acid by *Marchantia polymorpha* in cell culture. Phytochemistry. 30: 3255-3260.

Shinmen, Y., Shimizu, S., Akimoto, K., Kawasahima, H. and Yamada, H. 1989. Production of arachidonic acid by *Mortierella* fungi: selection of a potent producer and optimization of culture conditions for large-scale production. Appl. Microbiol. Biotechnol. 31: 11-16.

Shuman, S. 1991. Recombination mediated by *Vaccinia* virus DNA topoisomerase I in *Escherichia coli* is sequence specific. Proc. Natl. Acad. Sci. USA 88: 10104-10108.

Shuman, S. 1994. Novel approach to molecular cloning and polynucleotide synthesis using *Vaccinia* DNA topoisomerase. J. Biol. Chem. 269: 32678-32684.

Simopoulos, A. P. 2002. Omega-3 fatty acids in inflammation and autoimmune disease. J. Am. Coll. Nutr. 21: 495-505.

Singh, A. and Ward, O. P. 1997. Microbial production of docosahexaenoic acid (DHA, C22:6). In: Neidleman, S. L. and Laskin, A. I. (eds) Applied microbiology. Academic Press, London, pp 271-312.

Singh, A. and Ward, O.P. 1998. Docosapentaenoic acid (C22:5, ω-3) production by *Pythium acanthicum.* J. Ind. Microbiol. Biotechnol. 20: 187-191.

Smeekens, S. 2000. Sugar-induced signal transduction in plants. Annu. Rev. Plant Physiol. Plant Mol. Biol. 51: 49-81.

Song, L. Y., Lu, W. X., Hu, J., Zhang, Y., Yin, W. B., Chen, Y. H., Hao, S. T., Wang, B. L., Wang, R. R. C. and Hu, Z. M. 2010. Identification and function alanalysis of the genes encoding Δ^6-desaturase from *Ribes nigrum*. J. Exp. Bot. 61: 1827-1838.

Song, X., Zhang, X., Kuang, C., Zhu, L. and Guo, N. 2007. Optimization of fermentation parameters for the biomass and DHA production of *Schizochytrium limacinum* OUC88 using response surface methodology. Process Biochem. 42: 1391-1397.

Stam, M., Mol, J. N. M. and Kooter, J. M. 1997. The silence of genes in transgenic plants. Ann. Bot. 79: 3-12.

Stillwell, W. and Wassall, S. R. 2003. Docosahexaenoic acid: membrane properties of a unique fatty acid. Chem. Phys. Lipids 126: 1-27.

Streekstra, H. 1997. On the safety of *Mortierella alpina* for the production of food ingredients, such as arachidonic acid. J. Biotechnol. 56: 153-165.

Stumpe, M., Bode, J., Gobel, C., Wichard, T., Schaaf, A., Frank, W., Frank, M., Reski, R., Pohnert, G. and Feussner, I. 2006. Biosynthesis of C9-aldehydes in the moss *Physcomitrella patens*. Biochim. Biophys. Acta 1761: 301-312.

Stumpe, M., Gobel, C, Faltin, B., Beike, A. K., Hause, B., Himmelsbach, K., Bode, J., Kramell, R., Wasternack, C., Frank, W., Reski, R. and Feussner, I. 2010. The moss *Physcomitrella patens* contains cyclopentenones but no jasmonates: mutations in allene oxide cyclase lead to reduced fertility and altered sporophyte morphology. New Phytol. 188: 740-749.

Suppanz, I., Sarnighausen, E. and Reski, R. 2007. An integrated physiological and genetic approach to the dynamics of FtsZ targeting and organization in a moss, *Physcomitrella patens*. Protoplasma 232: 1-9.

Takeuchi, T. 2001. A review of feed development for early life stages of marine finfish in Japan. Aquaculture 200: 203-222.

Tan, L., Meesapyodsuk, D. and Qiu, X. 2011. Molecular analysis of Δ6 desaturase and Δ6 elongase from *Conidiobolus obscurus* in the biosynthesis of eicosatetraenoic acid, a ω3 fatty acid with nutraceutical potentials. Appl. Microbiol. Biotechnol. 90: 591-601.

Tanyildizi, M. S., Ozer, D. and Elibol, M. 2005. Optimization of α-amylase production by *Bacillus* sp. using response surface methodology. Process Biochem. 40: 2291-2296.

Taoka, Y., Nagano, N., Okita, Y., Izumida, H., Sugimoto, S. and Hayashi, M. 2009. Influences of culture temperature on the growth, lipid content and fatty acid composition of *Aurantiochytrium* sp. strain mh0186. Mar. Biotechnol. 11: 368-374.

Tardy, B., Bordet, J. C., Berruyer, M., Ffrench, P. and Dechavanne, M. 1992. Priming effect of adrenic acid (22:4(*n*-6)) on tissue factor activity expressed by thrombin-stimulated endothelial cells. Atherosclerosis 95: 51-58.

Tonon, T., Sayanova, O., Michaelson, L. V., Qing, R., Harvey, D., Larson, T. R., Li, Y., Napier, J. A. and Graham, I. A. 2005. Fatty acid desaturases from the microalga *Thalassiosira pseudonana*. FEBS J. 272: 3401-3412.

Trautwein, E. A. 2001. n-3 Fatty acids-physiological and technical aspects for their role in food. Eur. J. Lipid Sci. Technol. 103: 45-55.

Truksa, M., Wu, G., Vrinten, P. and Qiu, X. 2006. Metabolic engineering of plants to produce very long-chain polyunsaturated fatty acids. Transgenic Res. 15: 131-137.

Tvrdik, P., Westerberg, R., Silve, S., Asadi, A., Jakobsson, A., Cannon, B., Loison, G. and Jacobsson, A. 2000. Role of a new mammalian gene family in the biosynthesis of very long chain fatty acids and sphingolipids. J. Cell Biol. 149: 707-18.

Uauy, R. D., Birch, D. G., Birch, E. E., Tyson, J. E. and Hoffman, D. R., 1990. Effect of dietary omega-3 fatty acids on retinal function of very-low-birth-weight neonates. Pediatr. Res. 28: 485-492.

Uauy, R., Hoffman, D. R., Peirano, P., Birch, D. G. and Birch, E. E. 2001. Essential fatty acids in visual and brain development. Lipids 36: 885-895.

Uauy, R., Mena, P. and Rojas, C. 2000. Essential fatty acids in early life: structural and functional role. Proc. Nutri. Soc. 59:3-15.

Ueshima, H., Stamler, J., Elliott, P., Brown, I. J., Carnethon, M. R., Daviglus, M. L., He, K., Moag-Stahlberg, A., Rodriguez, B. L., Steffen, L. M., Van Hom, L., Yarnell, J. and Zhou, B. 2007. Food omega-3 fatty acid intake of individuals (total, linolenic acid, long-chain) and their blood pressure INTERMAP study. Hypertension 50: 313-319.

Unagul, P., Assantachai, C., Phadungruengluij, S., Suphantharika, M. and Verduyn, C. 2005. Properties of the docosahexaenoic acid-producer *Schizochytrium mangrovei* Sk-02: effects of glucose, temperature and salinity and their interaction. Bot. Mar. 48: 387-394.

VanRollins, M. L., Horrocks, L. and Sprecher, H. 1985. Metabolism of 7,10,13,16-docosatetraenoic acid to dihomo-thromboxane, 14-hydroxy-7,10,12-nonadecatrienoic acid and hydroxyl fatty acids by human platelets. Biochem. Biophys. Acta 833: 272-280.

Vaucheret, H., Beclin, C., Elmayan, T., Feuerbach, F., Godon, C., Morel, J. B., Morrain, P., Palauqui, J. C. and Vernhettes, S. 1998. Transgene-induced gene silencing in plants. Plant J. 16: 651-659.

VonArnim, A. G., Deng, X. W. and Stacey, M. 1998. Cloning vectors for the expression of green fluorescent protein fusion proteins in transgenic plants. Gene 221: 35-43.

vonSchacky, C. 2006. A review of omega-3 ethyl esters for cardiovascular prevention and treatment of increased blood triglyceride levels. Vasc. Health Risk Mang. 2: 251-262.

Walhout, A. J., Temple, G. F., Brasch, M. A., Hartley, J. L., Lorson, M. A., *et al.* 2000. GATEWAY recombinational cloning: application to the cloning of large numbers of open reading frames or ORFeomes. Methods Enzymol. 328: 575-592.

Wallis, J. G., Watts, J. L. and Browse, J. 2002. Polyunsaturated fatty acid synthesis: what will they think of next? Trends Biochem. Sci. 27: 467-470.

Wang, S. J. and Zhong, J. J. 2007. Bioreactor engineering. In: Yang, S. T. (ed) Bioprocessing for value-added products from renewable resources. Elsevier, The Netherlands, pp 131-161.

Wei, D., Li, M., Zhang, X., Ren, Y. and Xing, L. 2004. Identication and characterization of a novel Δ^{12}-fatty acid desaturase gene from *Rhizopus arrhizus*. FEBS Lett. 573: 45-50.

Wen, Z. Y. and Chen, F. 2000. Production potential of eicosapentaenoic acid by the diatom *Nitzschia laevis*. Biotechnol. Lett. 22: 727-733.

Wen, Z. Y. and Chen, F. 2001a. Application of statistically-based experimental designs for the optimization of eicosapentaenoic acid production by the diatom *Nitzschia laevis*. Biotechnol. Bioeng. 75: 159-169.

Wen, Z. Y. and Chen, F. 2001b. Optimization of nitrogen sources for heterotrophic production of eicosapentaenoic acid by diatom *Nitzschia laevis*. Enzyme Microb. Technol. 29: 341-347.

Wheeler, T. G., Benolken, R. M. and Anderson, R. E. 1975. Visual membranes: specificity of fatty acid precursors for the electrical response to illumination. Science 188: 1312-1314.

Wice, B. M., Reitzer, L. J. and Kennell, D. 1981. The continuous growth of vertebrate cells in the absence of sugar. J. Biol. Chem. 256: 7812-7819.

Wiedemann, G., Hermsen, C., Melzer, M., Buttner-Mainik, A., HeinzRennenberg, H., Reski, R. and Kopriva, S. 2010. Targeted knock-out of a gene encoding sulfate reductase in the moss *Physcomitrella patens* affects gametophytic and sporophytic development. FEBS Lett. 584: 2271-2278.

Wilson, R. and Sargent, J. R. 1993. Lipid and fatty acid composition of brain tissue from adrenoleukodystrophy patients. J. Nutr. 64: 577-586.

Wise, H. Z., Saxena, I. M. and Brown Jr., R. M. 2011. Isolation and characterization of the cellulose synthase genes *PpCesA6* and *PpCesA7* in *Physcomitrella patens*. Cellulose. 18: 371-384.

Wong, M. K. M., Tsui, C. K. M., Au D. W. T. and Vrijmoed, L. L. P. 2008. Docosahexaenoic acid production and ultrastructure of the thraustochytrid *Aurantiochytrium mangrovei* MP2 under high glucose concentrations. Mycoscience 49: 266-270.

Wu, G., Truksa, M., Datla, N., Vrinten, P., Bauer, J., Zank, T., Cirpus, P., Heinz, E. and Qiu, X. 2005a. Stepwise engineering to produce high yields of very long-chain polyunsaturated fatty acids in plants. Nat. Biotechnol. 23: 1013-1017.

Wu, S. T. and Lin, L. P. 2003. Application of response surface methodology to optimize docosahexaenoic acid production by *Schizochytrium* sp. S31. J. Food Biochem. 27: 127-139.

Wu, S. T., Yu, S. T. and Lin, L. P. 2005b. Effect of culture conditions on docosahexaenoic acid production by *Schizochytrium* sp. S31. Process Biochem. 40: 3103-3108.

Wynn, J. P., Hamid, A. A. and Ratledge, C. 1999. The role of malic enzyme in the regulation of lipid accumulation in filamentous fungi. Microbiology 145: 1911-1917.

Wynn, J. P., Hamid, A. A., Li, Y. and Ratledge, C. 2001. Biochemical events leading to the diversion of carbon into storage lipids in the oleaginous fungi Mucor circinelloides and *Mortierella alpina*. Microbiology 147: 2857-2864.

Yin, H., Fan, G. and Gu, Z. 2010. Optimization of culture parameters of selenium-enriched yeast (*Saccharomyces cerevisiae*) by response surface methodology (RSM). LWT-Food Sci. Technol. 43: 666-669.

Yi, X. Y., Gauthier, K. M., Cui, L., Nithipatikom, K., Falck, J. R. and Campbell, W. B. 2007. Metabolism of adrenic acid to vasodilatory 1α, 1β-dihomo-epoxyeicosatrienoic acids by bovine coronary arteries. Am. J. Physiol. Heart Circ. Physiol. 292: 2265-2274.

Yokochi, T., Honda, D. and Nakahara, T. 1998. Optimization of docosahexaenoic acid production by *Schizochutrium limacinum* SR21. Appl. Microbol. Biotechnol. 49: 72-76.

Yongmanitchai, W. and Ward, O. P. 1989. Omega-3 fatty acids: alternative sources of production. Process Biochem. 24: 117-25.

Yongmanitchai, W. and Ward, O. P. 1991. Growth of and omega-3 fatty acid production by *Phaeodactylum tricornutum* under different culture conditions. Appl. Environ. Microbiol. 57: 419-425.

Yuan, C., Wang, J., Shang, Y., Guohong, G., Yao, J. and Yu, Z. 2002. Production of arachidonic acid by *Mortierella alpina* I_{49}-N_{18}. Food Technol. Biotechnol. 40: 311-315.

Yu, L. J., Qin, W. M., Lan, W.Z., Zhou, P. P. and Zhu, M. 2003. Improved arachidonic acids production from the fungus *Mortierella alpina* by glutamate supplementation. Bioresour. Technol. 88: 265-268.

Zank, T. K., Zahringer, U., Beckmann, C., Pohnert, G., Boland, W., Holtorf, H., Reski, R., Lerchl, J. and Heinz, E. 2002. Cloning and functional characterisation of an enzyme involved in the elongation of Δ6-polyunsaturated fatty acids from the moss *Physcomitrella patens*. Plant J. 31: 255-268.

Zeidler, M., Gatz, C., Hartmann, E. and Hughes, J. 1996. Tetracycline-regulated reporter gene expression in the moss *Physcomitrella patens*. Plant Mol. Biol. 30: 199-205.

Zeng, Y., Ji, X. J., Lian, M,. Ren, L. J., Jin, L. J., Ouyang, P. K. and Huang, H. 2011. Development of a temperature shift strategy for efficient docosahexaenoic acid production by a marine fungoid protist, *Schizochytrium* sp. HX-308. Appl. Biochem. Biotechnol. 164: 249-255.

Zhang, D., Pirtle, I. L., Park, S. J., Nampaisansuk, M., Neogi, P., Wanjie, S. W., Pirtle, R. M. and Chapman, K. D. 2009. Identication and expression of a new delta-12 fatty acid desaturase (FAD2-4) gene in upland cotton and its functional expression in yeast and *Arabidopsis thaliana* plants. Plant Physiol. Biochem. 47: 462-471.

Zhang, S., Sakuradani, E., Ito, K. and Shimizu, S. 2007. Identication of a novel bifunctional Δ12/Δ15 fatty acid desaturase from a basidiomycete, *Coprinus cinereus* TD#822-2. FEBS Lett. 581: 315-319.

Zheng, X., Seiliez, I., Hastings, N., Tocher, D. R., Panserat, S., Dickson, C. A., Bergot, P. and Teale, A. J. 2004. Characterization and comparison of fatty acyl Δ6 desaturase cDNAs from fresh water and marine teleost fish species. Comp. Biochem. Physiol. B 139: 269-279.

Zhong, J. J. and Yoshida, T. 1995. High-density cultivation of *Perilla frutescens* cell suspensions for anthocyanin production: Effects of sucrose concentration and inoculum size. Enzyme Microb. Technol. 17: 1073-1079.

Zhong, J. J., Xu, G. R. and Yoshida, T. 1994. Effects of initial sucrose concentration on excretion of anthocyanin pigments in suspended cultures of *Perilla frutescens* cells. World J. Microbiol. Biotechnol. 10: 590-592.

Zhou, X. R., Horne, I., Damcevski, K., Haritos, V., Green, A. and Singh, S. 2008. Isolation and functional characterization of two independently-evolved fatty acid Δ12-desaturase genes from insects. Insect Mol. Biol. 17: 667-67.

Zhou, X. R., Robert, S. S., Petrie, J. R., Dion, M. F., Frampton, D. M. F., Mansour, M. P., Blackburn, S. I., Nichols, P. D., Green, A. G. and Singh, S. P. 2007. Isolation and characterization of genes from the marine microalg *Pavlova salina* encoding three front-end desaturases involved in docosahexaenoic acid biosynthesis. Phytochemistry 68: 785-796.

Zhu, M., Yu, L. J. and Wu, Y. X. 2003. An inexpensive medium for production of arachidonic acid by *Mortierella alpina*. J. Ind. Microbiol. Biotechnol. 30: 75-79.

Zhu, M., Yu, L. J., Li, W., Zhou, P. P. and Li, C. Y. 2006. Optimization of arachidonic acid production by fed-batch culture of *Mortierella alpina* based on dynamic analysis. Enzyme Microb. Technol. 38: 735-740.

APPENDIX A

Solutions and media for moss tissue culture and protoplast transformation

Stock solution for media making (Knight *et al*., 2002)

Solution B		
- $MgSO_4 \cdot 7H_2O$	25	g
- Distilled H_2O to	1000	ml
Solution C		
- KH_2PO_4	25	g
- Distilled H_2O to	1000	ml
Solution D		
- KNO_3	101	g
- $FeSO_4 \cdot 7H_2O$	1.25	g
- Distilled H_2O to	1000	ml
Trace element solution		
- H_3BO_3	614	mg
- $Al_2(SO_4)_3 \cdot K_2SO_4 \cdot 24H_2O$	55	mg
- $CuSO_4 \cdot 5H_2O$	55	mg
- KBr	28	mg
- LiCl	28	mg
- $Na_2MoO_4 \cdot 2H_2O$	25	mg
- $MnCl_2 \cdot 4H_2O$	389	mg
- $CoCl_2 \cdot 6H_2O$	55	mg
- $ZnSO_4 \cdot 7H_2O$	55	mg
- KI	28	mg
- $SnCl_2 \cdot 2H_2O$	28	mg
- $NiCl_2 \cdot 6H_2O$	59	mg
- Distilled H_2O to	1000	ml

Moss media recipes

Routine basal medium (BCD)		
- Stock B	10	ml
- Stock C	10	ml
- Stock D	10	ml
- Di-ammonium (+)-tartrate	920 (5)	mg (mM)
- Trace element solution	1	ml
- Agar	8	g
- Distilled H_2O to	1000	ml
- Sterilization by autoclaving and $CaCl_2$ was added immediately before pouring plates	1	mM
Protoplast regeneration medium-bottom layer (PRMB)		
	10	ml
- Stock B	10	ml
- Stock C	10	ml
- Stock D	920 (5)	mg (mM)
- Di-ammonium (+)-tartrate	1	ml
- Trace element solution	60	g
- D-mannitol	8	g
- Agar	1000	ml
- Distilled H_2O to	10	mM
- Sterilization by autoclaving and $CaCl_2$ was added immediately before use		

Protoplast regeneration medium-top layer (PRMT)		
- Stock B	10	ml
- Stock B	10	ml
- Stock B	10	ml
- Di-ammonium (+)-tartrate	920 (5)	mg (mM)
- Trace element solution	1	ml
- D-mannitol	80	g
- Agar	8	g
- Distilled H_2O to	1000	ml
- Sterilization by autoclaving and $CaCl_2$ was added immediately before use	10	mM

Solutions for protoplast transformation

8% D-mannitol solution		
- D-mannitol	80	g
- Distilled H_2O to	1000	ml
- Sterilization by autoclaving		
Calcium protoplast wash (CaPw)		
- D-mannitol	80	g
- $CaCl_2 \cdot 2H_2O$	10.95	g
- Distilled H_2O to	1000	ml
- Sterilization by autoclaving		
1M $MgCl_2$		
- $MgCl_2 \cdot 6H_2O$	203.3	g
- Distilled H_2O to	1000	ml
- Sterilization by autoclaving		
1% MES pH 5.6		
- N-morpholino ethanesulphonic	1	g
- Adjust to pH 5.6 with 0.1 M KOH		
- Distilled H_2O to	100	ml
- Sterilization by autoclaving		

1M $Ca(NO_3)_2$		
- $Ca(NO_3)_2 \cdot 4H_2O$	236.1	g
- Distilled H_2O to	1000	ml
- Sterilization by autoclaving		
D-mannitol/$MgCl_2$/MES solution (MMM)		
- D-mannitol	910	mg
- 1M $MgCl_2$ solution	150	µl
- 1% MES pH 5.6 solution	1	ml
- Distilled H_2O to	8.85	ml
- Filter sterilization		
D-mannitol/$Ca(NO_3)_2$ solution		
- 8% D-mannitol solution	9	ml
- 1M $Ca(NO_3)_2$ solution	1	ml
- 1M Tris buffer pH 8.0	100	µl
- Filter sterilization		
PEG solution		
- Polyethylene glycol (PEG) 6000	2	g
- Autoclave in a glass universal bottle		
- On day of transformation, melt PEG in microwave		
- Add D-mannitol/$Ca(NO_3)_2$ solution and mix well	5	ml
- Filter sterilization		
- Leave at room temperature for about 2 h before use		
0.5% Driselase solution		
- Driselase	0.125	g
- 8% D-mannitol solution	25	ml
- Gently mix (do not shake vigorously)		
- Leave to stand at room temperature for 15 min		
- Centrifuge at 2,500g for 5 min		
- Filter sterilization		

Genomic DNA extraction

Shortly extraction buffer		
- Tris-(hydroxymethyl) aminomethane hydrochloride (Tris-HCl, pH 9.0)	0.2	M
- LiCl	0.4	M
- Ethylenediaminetetraacetic acid (EDTA)	25	mM
- Sodium dodecyl sulfate (SDS)	10	g
- Distilled H_2O to	1000	ml
- Sterilization by autoclaving		

APPENDIX B

Standard curve of fatty acid methyl ester

Preparation of fatty acid standard solutions

Stock solutions of the reference standards, LA methyl ester (1 mg), ALA methyl ester (1 mg), GLA methyl ester (1 mg), EDA methyl ester (1 mg), DHGLA methyl ester (0.5 mg), ARA methyl ester (0.2 mg), EPA methyl ester (0.1 mg), ADA methyl ester (0.5 mg) and ω-3 DPA methyl ester (0.5 mg) were made by dissolving in heptane and these stock solutions were two-fold serial dilution to six concentrations.

Fatty acid methyl esters (FAMEs), LA, ALA, GLA and EDA methyl esters ranging from 31-1,000 µg/ml, DHGLA, ADA and ω-3 DPA methyl esters ranging from 15-500 µg/ml, ARA methyl ester ranging from 6-200 µg/ml and EPA methyl ester ranging from 6-100 µg/ml were used for construction of calibration curves.

GC analysis of FAMEs was conducted using an Agilent 6890N equipped with an HP-INNOWax capillary column (0.25 mm x 30 m x 0.25 µM), a flame ionization detector, using helium as the carrier gas. An aliquot (2 µl) of each sample extract was injected onto the GC column using the injector in the split mode. The initial column temperature was 185^{o}C (0.5 min) and was increased at a rate of 3.5^{o}C/min to 235^{o}C (14.3 min), and then maintained at 235^{o}Cfor 1.0 min. Calibration curves were established by analysis of the standard compounds at six concentrations and plotted peak area against the concentration of each reference standards.

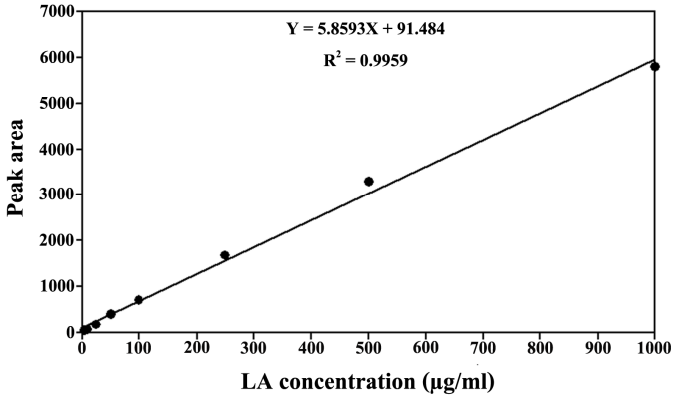

Figure 1B Standard curve of LA methyl ester (Retention time = 6.8 min).

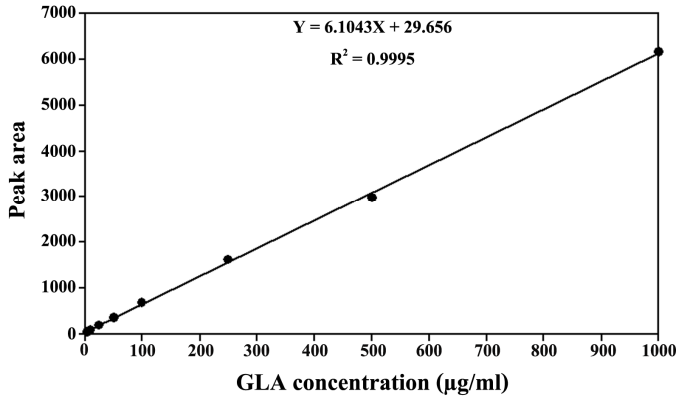

Figure 2B Standard curve of GLA methyl ester (Retention time = 7.1 min).

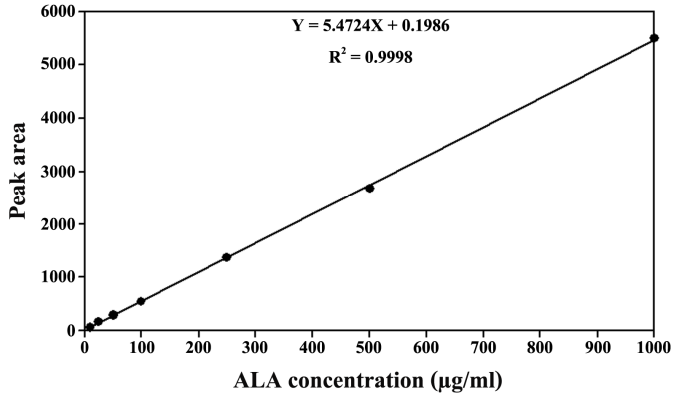

Figure 3B Standard curve of ALA methyl ester (Retention time = 7.4 min).

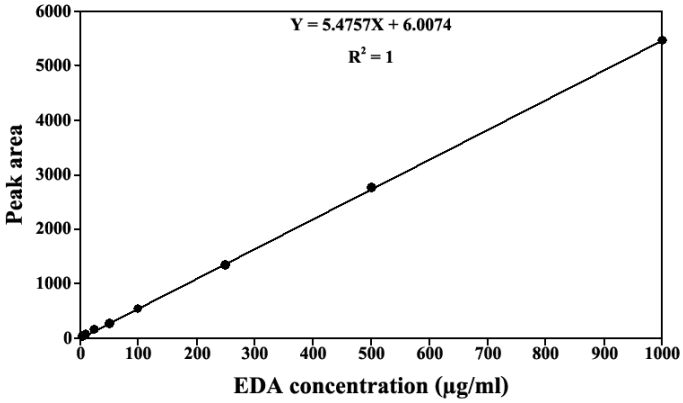

Figure 4B Standard curve of EDA methyl ester (Retention time = 9.2 min).

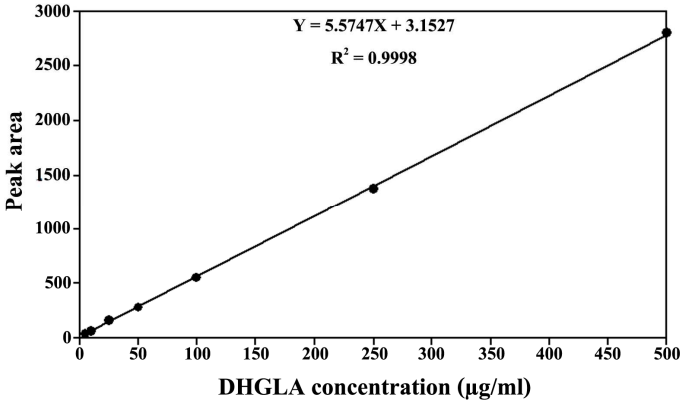

Figure 5B Standard curve of DHGLA methyl ester (Retention time = 9.7 min).

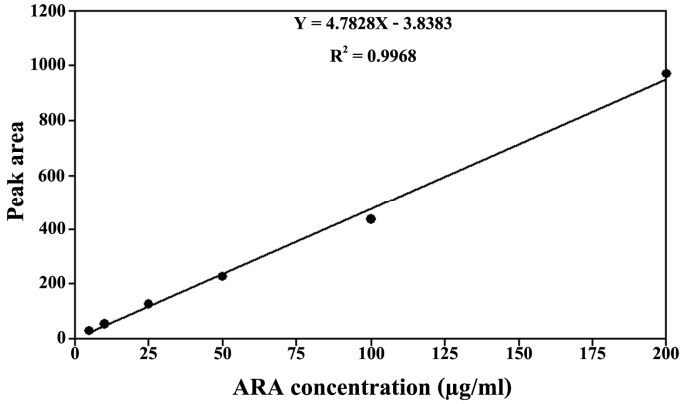

Figure 6B Standard curve of ARA methyl ester (Retention time = 10.2 min).

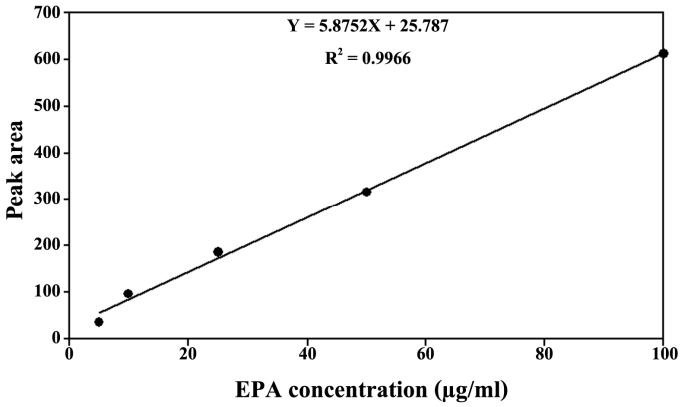

Figure 7B Standard curve of EPA methyl ester (Retention time = 11.4 min).

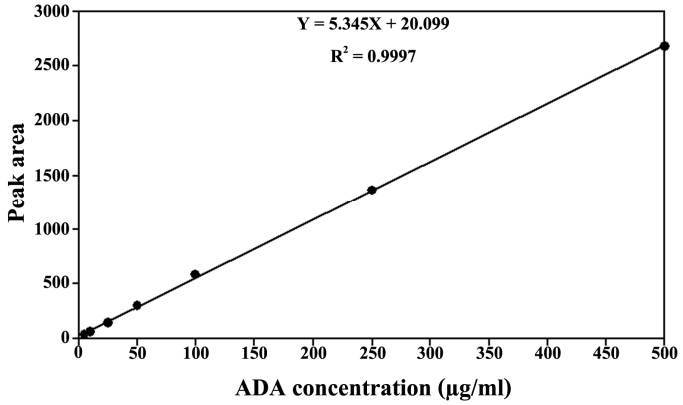

Figure 8B Standard curve of ADA methyl ester (Retention time = 14.7 min).

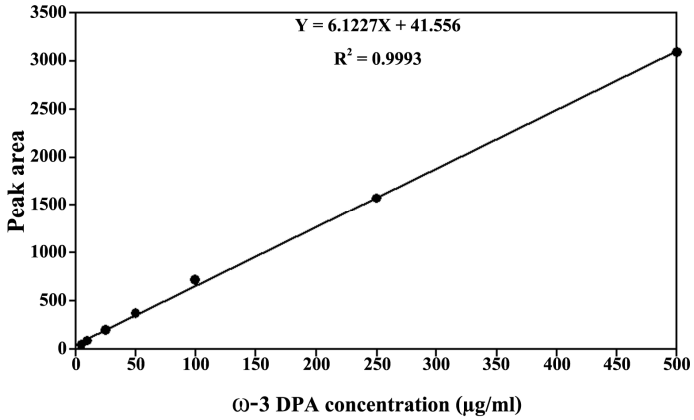

Figure 9B Standard curve of ω-3 DPA methyl ester (Retention time = 15.7 min).

APPENDIX C

Gateway cloning technology

A Gateway™ cloning vector set for high-throughput functional analysis of genes *in planta* (Curtis and Grossniklaus, 2003)

1. 35S induction construct (pMDC32)

- Backbone pCambia 1300
- Kan^r in bacteria
- Hyg^r in plants

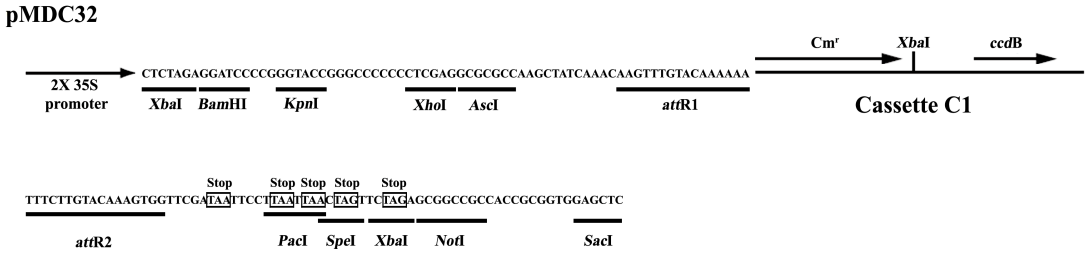

2. GFP C-terminal fusions (pMDC43)

- Backbone pCambia 1300
- Kan^r in bacteria
- Hyg^r in plants

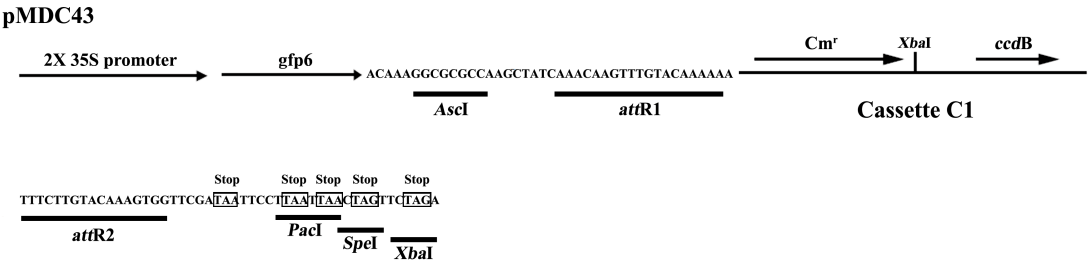

VITAE

Name Mr. Pichit Chodok

Student ID 5010730010

Educational Attainment

Degree	Name of Institution	Year of Graduation
Bachelor of Science (Agriculture)	Prince of Songkla University	2001
Master of Science (Biotechnology)	Walailak University	2007

Scholarship Awards during Enrolment

2007-2010 The Academic Excellence Enhancing Program in Pharmaceutical Sciences, Prince of Songkla University.

List of publication and proceeding

Kaewsuwan, S., Bunyapraphatsara, N., Cove, D.J., Quatrano, R.S. and Chodok, P. 2010. High level production of adrenic acid in *Physcomitrella patens* using the algae *Pavlova* sp. Δ^5-elongase gene. Bioresour. Technol. 101: 4081-4088.

Chodok, P., Kanjana-Opas, A. and Kaewsuwan, S. 2010. The Plackett–Burman design for evaluating the production of polyunsaturated fatty acids by *Physcomitrella patens*. J. Am. Oil Chem. Soc. 87: 521-529.

Chodok, P., Cove, D.J., Quatrano, R.S., Kanjana-Opas, A. and Kaewsuwan, S. 2012. Metabolic engineering and oil supplementation of *Physcomitrella patens* for activation of C_{22} polyunsaturated fatty acid production. J. Am. Oil Chem. Soc. 89: 465-476.

Chodok, P. and Kaewsuwan, S. Production of polyunsaturated fatty acids (PUFAs) in the moss *Physcomitrella patens* by using sucrose as a carbon source. The 20th Annual Meeting and International Conference of the Thai Society for Biotechnology. “TSB 2008: Biotechnology for Global Care”. Taksila Hotel, Maha SaraKham, Thailand, 14th-17th October 2008.

Chodok, P., Kanjana-Opas, A. and Kaewsuwan, S. Activation of docosahexaenoic acid (DHA) precursor in the moss *Physcomitrella patens* by marine algae *Pavlova* sp. Δ^5-elongase and vegetable oil supplements. 13th International Symposium on Marine Natural Products (MaNaPro XIII). Hilton Phuket Arcadia Resort & Spa, Phuket, Thailand, 17th-22th October 2010.